

## INFORMATION TO USERS

This manuscript has been reproduced from the microfilm master. UMI films the text directly from the original or copy submitted. Thus, some thesis and dissertation copies are in typewriter face, while others may be from any type of computer printer.

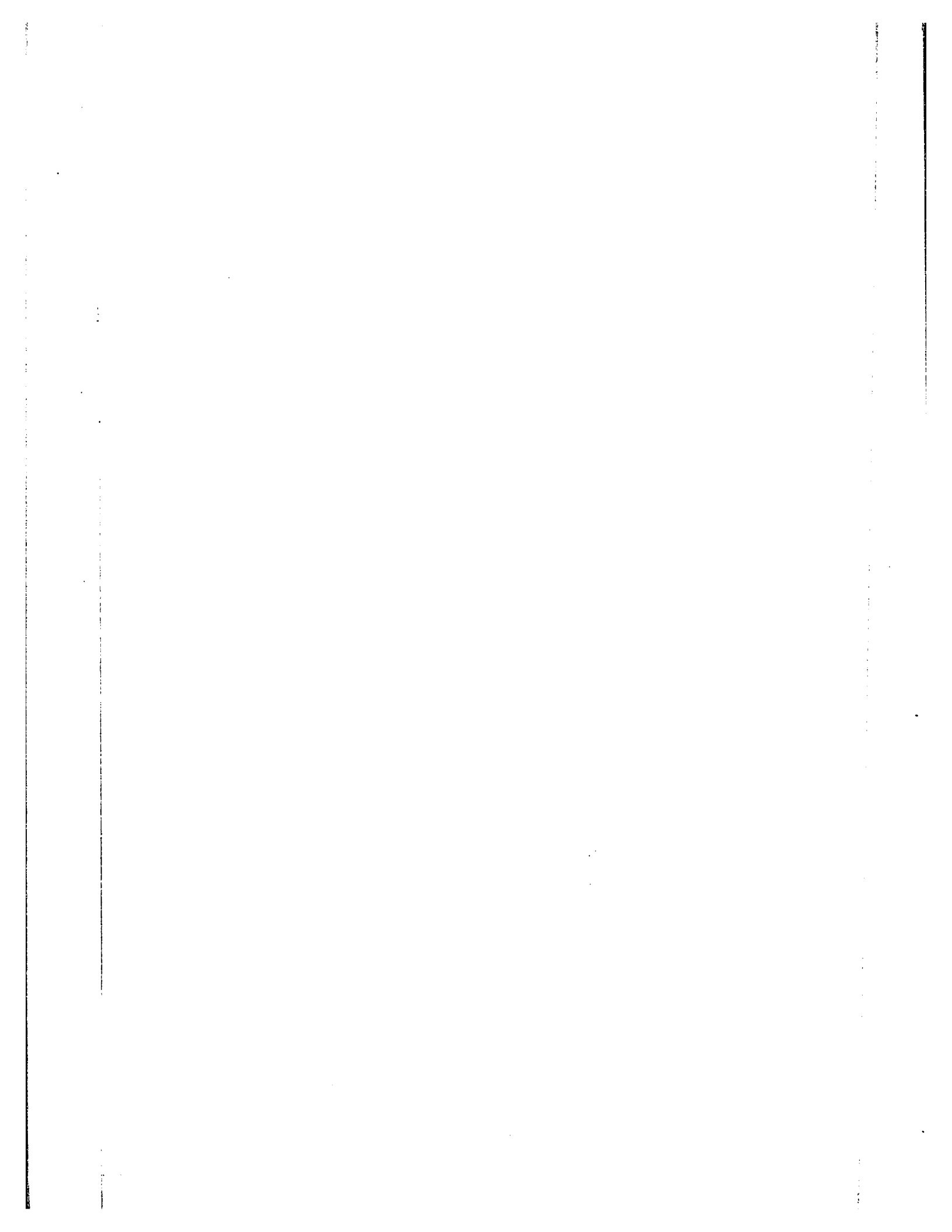
**The quality of this reproduction is dependent upon the quality of the copy submitted.** Broken or indistinct print, colored or poor quality illustrations and photographs, print bleedthrough, substandard margins, and improper alignment can adversely affect reproduction.

In the unlikely event that the author did not send UMI a complete manuscript and there are missing pages, these will be noted. Also, if unauthorized copyright material had to be removed, a note will indicate the deletion.

Oversize materials (e.g., maps, drawings, charts) are reproduced by sectioning the original, beginning at the upper left-hand corner and continuing from left to right in equal sections with small overlaps.

ProQuest Information and Learning  
300 North Zeeb Road, Ann Arbor, MI 48106-1346 USA  
800-521-0600

**UMI<sup>®</sup>**



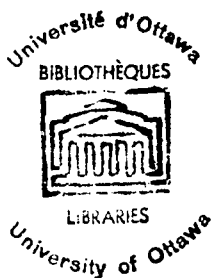
30

KINETICS AND MECHANISMS OF SOME  
COMBINATION AND DECOMPOSITION REACTIONS

by

Muhammad Eusuf

A thesis submitted in partial fulfillment  
of the requirements for the degree of  
Doctor of Philosophy  
in the  
Department of Chemistry  
University of Ottawa  
Ottawa, Canada



---

K.J. Laidler  
Professor of Chemistry  
Research Supervisor

---

M. Eusuf  
Ph.D. Candidate

UMI Number: DC52433

### INFORMATION TO USERS

The quality of this reproduction is dependent upon the quality of the copy submitted. Broken or indistinct print, colored or poor quality illustrations and photographs, print bleed-through, substandard margins, and improper alignment can adversely affect reproduction.

In the unlikely event that the author did not send a complete manuscript and there are missing pages, these will be noted. Also, if unauthorized copyright material had to be removed, a note will indicate the deletion.

**UMI<sup>®</sup>**

---

UMI Microform DC52433  
Copyright 2007 by ProQuest LLC  
All rights reserved. This microform edition is protected against  
unauthorized copying under Title 17, United States Code.

---

ProQuest LLC  
789 East Eisenhower Parkway  
P.O. Box 1346  
Ann Arbor, MI 48106-1346

PREFACE

Atom and free-radical combination reactions play a very important role in chemical kinetics. They constitute the chain-ending steps in chain reactions and influence the overall kinetic behaviour. During recent years there has been considerable interest in these combination reactions from both the experimental and theoretical points of view. The mechanisms of these reactions comprise two main classes: (i) the energy-transfer mechanism, in which two atoms or radicals form a complex which is deactivated by a collision with a foreign molecule, (ii) the radical-molecule complex mechanism, in which an atom or radical forms a complex with a foreign molecule; this complex is deactivated by collisions and finally undergoes reaction with a second atom or free radical. The binding energy between a free radical or an atom and a foreign molecule is the deciding factor whether the latter mechanism plays a role in these reactions. Part I describes a theoretical study of the combination of iodine atoms. The binding energies between iodine atoms and various chaperon molecules have been calculated. An attempt has been made to draw a conclusion from a comparison of the experimental and calculated rate constants as to the type of mechanism applicable in this reaction in the presence of various foreign molecules.

The combination of methyl radicals is the main chain-ending step in the decomposition of many organic compounds e.g.  $\text{CH}_3\text{OCH}_3$ ,  $\text{CH}_3\text{CHO}$  etc. Although it is now generally agreed that at low pressures this combination reaction is a third order process, the order of this reaction under ordinary pyrolysis conditions is a subject of great controversy. In Part 2

this reaction is considered on the basis of the experimental results obtained in the photolysis and pyrolysis of various organic compounds.

It was believed by early workers that in organic decompositions molecules acquire energy by collisions and then split up into fragments of stable molecules. In 1934, Rice and Herzfeld suggested a free-radical mechanism for these reactions on the basis of the fact that free radicals were detected in these systems by Rice and his coworkers. Although this mechanism is essentially correct as far as the overall process is concerned, many of the postulated elementary processes still lack verification or need modification. The thermal decomposition of acetaldehyde and propionaldehyde (Parts 3 and 5) have been studied with a view to establishing the important elementary processes and to elucidating the details of the mechanisms.

It has been believed by Hinshelwood and his students that the decomposition of organic compounds takes place by the concurrent occurrence of both molecular and free radical processes and that the maximally inhibited reaction is a non-chain molecular process. There are experimental facts that the degree of isotopic mixing and the nature of the products are the same both in the presence and absence of nitric oxide, showing that the molecular decomposition is of minor importance. The view of Hinshelwood has been maintained against these strong objections for the last three decades only because no satisfactory mechanism was available to explain the experimental results. In 1960, Laidler and Wojciechowski suggested a new type of mechanism in which nitric oxide initiates chains by abstracting a hydrogen atom and terminates then by being involved in chain-ending processes. This mechanism could lead to a quantitative interpretation of the results of the decomposition of hydrocarbons and ethers. In order to establish the

generality of this mechanism, work has to be done on different types of compounds. Parts 4 and 6 of this thesis present the results of the pyrolysis of acetaldehyde and propionaldehyde respectively in the presence of nitric oxide. These results have been explained on the basis of the above ideas.

Part 1 has been published in the Transactions of the Faraday Society 59, 2750 (1963). Parts 3 and 4 have been accepted for publication in the Canadian Journal of Chemistry and Parts 5 and 6 have been submitted for publication in the Canadian Journal of Chemistry.

#### ACKNOWLEDGMENT

The author is indebted to Professor K.J. Laidler under whose expert guidance this work was carried out. Professor Laidler's constant attention, infinite patience and timely encouragement are most gratefully appreciated. The author wishes to remember Drs. M.H. Back, B.M. Wojciechowski and J.L. Holmes for valuable help, useful suggestions and constructive criticisms. He wishes to thank Dr. A.D. Trenwith for discussions and information about his recent unpublished work. Thanks are also due to Drs. P.J. Thomas and T.M. Bell for helpful discussions.

The author is grateful to the Canadian Commonwealth Scholarship and Fellowship Committee for the award of a scholarship.

TABLE OF CONTENTS

	<u>Page No.</u>
PREFACE	1
ACKNOWLEDGMENTS	iii
TABLE OF CONTENTS	iv
LIST OF TABLES	viii
LIST OF FIGURES	ix
LIST OF PLATES	xiii
ABSTRACTS	1
Theoretical Aspects of Atom and Radical Combination Reaction	1
The Kinetics of the Dissociation of Ethane and the Combination of Methyl Radicals.	2
The Uninhibited Decomposition of Acetaldehyde.	2
The Decomposition of Acetaldehyde in the Presence of Nitric Oxide.	3
The Uninhibited Decomposition of Propionaldehyde.	4
The Decomposition of Propionaldehyde in the Presence of Nitric Oxide.	5
Part I - <u>THEORETICAL ASPECTS OF ATOM</u>	
<u>RADICAL COMBINATION REACTIONS</u>	6
INTRODUCTION	6
FORMULATION OF THE RATE EQUATIONS	8
BINDING ENERGIES	12
Dispersion Forces	12
Charge Transfer	16
SIGNIFICANCE OF THE BINDING ENERGIES	19
RATE CONSTANT CALCULATIONS	19
DISCUSSION	23

	<u>Page No.</u>
Part II - <u>THE KINETICS OF THE DISSOCIATION OF ETHANE AND</u>	
<u>THE COMBINATION OF METHYL RADICALS.</u>	25
INTRODUCTION	25
THE PYROLYSIS OF ACETALDEHYDE	28
THE PHOTOLYSIS OF ACETONE	30
THE PHOTOLYSIS OF ACETALDEHYDE	34
DIRECT STUDIES OF THE COMBINATION OF METHYL RADICALS	38
THE PYROLYSIS OF ETHANE	39
Part III - <u>THE UNINHIBITED DECOMPOSITION OF ACETALDEHYDE</u>	42
INTRODUCTION	42
Review of the Earlier Work	42
Evidence for Free Radicals	44
Inhibition by Inert Gases	48
EXPERIMENTAL	49
Apparatus	49
Method	56
Results	57
DISCUSSION	61
The Reaction Mechanism	61
Influence of Foreign Gases	70
Formation of Ethane	71
Formation of Hydrogen	72
Formation of Acetone	74
Formation of Other Minor Products	75

	<u>Page No.</u>
Part IV - <u>THE DECOMPOSITION OF ACETALDEHYDE IN THE PRESENCE</u>	
<u>OF NITRIC OXIDE</u>	77
INTRODUCTION	77
Review of the Earlier Work	77
EXPERIMENTAL	81
Results	82
THE REACTION MECHANISM	88
THE ELEMENTARY REACTIONS	99
Part V - <u>THE UNINHIBITED DECOMPOSITION OF PROPIONALDEHYDE</u>	102
INTRODUCTION	102
Review of the Earlier Work	102
EXPERIMENTAL	105
Results	106
DISCUSSION	116
Overall Reaction Mechanism	116
Comparison of the Experimental and Predicted	
Values of the Ratio $v_{C_2H_6} / v_{C_2H_4}$	122
Contribution of the Molecular Process	
$C_2H_5 \rightarrow C_2H_6 + CO$	123
Activation Energies	124
Part VI - <u>THE DECOMPOSITION OF PROPIONALDEHYDE IN THE PRESENCE</u>	
<u>OF NITRIC OXIDE</u>	128
INTRODUCTION	128
Review of the Earlier Work	128

	<u>Page No.</u>
EXPERIMENTAL	133
Results	133
DISCUSSION	146
Overall Reaction Mechanism	146
Activation Energies	154
The Production of Methane	155
The Termination Steps	156
CLAIMS TO ORIGINAL RESEARCH	158
REFERENCES	162

LIST OF TABLES

<u>Table No.</u>		<u>Page No.</u>
1.	Binding Energies and Other Properties of Complexes (Dispersion Forces)	14
2.	Resonance Integral $\beta$ , Estimated from Experimental Data	18
3.	Binding Energies due to Charge-Transfer	20
4.	Observed and Calculated Rate Constants for Iodine Atom Combinations	22
5.	Results for the Photolysis of Acetone	33
6.	One-half and three-halves Order Rate Constants for the Uninhibited Decomposition of Propionaldehyde	117
7.	Ratios of Products for the Uninhibited Decomposition of Propionaldehyde	121
8.	Kinetic Parameters for Elementary Reactions (Uninhibited Decomposition of Propionaldehyde)	125
9.	Rate Constants for the Propionaldehyde Decomposition Catalysed by Nitric Oxide	144
10.	Kinetic Parameters for Elementary Reactions (Propional- dehyde Decomposition in the Presence of Nitric Oxide)	153

LIST OF FIGURES

<u>Figure No.</u>		<u>Page No.</u>
1	Plot of Binding Energy, due to Dispersion Forces, against the Internuclear Separation for the System Ar...I.	21
2.	Plot of $\log v_{\text{CH}_4} / v_{\text{C}_2\text{H}_6}^{1/2} [\text{CH}_3\text{COCH}_3]$ against $1/T$ for the Photolysis of Acetone	35
3.	Plot of $\log v_{\text{CH}_4} / v_{\text{C}_2\text{H}_6}^{1/2}$ against $\log P_{\text{CH}_3\text{CHO}}$ for the Photolysis of Acetaldehyde	37
4.	Schematic Diagram of the Apparatus	50
5A.	Schematic Circuit of the Transducer	54
5B.	Schematic Diagram of the Measuring Part of the Recorder	54
6.	Typical Pressure-Time Curve for the Uninhibited Decomposition of Acetaldehyde	58
7.	Double Logarithmic Plots of Initial Rate against Initial Pressure of Acetaldehyde	59
8.	Arrhenius Plot for the Uninhibited Reaction of Acetaldehyde	60
9.	Plots of Log Rate against log Pressure of Acetaldehyde showing the Effects of 100 mm of Added Foreign Gases.	62
10.	Plots of the Amount of Ethane formed against Time.	63
11.	Double Logarithmic Plot of Initial Rate of Formation of Ethane against Initial Pressure of Acetaldehyde	64

<u>Figure No.</u>		<u>Page No.</u>
12.	Typical Pressure-Time Curve for the Acetaldehyde Decomposition in the Presence of Nitric Oxide.	83
13.	Effect of Temperature on the Inhibition by Nitric Oxide.	84
14.	Plots of Rates against Nitric Oxide Pressures Added at Various Acetaldehyde Pressures.	85
15.	Plots of Rates against Nitric Oxide Pressures at Different Temperatures.	86
16.	Arrhenius Plot for the Hydrogen Abstraction Reaction	87
17.	Effect of Nitric Oxide Pressure on the Order with respect to Acetaldehyde.	89
18.	Double Logarithmic Plots of Rate against Acetaldehyde Pressure with 50 mm of Nitric Oxide.	90
19.	Double Logarithmic Plot of Rate against Nitric Oxide Pressure (Acetaldehyde Decomposition).	91
20.	Arrhenius Plot for the Nitric Oxide Catalysed Decomposition of Acetaldehyde.	92
21.	Schematic Diagram Showing the Reaction Orders at Various Nitric Concentrations.	93
22.	Typical $\Delta P-t$ Curve for the Uninhibited Decomposition of Propionaldehyde.	107
23.	Pressure of Carbon Monoxide Formed against Time for the Propionaldehyde Decomposition.	108

<u>Figure No.</u>	<u>Page No.</u>
24. Log v against $\text{Log } P_{\text{C}_2\text{H}_5\text{CHO}}$ at different Temperatures.	109
25. Effect of Adding $\text{CO}_2$ and $\text{C}_2\text{H}_6$ on the Decomposition of Propionaldehyde.	111
26. Effect of $\text{CO}_2$ on the Rates of Formation of $\text{C}_2\text{H}_4$ and $\text{C}_2\text{H}_6$ .	112
27. Plot of the Ratio $P_{\text{C}_2\text{H}_6}/P_{\text{C}_2\text{H}_4}$ against $P_{\text{C}_2\text{H}_5\text{CHO}}$ .	113
28. Plot of $v_{\text{C}_2\text{H}_6}/v_{\text{C}_2\text{H}_4} [\text{C}_2\text{H}_5\text{CHO}]^{1/2}$ against $[\text{C}_2\text{H}_5\text{CHO}]^{1/2}$ .	114
29. Plots of $v/P_{\text{C}_2\text{H}_5\text{CHO}}^{1/2}$ against $P_{\text{C}_2\text{H}_5\text{CHO}}$ at Different Temperatures.	115
30. Arrhenius Plots of the one-half and three-halves Order Rate Constants for the Uninhibited Decomposition of Propionaldehyde.	118
31. Arrhenius Plots of the Ratios Involving the Rate Constants of the Chain-Ending and Chain-Propagating Steps (Results of Szabó and Márta).	131
32. Typical $\Delta P-t$ Curve for the Propionaldehyde Decomposition Catalysed by Nitric Oxide.	134
33. Pressure of Carbon Monoxide Formed against Time (Propionaldehyde Decomposition in the Presence of Nitric Oxide)	135
34. Comparison of the Rates of Formation of the Products in the Presence and Absence of Nitric Oxide (Propionaldehyde Decomposition).	137

<u>Figure No.</u>		<u>Page No.</u>
35.	Plots of Relative Rate against Nitric Oxide Pressure (Propionaldehyde Decomposition).	138
36.	Effect of Nitric Oxide Pressure on the Order of Reaction with respect to Propionaldehyde.	139
37.	Plot of $\log v$ against $\log P_{\text{C}_2\text{H}_5\text{CHO}}$ with 60 mm of Nitric Oxide.	140
38.	Log Relative Rate against Log Pressure of Nitric Oxide.	142
39.	Plot of $v/P_{\text{C}_2\text{H}_5\text{CHO}}$ against $P_{\text{C}_2\text{H}_5\text{CHO}}^{1/2}$ with 60 mm of Nitric Oxide.	
40.	Arrhenius Plots for the Propionaldehyde Decomposition Catalysed by Nitric Oxide.	145

- xiii -

LIST OF PLATES

Plate No.

Page No.

1. View of the Apparatus

52

ABSTRACT

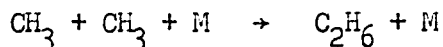
Theoretical Aspects of Atom and Radical Combination Reaction

Atom and free radical combinations in the gas phase are considered on the basis of (i) the energy transfer mechanism, in which the two atoms or radicals form a complex which is deactivated by a collision with a foreign molecule; (ii) the radical molecule complex mechanism, in which the atom or radical forms a complex with the foreign molecule; this complex is deactivated by collisions and finally undergoes a reaction with a second atom or free radical. Estimates are made of the binding energies between iodine atoms and various chaperon molecules, dispersion forces and charge transfer being taken into account. Calculations are made of the rates of iodine atom combinations in the presence of a variety of chaperons. For certain simple molecules, including the inert gases, there is little binding due to either charge transfer or to the quantum-mechanical dispersion forces. The binding energies for these molecules are less than the average thermal energy; the complexes therefore cannot be deactivated, and can play no role in atom combinations. For these systems, the energy transfer mechanism gives good agreement between theory and experiment. With n-butane, benzene and molecular iodine as chaperons, on the other hand, the rates are higher than can be explained on the basis of energy transfer; complex formation, involving dispersion forces and charge transfer, therefore plays a role in the reactions.

The Kinetics of the Dissociation of Ethane and the Combination of Methyl

Radicals

The evidence is reviewed with regard to the mechanisms of the ethane and acetaldehyde pyrolyses, and of related processes. It is shown that the acetaldehyde results cannot be interpreted except in terms of the hypothesis that the main chain ending step is



in its third order region. An analysis is made of the results on the photolysis of acetaldehyde and acetone, and these are also shown to lead to the conclusion that the reaction is third order. This being so, the initiation reaction in the ethane decomposition must be  $\text{C}_2\text{H}_6 \rightarrow 2 \text{CH}_3$  in its second order region, and termination must be  $2 \text{C}_2\text{H}_5 \rightarrow \text{C}_4\text{H}_{10}$  or  $\text{C}_2\text{H}_6 + \text{C}_2\text{H}_4$  (the Kùchler-Theile mechanism). Quinn's result that the initial rate of methane production in the ethane decomposition is first-order is interpreted in terms of the fact that methane is formed largely by the process  $\text{C}_2\text{H}_6 \rightarrow \text{CH}_4 + \text{CH}_2$  and only to a minor extent from methyl radicals.

The Uninhibited Decomposition of Acetaldehyde

The kinetics of the uninhibited decomposition of acetaldehyde have been re-examined. The initial rates of the decomposition of pure acetaldehyde show strict three-halves order dependence at temperatures from 480° to 525°C, and the activation energy is 47.6 kcal. per mole. Foreign gases, which de-

crease the rate of reaction, cause a significant increase in order. The rate of ethane formation is second order in acetaldehyde, and Trenwith has found the hydrogen formation to be second-order in acetaldehyde. The results are shown to be consistent only with a mechanism involving second-order initiation, and the third-order reaction  $2 \text{CH}_3 + \text{M} \rightarrow \text{C}_2\text{H}_6 + \text{M}$  as the terminating step. The rate of the initiation process is only slightly affected by the addition of inert foreign gases; it is suggested that the initial process may be  $\text{CH}_3\text{CHO} + \text{CH}_3\text{CHO} \rightarrow \text{CH}_3\text{CHOH} + \text{CH}_3\text{CO}$ , with a subsequent breakdown of  $\text{CH}_3\text{CHOH}$  into  $\text{CH}_3\text{CHO} + \text{H}$ . The mechanism is shown to account for the over-all kinetic behaviour and for the formation of the minor products.

#### The Decomposition of Acetaldehyde in the Presence of Nitric Oxide

The decomposition of acetaldehyde has been reinvestigated in the presence of various amounts of nitric oxide, and over a range temperatures (495 to 525°C) and acetaldehyde pressures (36 to 240 mm Hg). At higher acetaldehyde pressures there is no inhibition, the rate steadily increasing with increasing nitric oxide concentration; at low acetaldehyde concentrations increasing amounts of nitric oxide first give inhibition and then give catalysis. The degree of inhibition increases with decrease in temperature. As the nitric oxide concentration is increased the order rises above 3/2 and then falls to 3/2 again. At higher nitric oxide concentrations the rate varies with  $[\text{CH}_3\text{CHO}]^{3/2} [\text{NO}]^{1/2}$ . All of the facts are explained by a mechanism according to which initiation occurs by  $\text{CH}_3\text{CHO} + \text{NO} \rightarrow \text{CH}_3\text{CO} + \text{HNO}$  together with the processes occurring in the

absence of nitric oxide (cf. Part 3). Termination is considered to involve the reaction occurring in the case of no inhibition ( $\text{CH}_3 + \text{CH}_3 + \text{X} \rightarrow \text{C}_2\text{H}_6 + \text{X}$ ) together with  $\text{CH}_3 + \text{CH}_3\text{NO} \rightarrow \text{C}_2\text{H}_6 + \text{NO}$  and  $2 \text{CH}_3\text{NO} \rightarrow \text{C}_2\text{H}_6 + 2 \text{NO}$ . Application of the mechanism to the results is discussed in details.

#### The Uninhibited Decomposition of Propionaldehyde

The propionaldehyde decomposition was studied in the temperature range 520 - 560°C and from pressures from 21 to 362 mm Hg. The reaction was followed by pressure change as well as by gas chromatography. The overall order was found to be between 1.25 and 1.30 over the whole range of temperatures and pressures studied. Inert gases have no effect on the rates of formation of the products of reaction. The results are consistent with a mechanism consisting of first-order initiation,  $\text{C}_2\text{H}_5\text{CHO} \rightarrow \text{C}_2\text{H}_5 + \text{CHO}$ , and second-order termination,  $\text{C}_2\text{H}_5 + \text{C}_2\text{H}_5 \rightarrow \text{C}_4\text{H}_{10}$  or  $\text{C}_2\text{H}_6 + \text{C}_2\text{H}_4$ . The overall rate can be expressed as

$$v = k [\text{C}_2\text{H}_5\text{CHO}]^{3/2} + k' [\text{C}_2\text{H}_5\text{CHO}]^{1/2}.$$

The molecular reaction,  $\text{C}_2\text{H}_5\text{CHO} \rightarrow \text{C}_2\text{H}_6 + \text{CO}$ , has been shown to be of minor importance. The reaction  $\text{C}_2\text{H}_5 \rightarrow \text{C}_2\text{H}_4 + \text{H}$ , was found to take place in its first-order high pressure region under the conditions of the present investigation.

The Decomposition of Propionaldehyde in the Presence of Nitric Oxide.

The decomposition of propionaldehyde in the presence of various amounts of nitric oxide has been studied in the temperature range 520 - 560°C and at propionaldehyde pressures from 30 to 292 mm Hg. The reaction was found to be inhibited by small amounts of nitric oxide. Higher pressures of nitric oxide show strong catalysis. The order of the maximally inhibited reaction is 1.5 and the degree of inhibition decreases with the increase of propionaldehyde pressure. In the catalytic region the order of the overall reaction is 1.25 with respect to propionaldehyde and the relative rate (the ratio of rates in the presence and absence of nitric oxide) is independent of propionaldehyde pressure. The overall rate in the catalytic region can be expressed as

$$v = 8.38 \times 10^{12} e^{-36800/RT} [C_2H_5CHO][NO] + 2.35 \times 10^{14} e^{-42300/RT} [C_2H_5CHO]^{3/2} [NO]^{1/2} \text{ sec.}^{-1}.$$

the unit of concentration being mole per cc. A mechanism in which nitric oxide initiates chains by the reaction,  $C_2H_5CHO + NO \rightarrow C_2H_5CO + HNO$ , propagates them by  $C_2H_5NO + C_2H_5CHO \rightarrow C_2H_6 + C_2H_5CO + NO$  and terminates them by  $C_2H_5 + C_2H_5NO \rightarrow C_4H_{10} + NO$  or  $C_2H_6 + C_2H_4 + NO$  and  $C_2H_5NO + C_2H_5NO \rightarrow C_4H_{10} + 2 NO$  or  $C_2H_6 + C_2H_4 + 2 NO$  has been proposed. The proposed mechanism is found to be entirely consistent with the results.

PART I

THEORETICAL ASPECTS OF ATOM AND RADICAL COMBINATION

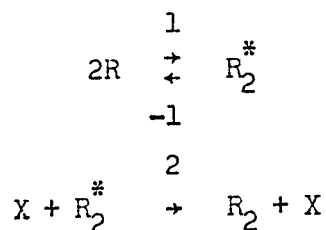
REACTIONS

INTRODUCTION

Recently there has been interest, experimentally (1-11) and theoretically (7, 12-22) in the gas-phase combinations of atoms and free radicals in the presence of foreign gases. Third-order rate constants have been obtained for the combinations of hydrogen (2), and iodine (3-9) atoms and of methyl (10, 11) and other radicals. Many of the reactions have small negative activation energies. The third-order rate constants for atom combination reactions fall into two classes: with the inert gases and certain simple molecules (such as hydrogen) the values at ordinary temperatures are about  $3 \times 10^9 \text{ l.}^2 \text{ mole}^{-2} \text{ sec}^{-1}$ , while with more complex molecules much higher rates are observed.

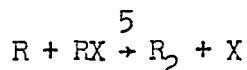
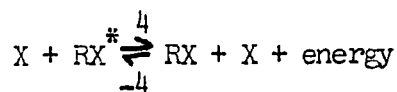
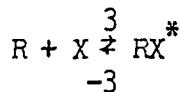
Various theoretical treatments (7, 12-22) have been put forward; these comprise two main classes.

(i) ENERGY-TRANSFER (ET) mechanisms, which may be formulated as



where R is the atom or radical and X the foreign molecule.

(ii) RADICAL-MOLECULE COMPLEX (RMC) mechanisms, formulated as



When R is a free radical, the life-time of  $R_2^*$  is usually sufficiently long for the ET mechanism to be the more important. Also atom combinations in the presence of polyatomic and particularly of chemically reactive, foreign molecules, occur largely by the RMC mechanism, the reason being that  $RX^*$ , because of its complexity, has a long life and is readily deactivated to give the more stable species RX which brings about the combination process. The greater the energy released in the conversion of  $RX^*$  into RX the greater the rate constant for the combination process; support for this has been obtained experimentally.

The situation is not, however, so clear-cut for the combinations of atoms in the presence of simple foreign molecules, such as inert gases, hydrogen and oxygen. Neither mechanism is now particularly favoured; the  $R_2^*$  complex is of very short life ( $10^{-13}$  sec), as also will be the complexes  $RX^*$  and RX in view of the very low binding energies. This question of the binding between R and X and of the possible energy levels of the complex RX, is important in deciding

whether the RMC mechanism plays a role in these reactions. This question is examined theoretically in the present paper.

Porter (17) believes that the RMC mechanism is the important one in all atom combination reactions, but Laidler (18) has questioned whether the binding energy can be great enough when the foreign gas is inert and concluded that the energy-transfer mechanism applies in such cases. The calculations described below provide further evidence for this point of view.

#### FORMULATION OF THE RATE EQUATIONS

To an approximation equivalent to the Lindemann-Hinshelwood treatment of unimolecular reactions the rate equations for the two mechanisms for atom and free-radical combinations may be formulated as follows. Application of the steady-state treatment to the ET mechanism leads to a rate of disappearance of R,

$$v = \frac{2k_1k_2[R]^2[X]}{k_{-1} + k_2[X]} \quad (1)$$

At low [X], the region of special experimental interest,

$$v = 2K_1k_2[R]^2[X], \quad (2)$$

where  $K_1$  is the equilibrium constant for the formation of  $R_2^*$  from  $2R$  where\*

$$k_1 = \frac{f_{R_2^*}}{f_R^2} \left( \frac{\epsilon}{kT} \right)^{s-1} \frac{1}{(s-1)!} \quad (3)$$

The  $f$ 's are the conventional partition functions,  $\epsilon$  is the energy of  $R_2^*$  with respect to the ground vibrational state of  $R_2$ , and  $s$  is the number of effective normal modes between which flow can occur. The statistical factor  $(\epsilon/kT)^{s-1}/(s-1)!$  takes account of the fact that the energy  $\epsilon$  is distributed between  $s$  modes; no exponential term enters into eqn. (3), since no energy is released in the process. The third-order

\* The question arises as to the precise definition of the excited species  $R_2^*$ . When  $R$  is a radical, the species  $R_2^*$  has a lifetime that is much longer than a vibrational frequency, and  $R_2^*$  is sharply distinguished from  $R + R$ . When  $R$  is an atom, however, the two atoms simply approach and separate within the period of the first vibration. The conventional statistical-mechanical treatment that is employed here regards the bound state of  $R_2$  as a species undergoing a purely harmonic oscillation, and the excited species  $R_2^*$  as a vibrationally-excited state of the harmonic oscillator. The average internuclear separation, the one used in the calculations of partition functions, is that corresponding to the minimum in the potential-energy curve. This point of view is roughly equivalent to defining the species  $R_2^*$  as one having an internuclear separation equal to or less than that corresponding to the rotational-energy barrier.

combination constant can thus be written as

$$k_{e.t.}^{111} = 2k_2 \frac{f_{R_2}^*}{f_R^2} \left( \frac{\epsilon}{kT} \right)^{s-1} \frac{1}{(s-1)!} \quad (4)$$

The rate constant  $k_2$  is usually identified with the collision number. Reaction is favoured by large values of  $\epsilon$  and  $s$  and undoubtedly most radical combinations occur by this mechanism. For atom combinations, where  $s$  is unity, the rate constant reduces to  $2k_2 f_{R_2} / f_R^2$ , which is usually about  $10^9$  to  $10^{10}$  l.<sup>2</sup> mole<sup>-2</sup> sec<sup>-1</sup>. This mechanism is then not particularly favoured, but reactions will occur largely by this mechanism if the alternative one is difficult.

A similar application of the steady-state method to the RMC mechanism leads to

$$v = \frac{2k_3 k_4 k_5 [R]^2 [X]^2}{k_{-3} k_{-4} [X] + k_{-3} k_5 [R] + k_4 k_5 [R] [X]} \quad (5)$$

Under most conditions,  $[R]$  is sufficiently small so that

$$v = 2k_5 K_3 K_4 [R]^2 [X], \quad (6)$$

where  $K_3$  and  $K_4$  are the equilibrium constants. According to this mechanism the reaction does not become second order at high pressures of  $X$ . The equilibrium constant  $K_3$  can be written as

$$K_3 = \frac{f_{RX}}{f_R f_X} \left( \frac{\epsilon^*}{kT} \right)^{s'-1} \frac{1}{(s'-1)!} \quad (7)$$

where the f's are the ordinary partition functions,  $\epsilon^*$  is the energy of  $RX^*$  with respect to the zero-point level of RX, and  $s'$  is the number of effective degrees of freedom in the complex RX. The factor  $(\epsilon^*/kT)^{s'-1}/(s'-1)!$  takes account of the flow of energy  $\epsilon^*$  between the  $s'$  modes.

The equilibrium constant  $K_4$  is expressed as

$$K_4 = \frac{\exp(\epsilon^*/kT)(s'-1)!}{(\epsilon^*/kT)^{s'-1}} \quad (8)$$

The factor  $\exp(\epsilon^*/kT)$  takes account of the loss of energy  $\epsilon^*$  in the process, the partition functions otherwise remaining the same. The factor  $(s'-1)/(\epsilon^*/kT)^{s'-1}$  is introduced because, whereas in  $RX^*$  the energy  $\epsilon^*$  flows between  $s'$  normal modes, it does not in RX.

The third-order combination rate constant therefore becomes

$$k_c^{111} = 2k_5 \frac{f_{RX}}{f_R f_X} \exp\left(\frac{\epsilon^*}{kT}\right) \quad (9)$$

This mechanism is therefore favoured when  $\epsilon^*$  is large. The number  $s'$  of effective degrees of freedom does not enter into the final rate expression; the mechanism is thus favoured not by the complexity of the chaperon molecule but by its ability to form a complex with R.

BINDING ENERGIES

The magnitude of the energy  $\epsilon^*$  is now considered. Three types of binding may be involved, namely: (i) binding due to dispersion forces, (ii) binding due to charge transfer, (iii) binding due to covalent forces.

DISPERSION FORCES

These energies have been calculated using the usual combining rules

$$\epsilon_{RX}^i = (\epsilon_{RR}^i \epsilon_{XX}^i)^{1/2} \quad (10)$$

$$\sigma_{RX} = \frac{1}{2}(\sigma_{RR} + \sigma_{XX}) \quad (11)$$

where the  $\epsilon$ 's are the appropriate binding energies (with respect to the minimum energy) and the  $\sigma$ 's are the collision diameters. Values of  $\epsilon_{RR}^i$  and  $\epsilon_{XX}^i$  for non-polar molecules can be calculated with reasonable accuracy using either the Lennard-Jones 12-6 potential

$$\epsilon(r) = 4\epsilon^i \left[ \left( \frac{\sigma}{r} \right)^{12} - \left( \frac{\sigma}{r} \right)^6 \right] \quad (12)$$

or the exp-6 potential

$$\epsilon(r) = \frac{\epsilon'}{1 - (6/\alpha)} \left[ \frac{6}{\alpha} \exp\left\{ \alpha \left( 1 - \frac{r}{r_m} \right) \right\} - \left( \frac{r_m}{r} \right)^6 \right] \quad (13)$$

where  $r$  is the distance between the atoms. The attractive terms have been calculated using a modification of the Slater-Kirkwood formula (23) which gives for the value of  $B$  in the  $B/r^6$  term the expression

$$B = 3eh\alpha^{\frac{3}{2}} N^{\frac{1}{2}} / 4m^{\frac{1}{2}} \quad (14)$$

Here  $e$  is the electronic charge,  $h$  is Planck's constant divided by  $2\pi$ ,  $\alpha$  is the polarizability of the atom and  $m$  the electronic mass. In the original Slater-Kirkwood formula  $N$  is the number of outer-shell electrons, but Pitzer (24) has shown that the value should be larger than this; for Xe, using the Lennard-Jones potential, the value is calculated to be 32 and following Peterson and Pitzer (25) the value for the iodine atom has been taken as 31.

The polarizability and van der Waals diameter for the iodine atom have been taken from Ketelaar (26); the I...I binding energy, due to dispersion forces, was then calculated to be  $31.9 \times 10^{-15}$  ergs, and the equilibrium separation  $4.83 \text{ \AA}$ . The  $\epsilon_{XX}$  and  $\sigma_X$  values were taken from Hirschfelder, Curtiss and Bird (27); the values used were those obtained from second virial coefficients, except for  $I_2$  and benzene for which the viscosity data were employed. The second column of Table 1 includes  $\epsilon'_{RX}$  values, for  $R$  equal to iodine, for a number of foreign molecules  $X$ , using the combining rule. For  $ArI$ ,

Table 1

BINDING ENERGIES AND OTHER PROPERTIES OF COMPLEXES (DISPERSION FORCES)

Chaperon	binding energy $\epsilon'$ (ergs $\times 10^5$ )	equilibrium separation $r$ (cm $\times 10^8$ )	morse constant ( $\text{cm}^{-1} \times 10^{-8}$ )	zero-point energy $\epsilon_0$ (ergs $\times 10^{15}$ )	$\epsilon^*$ ( $= \epsilon' - \epsilon_0$ ) (ergs $\times 10^{15}$ )
He	6.7	3.85	1.56	3.2	3.5
Ar	23.0	4.32	1.39	2.2	20.8
	22.2 <sup>a</sup>	--	--	2.2	20.0
	19.6 <sup>b</sup>	--	--	2.2	17.4
H <sub>2</sub>	12.7	4.09	1.47	5.9	6.8
O <sub>2</sub>	22.7	4.42	1.36	2.3	20.4
CO <sub>2</sub>	28.8	4.93	1.22	2.0	26.8
n-C <sub>4</sub> H <sub>10</sub>	36.1	5.20	1.15	1.98	39.12
C <sub>6</sub> H <sub>6</sub>	44.0	5.37	1.12	1.9	44.1
I <sub>2</sub>	49.2	5.21	1.15	1.6	47.6

<sup>a</sup>calculated directly using the 12-6 potential; <sup>b</sup>calculated using the exp-6 potential

All other values were calculated using the combining rule.

calculations have also been made using the 12-6 potential directly and using the exp-6 potential. The agreement is satisfactory. Table 1 also gives the values of  $r_e$ , the equilibrium separation, calculated on the basis of the Lennard-Jones potential using the relationship

$$r_e = (2^{1/6}/2)(\sigma_I + \sigma_X). \quad (15)$$

The  $\sigma_X$  values were taken from Hirschfelder, Curtiss and Bird (27).

The Lennard-Jones 6-12 potential is equivalent to the Morse equation

$$\epsilon(r) = \epsilon'(1 - \exp[-a(r - r_e)])^2 \quad (16)$$

where  $a = 6/r_e$ . The equilibrium frequency  $\nu_e$  is given by

$$\nu_e = \frac{a}{\pi} \left( \frac{\epsilon'}{2\mu} \right)^{1/2} \quad (17)$$

where  $\mu$  is the reduced mass. The heights  $\epsilon_0$  of the zero-point levels with respect to the minimum in the curve were calculated using the expression

$$\epsilon_0 = hcw_e \left( v + \frac{1}{2} \right) - hcw_e x \left( v + \frac{1}{2} \right)^2$$

with  $v = 0$ ;  $h$  is Planck's constant,  $c$  the velocity of light and  $x = w_e/4D$ , where  $D$  is the binding energy in wave numbers. The values obtained, together with  $\epsilon^* = \epsilon' - \epsilon_0$ , which is the dissociation

energy with respect to the zero-point level, are included in Table 1.

CHARGE TRANSFER

The wave function for a charge-transfer complex is (28)

$$\psi = a\psi_0 + b\psi_1 \quad (19)$$

where  $\psi_0$  is a no-bond wave function and  $\psi_1$  is a wave function for the complex in which an electron has been transferred. The corresponding binding energy is

$$W = -(H_{01} - SW_0)^2 / (W_1 - W_0) \quad (20)$$

where

$$\begin{aligned} H_{01} &= \int \psi_0 H \psi_1 d\tau, & S &= \int \psi_0 \psi_1 d\tau, \\ W_1 &= \int \psi_1 H \psi_1 d\tau, & W_0 &= \int \psi_0 H \psi_0 d\tau \end{aligned}$$

To a good approximation S can be neglected and according to Hastings, Franklin, Schiller and Matsen (27) W can be expressed as

$$W = - \frac{\beta^2}{I_B - E_A - (e^2/r) + C'} \quad (21)$$

where  $\beta$  is the resonance integral  $H_{01}$  (approximately constant),  $I_B$

is the ionization potential of the electron donor,  $E_A$  is the electron affinity of the acceptor,  $e^2/r$  is the coulomb energy corresponding to a separation  $r$ , and  $C$  is a small energy term arising from repulsion, etc. We have estimated  $\beta$  by using the experimental binding energies (26) for a number of molecular iodine complexes;  $r$  was taken as  $3.4 \text{ \AA}$  and  $E_A$  as 1.8 eV, following Mulliken (28) and a value of zero was taken for  $C$ ;  $W$  is then given by

$$W = -\beta^2 / (I_B - 6.03) \quad (22)$$

a relationship similar to one employed by Hastings et al. (29). Values of  $\beta$  are shown in Table 2; as expected, they are approximately constant, and the average value of 0.444 eV has been used in subsequent calculations. The small variations of the transition energies (30) for benzene complexes with different acceptor molecules (probably having similar electron affinities) also indicate the approximate constancy of  $\beta$ .

The charge-transfer energies for the atomic iodine-chaperon complexes have therefore been calculated from

$$W = \frac{3.15 \times 10^{-13}}{I_x - E_I - (e^2/r)} \quad (23)$$

with  $E_I$  taken as 3.24 eV (31) and  $I_x$  taken from various sources (29, 31-34). There is no direct information about  $r$ ; Mulliken's value of  $3.4 \text{ \AA}$ , which is slightly less than the collision diameters,

Table 2

RESONANCE INTEGRAL  $\beta$ , ESTIMATED FROM EXPERIMENTAL DATA

<u>complex</u>	<u><math>I_B</math> (eV)</u>	<u><math>\beta</math> (eV)</u>
benzene-iodine	9.247 (34)	0.424
toluene-iodine	8.82 (29)	0.465
xylylene-iodine	8.53 (29)	0.465
naphthalene-iodine	8.26 (36)	0.417

has been used. The observed stabilities of the various organic compounds containing  $\pi$  bonds with different bond lengths can be well correlated by means of a single value of  $\beta$  calculated from the observed resonance energy of benzene.

The results of the calculations are given in Table 3. The values, which in view of the approximations are upper limits, are somewhat larger than those arising from dispersion forces, especially for  $O_2$ ,  $CO_2$ ,  $n-C_4H_{10}$ ,  $C_6H_6$  and  $I_2$ .

#### SIGNIFICANCE OF THE BINDING ENERGIES

For He, Ar and  $H_2$  the  $\epsilon^*$  values, arising from both dispersion forces and charge transfer, are so small that no true binding can be said to occur. This is illustrated in Fig. 1 for ArI, for which  $\epsilon^*$  arising from dispersion forces is considerably less than  $kT$  ( $= 41.4 \times 10^{-15}$  ergs) at  $300^\circ K$ . At this temperature there will therefore be no binding when an argon atom and an iodine atom come together; the majority of such systems will at once dissociate. With  $n-C_4H_{10}$ ,  $C_6H_6$  and  $I_2$ , on the other hand, the binding energies are greater than  $kT$  and true binding occurs.

#### RATE CONSTANT CALCULATIONS

Experimental values of third-order rate constants, taken from Porter (17) are shown in column 2 of Table 4. The results of

Table 3

BINDING ENERGIES DUE TO CHARGE-TRANSFER

<u>chaperon</u>	<u>I<sub>x</sub> (eV)</u>	<u>binding energy ε'</u> <u>(ergs x 10<sup>15</sup>)</u>	<u>ε* (ergs x 10<sup>15</sup>)</u>
He	24.580 (31)	18.4	12.7
Ar	15.755 (31)	38.2	35.4
H <sub>2</sub>	15.6 (32)	38.7	27.7
O <sub>2</sub>	12.5 (32)	62.7	59.4
CO <sub>2</sub>	14.4 (32)	45.4	42.8
n-C <sub>4</sub> H <sub>10</sub>	10.63 (33)	99.8	96.5
C <sub>6</sub> H <sub>6</sub>	9.247 (34)	177.1	173.2
I <sub>2</sub>	9.7 (32)	141.4	138.7

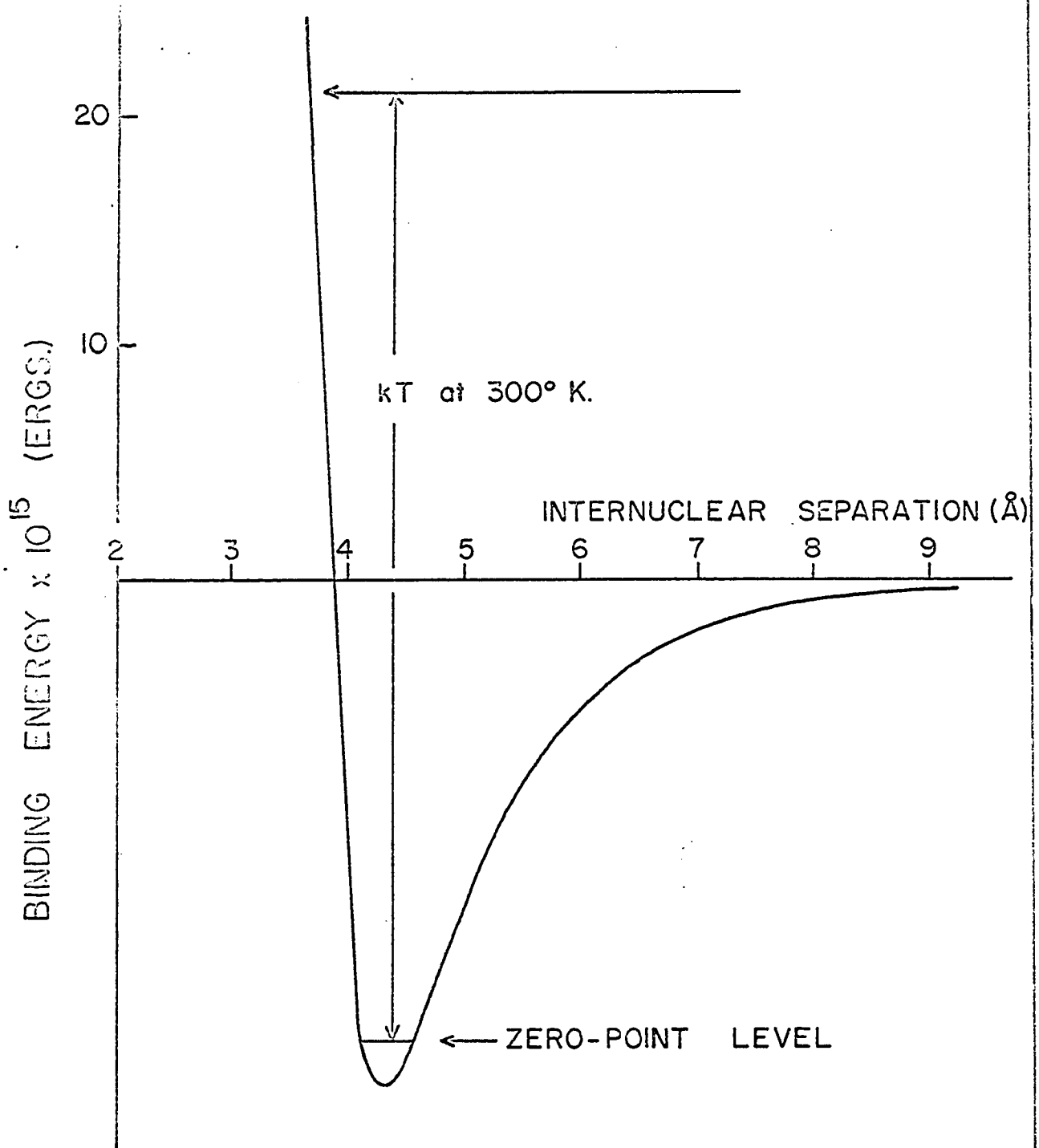


Figure 1. Plot of binding energy, due to dispersion forces, against the internuclear separation for the system Ar...I.

Table 4

OBSERVED AND CALCULATED RATE CONSTANTS FOR IODINE ATOM COMBINATIONS

rate constant x  $10^{32}$  (27°C)(cm<sup>6</sup> molecule<sup>-2</sup> sec<sup>-1</sup>)

<u>chaperon</u>	<u>RMC mechanism</u>			
	<u>expt. energy transfer mechanisms</u>		<u>dispersion</u>	<u>charge transfer</u>
He	0.42 <sup>*</sup>	2.9	(23)	(18)
Ar	0.83	1.2	(24)	(27)
H <sub>2</sub>	1.57	4.4	(23)	(25)
O <sub>2</sub>	1.87	1.3	(26)	(42)
CO <sub>2</sub>	3.7	1.3	(38)	(43)
n-C <sub>4</sub> H <sub>10</sub>	9.9	1.2	47	130
C <sub>6</sub> H <sub>6</sub>	25	1.2	56	660
I <sub>2</sub>	440	0.8	48	260

\* This value for helium is doubtful experimentally, and difficult to explain theoretically since He should be much more effective than argon. Hilferding and Steiner (2) found that He was four times as effective as Ar in bringing about the combination of bromine atoms.

rate calculations on the basis of the ET mechanism are shown in column 3. These calculations, based on eqn. (4) involve some uncertainty as to the statistical factor. Of the 16 possible states arising from two  $^2P_{3/2}$  iodine atoms, eight are attractive (35). Any one of these attractive steps can lead to combination by transfer of energy on collision with a foreign molecule, and the statistical factor is therefore taken as  $\frac{1}{2}$ . The rate constant  $k_2$  has been taken to be the collision number, with a collision diameter equal to the van der Waals diameter of an iodine atom plus half the diameter of X; this may be slightly too large, since the effective radius of the iodine molecule may be somewhat less than the diameter of the atom.

In making calculations based on the RMC mechanism (eqn.(9)) the collision diameter was taken to be the van der Waals diameter for an iodine atom, and the  $\epsilon^*$  values obtained above were employed. When the  $\epsilon^*$  values are less than  $kT$  they are of no significance from the present point of view; the corresponding rates are given in brackets in Table 4.

#### DISCUSSION

In view of the assumptions and approximations made in the calculations the rate constants in column 3 of Table 2, for He, Ar,  $H_2$ ,  $O_2$  and  $CO_2$ , agree satisfactorily with the experimental values. The RMC mechanism is not required to explain the rates.

With  $n-C_4H_{10}$ ,  $C_6H_6$  and  $I_2$ , on the other hand, the experimental rates are much greater than those calculated on the basis of energy

transfer, and the results must be explained in terms of an atom-molecule complex. For  $n\text{-C}_4\text{H}_{10}$  and  $\text{C}_6\text{H}_6$  the rates calculated for the RMC mechanism, for both types of binding, are appreciably higher than the experimental rates. If this difference is significant, reaction may occur by a combination of the two mechanisms, i.e. the ternary complex  $\text{X}\cdots\text{I}\cdots\text{I}$  can be formed in two different ways, either via  $\text{X} + \text{I}\cdots\text{I}$  or via  $\text{X}\cdots\text{I} + \text{I}$ . The generalized computational treatment of Keck (12, 16) is, in fact, equivalent to a combination of the two mechanisms.

With  $\text{I}_2$  as chaperon the observed rate is much larger than that calculated on the basis of either mechanism. The complexing is evidently much stronger than can be interpreted on the basis of dispersion forces and charge-transfer, and covalent bonding is involved.

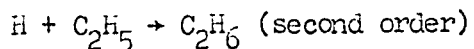
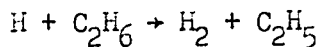
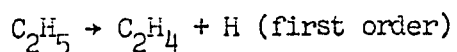
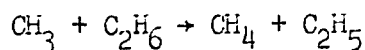
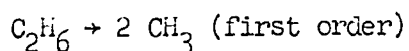
Part II

The Kinetics of the Dissociation of Ethane and  
the Combination of Methyl Radicals

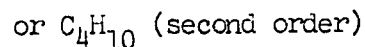
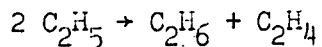
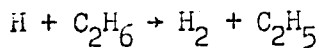
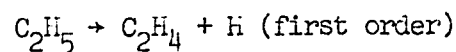
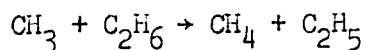
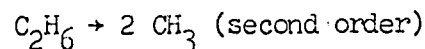
INTRODUCTION

The two chemical mechanisms for the ethane decomposition are as follows:

Rice - Herzfeld (37)



Küchler - Theile (38)



In the terminology of Laidler, Sagert and Wojciechowski (39) the Rice-Herzfeld mechanism is of the  $^1\beta_{u_1}$  type, and the Küchler-Theile mechanism is of the  $^2_{uu_1}$  type. Both correspond to first-order over-all kinetics, in agreement with experiment under the usual conditions (temperatures from 550 - 650°C, pressures from 20 mm to atmospheric).

In a recent experimental and theoretical investigation of the whole problem Laidler and Wojciechowski (40) have concluded that the K $\ddot{u}$ chler-Theile mechanism is the correct one. Their main arguments may be summarized as follows:

1) From the results of Dodd and Steacie (10), and of other investigators to be referred to later, at 200°C the methyl radical recombination is third-order at 1 mm pressure and probably at considerably higher pressures. The theories of unimolecular reactions predict that the transition pressure varies with the  $(s-1)/2$  th power of the temperature, where  $s$ , the number of effective degrees of freedom, is probably about 9. It follows that at the temperatures of the pyrolysis experiments the combination is third-order over the usual pressure range. By the principle of microscopic reversibility the dissociation  $C_2H_6 \rightarrow 2 CH_3$  must be second order.

2) Calculations of the concentrations of H and  $C_2H_5$  show that in the higher pressure range the reaction  $H + C_2H_5 \rightarrow C_2H_6$  will be much less important than  $2 C_2H_5 \rightarrow C_4H_{10}$  or  $C_2H_6 + C_2H_4$ .

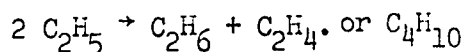
3) The experimental activation energy for the reaction could easily be reconciled with the K $\ddot{u}$ chler-Theile mechanism, but not with the Rice-Herzfeld mechanism.

4) Inert gases increase the rate, a result that is attributed to their effect on the ethane dissociation. This result is, however, capable of the alternative explanation that the effect of inert gases is on the reaction  $C_2H_5 \rightarrow C_2H_4 + H$ .

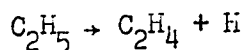
5) It is predicted that at low pressures the K $\ddot{u}$ chler-Theile  ${}^2_{uu_1}$  mechanism will become  ${}^2_{su_{3/2}}$ , so that a transition to three-halves order is to be expected. Such a transition was actually found, at

approximately the predicted pressure. No such transition is expected on the basis of the Rice-Herzfeld mechanism.

More recently Quinn (41, 42) has made a study of the kinetics of formation of the minor product methane in the ethane decomposition, and finds that the initial rate of formation is proportional to the first power of the ethane pressure. This he takes to indicate that the ethane dissociation is first order, since he assumes that the methane is initially formed largely from the methyl radicals. Quinn accepts the argument that the higher concentration of ethyl radicals requires the main chain-ending step to be



In order to explain the first-order over-all kinetics he concludes that the process



is in the pressure region in which the rate is roughly proportional to the square root of the ethane pressure (i.e., the  $\text{C}_2\text{H}_5$  radical is half way between a  $\beta$  radical and a  $\mu$  radical). This mechanism also satisfactorily explains the inert-gas effect (as an effect on  $\text{C}_2\text{H}_5 \rightarrow \text{C}_2\text{H}_4 + \text{H}$ ). It also explains the increase in order at lower pressures (since the radicals will gain more  $\beta$  character as the pressure is lowered); however the predicted change of order, in terms of this mechanism, is nothing like as sharp as found by Laidler and Wojciechowski and as predicted by the  ${}^2\mu\mu_1$  mechanism.

Quinn's mechanism also leads to a quantitative interpretation of the overall reaction, in terms of the elementary steps, which is at least as satisfactory as that of Laidler and Wojciechowski.

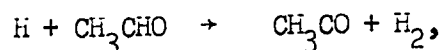
At first sight Quinn's results on the rate of methane production seem to lead unequivocally to the mechanism he proposes, involving first-order initiation. Certain results on the acetaldehyde decomposition obtained by Brill, Goldfinger, Letort, Mattys, and Niclause (43), and also more recently by Trenwith (44) and in these laboratories (see following part) lead, on the other hand, to the equally strong conclusion that the methyl radical combination must be in its third-order region, and that the ethane dissociation is therefore in its second-order regions. These results will now be outlined and discussed briefly, after which other evidence will be adduced. In a final section an alternative explanation will be given of Quinn's results, the conclusion being drawn that the K $\ddot{u}$ chler-Theile mechanism is after all the correct one.

#### THE PYROLYSIS OF ACETALDEHYDE

The important result obtained by Brill, et al. (43), and confirmed in more detail in these laboratories (see following part), is that the rate of the acetaldehyde decomposition is strongly decreased by adding inert gases. Such a result can only be explained if the inert gases aid the chain-ending step. The main chain carriers are CH<sub>3</sub> and CH<sub>3</sub>CO, with the former in excess, so that the main chain-ending step is the methyl radical recombination. It therefore seems impossible to escape the conclusion that

inert gases have a strong effect on the rate of this reaction, which cannot therefore be in its high-pressure second-order region. The quantitative analysis of the results obtained in these laboratories, described in the preceding papers, seem to leave no alternative to the conclusion that the combination process is in the third-order region, and that the acetaldehyde dissociation is second-order. The temperatures used in the study of the acetaldehyde decomposition are somewhat lower than in the ethane decomposition, so that the ethane dissociation should be second-order a fortiori.

Trenwith (44) has studied the rate of hydrogen production in the acetaldehyde decomposition, and has found that it is proportional to the square of the acetaldehyde concentration. The main source of hydrogen is almost certainly hydrogen atoms, which produce  $H_2$  by



so that the hydrogen atoms must be produced by a second-order initiation process.

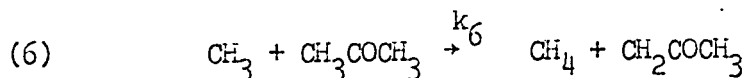
The same conclusion is to be drawn from the result, obtained in these laboratories (see following part ), that the initial rate of ethane production is proportional to the square of the acetaldehyde concentration. In the steady state the rate of production of methyl radicals is equal to the rate of their disappearance; it follows that the initiation reaction is second-order in acetaldehyde, and that the methyl radical combination is third-order.

These results on the kinetics of the formation of minor products in the ethane and acetaldehyde decompositions have thus, led, at first sight, to conflicting conclusions. In the next section we cite additional evidence supporting the view that the methyl radical combination is third-order under the usual conditions of pyrolysis experiments.

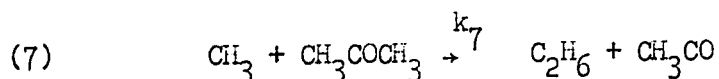
#### THE PHOTOLYSIS OF ACETONE

The work of Dodd and Steacie (10) and of Trotman-Dickenson and Steacie (45) on the photolysis of acetone at fairly low temperatures (<200°C) has indicated that the methyl radical recombination becomes third-order at pressures of a few millimeters. More positive evidence is provided by the work of Brinton (46) who has studied the acetone photolysis in a higher temperature range (200 - 475°C) and at pressures from 25 to 100 mm Hg. It will now be shown that Brinton's results leads to the conclusion that at the highest temperatures the methyl radical combination is a third-order reaction.

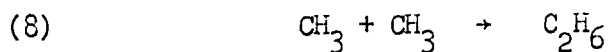
Methane is formed in the acetone photolysis by the reaction



Ethane might be formed by the second-order abstraction reaction



as well as by the combination of methyl radicals



The rates of methane and ethane formation are

$$v_{\text{CH}_4} = k_6 [\text{CH}_3] [\text{CH}_3\text{COCH}] \quad (24)$$

and

$$v_{\text{C}_2\text{H}_6} = k_7 [\text{CH}_3] [\text{CH}_3\text{COCH}_3] + k_8 [\text{CH}_3]^2 \quad (25)$$

The following special cases are of interest:

- 1) Ethane is mainly formed by reaction (7), in which case

$$\frac{v_{\text{CH}_4}}{v_{\text{C}_2\text{H}_6}} = \frac{k_1}{k_7} \quad (26)$$

- 2) Ethane is formed mainly by the methyl radical combination in its second-order region:

$$\frac{v_{\text{CH}_4}}{v_{\text{C}_2\text{H}_6}^{1/2} [\text{CH}_3\text{COCH}_3]} = \frac{k_1}{k_8^{1/2}} \quad (27)$$

- 3) Ethane is formed mainly by the methyl radical combination in its third-order region ( $k_8 = k_8' [\text{CH}_3\text{COCH}_3]$ ):

$$\frac{v_{\text{CH}_4}}{v_{\text{C}_2\text{H}_6}^{1/2} [\text{CH}_3\text{COCH}_3]^{1/2}} = \frac{k_6}{k_8^{1/2}} \quad (28)$$

Brinton's data are given, and analyzed from this point of view, in Table 5; they have been collected in such a way that the light intensity variation, as measured by the rate of carbon monoxide production, is at a minimum. It is clear that Case 1 can be excluded since  $v_{\text{CH}_4}/v_{\text{C}_2\text{H}_6}$  shows large variations. The ratio  $v_{\text{CH}_4}/v_{\text{C}_2\text{H}_6}^{1/2} [\text{CH}_3\text{COCH}_3]^{1/2}$  is seen to be approximately constant with respect to acetone pressure at 400 and 435°C: this suggests that Case 3 is applicable. At 305°C the ratio  $v_{\text{CH}_4}/v_{\text{C}_2\text{H}_6}^{1/2} [\text{CH}_3\text{COCH}_3]$  shows more constancy than  $v_{\text{CH}_4}/v_{\text{C}_2\text{H}_6}^{1/2} [\text{CH}_3\text{COCH}_3]^{1/2}$ , indicating that the third-body effect on the radical recombination is less important at this lower temperature.

At first sight the results therefore suggest that the methyl radical combination is largely third order at 400 and 435°C, but it might be argued that the situation is complicated by the simultaneous occurrence of reaction 7. If the radical combination were second-order and reactions 6, 7, and 8 are all taken into account

$$\frac{v_{\text{CH}_4}}{v_{\text{C}_2\text{H}_6}^{1/2} [\text{CH}_3\text{COCH}_3]} = \frac{k_6 [\text{CH}_3]}{(k_7 [\text{CH}_3] [\text{CH}_3\text{COCH}_3] + k_8 [\text{CH}_3]^2)^{1/2}} \quad (29)$$

Since  $E_6 = 9.1$  kcal. (10) and  $E_8 = 0$  a plot of  $\log v_{\text{CH}_4}/v_{\text{C}_2\text{H}_6}^{1/2} [\text{CH}_3\text{COCH}_3]$

Table 5

## RESULTS OF THE PHOTOLYSIS OF ACETONE

Temperature (°C)	$v_{CO} \times 10^{12}$ (mole $cc^{-1} sec^{-1}$ )	$[CH_3COCH_3] \times 10^6$ (mole $cc^{-1}$ )	$\frac{v_{CH_4}}{v_{C_2H_6}^{1/2} [CH_3COCH_3]}$ ( $cc^{1/2} mole^{-1/2} sec^{-1/2}$ )	$\frac{v_{CH_4}}{v_{C_2H_6}^{1/2} [CH_3COCH_3]^{3/2}} \times 10^3$ ( $sec^{-1/2}$ )	$\frac{v_{CH_4}}{v_{C_2H_6}}$
305	35.3	1.399	19.2	22.7	14.4
305	6.2	1.418	19.1	22.1	62.4
305	3.6	0.675	21.6	17.2	33.8
305	9.7	2.790	15.6	27.0	103.5
400	34.7	1.196	57.2	62.4	76.9
400	28.2	1.255	55.4	62.5	100.8
400	22.8	2.470	30.4	48.4	132.8
400	21.8	0.608	72.2	56.6	52.5
435	8.9	2.040	18.5	30.4	110.3
435	7.9	2.040	18.3	31.0	120.0
435	6.9	1.138	28.5	30.4	82.1
435	5.9	1.141	33.5	35.6	105.4
435	5.1	1.139	31.1	33.1	102.5

against  $1/T$  at constant acetone pressure and constant light intensity should bend downwards at higher temperatures (when  $k_7$  becomes more important). In fact, as shown in Figure 2, the curve actually bends upwards at higher temperatures; the activation energy increases from 10.0 kcal at lower temperatures (in good agreement with the above value for  $E_6$ ) and has become 14.6 kcal. at  $435^\circ\text{C}$ . This result can only be explained if reaction [7] is unimportant and if there is a negative activation energy associated with reaction (8). This negative activation energy is  $2(9.7 - 14.6) = -9.8$  kcal., in surprisingly good agreement with the value of -11.7 kcal estimated by Gill and Laidler (15) on the basis of a theoretical treatment of the third-order methyl radical combination.

The conclusion is therefore that Brinton's results show that the combination is largely third-order at the highest temperatures of the investigation, and cannot be reconciled with any other interpretations of the process.

#### THE PHOTOLYSIS OF ACETALDEHYDE

Experiments on the photolysis of acetaldehyde have been carried out in a lower temperature range ( $<340^\circ\text{C}$ ), and clear-cut evidence for third-order behaviour of the methyl radical recombination is therefore not expected. The results do, however, indicate distinct pressure dependence of the reaction, and are entirely consistent with the conclusions drawn above from the results of the acetone photolysis.

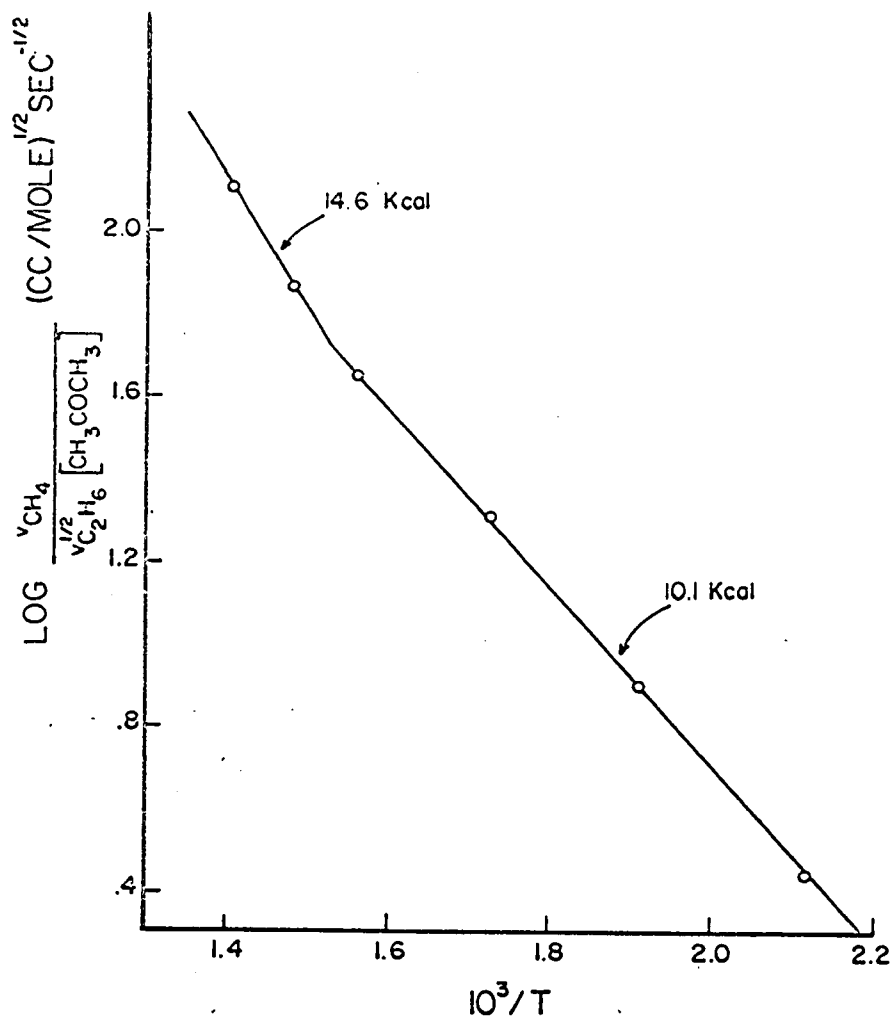
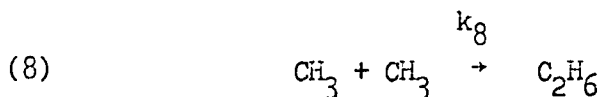
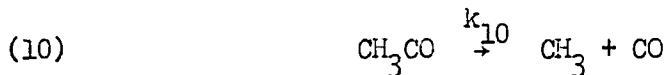
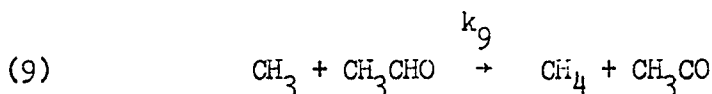
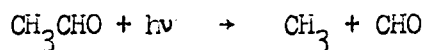


Figure 2. Plot of  $\log v_{\text{CH}_4} / v_{\text{C}_2\text{H}_6}^{1/2} [\text{CH}_3\text{COCH}_3]^{1/2}$  against  $1/T$  for the photolysis of acetone.

Danby, Buchanan and Henderson (47) studied the photolysis of acetaldehyde in the temperature range 212 - 340°C and pressure range 19 - 317 mm Hg. Analysis of their results at 300°C shows (Fig. 3) that  $v_{\text{CH}_4}/v_{\text{C}_2\text{H}_6}^{1/2}$  is proportional to  $[\text{CH}_3\text{CHO}]^{0.85}$ . The mechanism of the photolysis is



The steady-state treatment leads to the result that

$$\frac{v_{\text{CH}_4}}{v_{\text{C}_2\text{H}_6}^{1/2}} = \frac{k_9[\text{CH}_3\text{CHO}]}{k_8^{1/2}} \quad (30)$$

It therefore follows that  $k_8$  is proportional to  $[\text{CH}_3\text{CHO}]^{0.3}$  at this temperature; the recombination is therefore closer to second- than to third-order, but is well in the pressure-dependent region. This result is similar to that obtained in the acetone photolysis in the same temperature range.

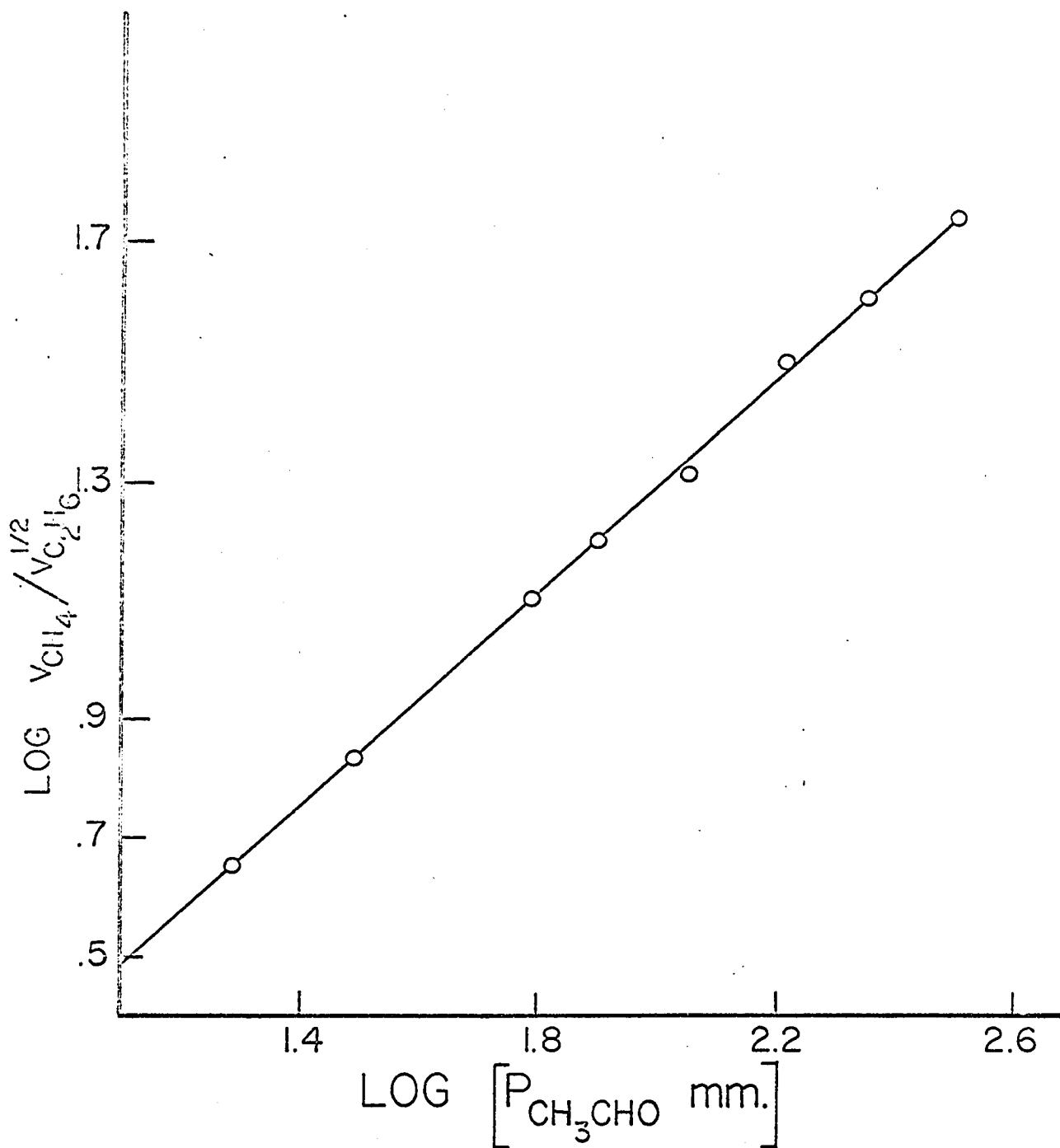


Figure 3. Plot of  $\log v_{\text{CH}_4} / v_{\text{C}_2\text{H}_6}^{1/2}$  against  $\log$  acetaldehyde pressure .  
for the photolysis of acetaldehyde at 300°C.

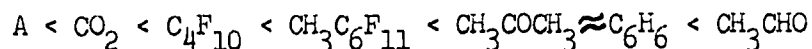
DIRECT STUDIES OF THE  
COMBINATION OF METHYL RADICALS

Ingold and Lossing (48) studied the combination of methyl radicals mass spectrometrically in the temperature range 161 - 814°C and at various pressures (4.8 - 18.5 mm) of helium, and found that the reaction was partly heterogenous and partly homogenous. The rate of the reaction decreased with the increase of temperature, and an activation energy of - 2.2 kcal. was obtained. In this investigation no effect of the carrier gas pressure was detected, but in a later investigation with an improved technique, Ingold, Henderson and Lossing (49) found that the rate of combination showed a linear dependence on the helium pressure at 1000°C in the pressure range 3.2 - 15.0 mm Hg. These facts were attributed to the third-order recombination of methyl radicals. The negative activation energy of 2.2 Kcal/mole is too low compared to that calculated following Gill and Laidler<sup>(15)</sup> but this is understandable in view of the significant surface combination they observed under their conditions at low total pressures.

Kistiakowsky and Roberts (50), in an investigation of the photolysis of acetone below 240°C, found that ethane formation is significantly pressure dependent below 10 mm of acetone pressure and that CO<sub>2</sub> is about twenty times less effective than acetone in bringing about the combination of methyl radicals.

Dodd and Steacie (10), studying the photo-decomposition of acetone below 250°C, concluded that the combination of methyl radicals was strongly dependent on the pressure of the third body below 20 mm

acetone pressure and that the following substances may be arranged in the increasing order of efficiency of energy transfer as shown below



The above mentioned relative efficiencies of different gases reported by Dodd and Steacie, and by Kistiakowski and Roberts must be accepted with reserve in view of the significant surface effect observed by Dodd and Steacie at low pressure and low temperature.

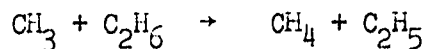
All of the above results are consistent with the conclusion that the methyl radical combination is not in its second-order region under the conditions of the experiments.

#### THE PYROLYSIS OF ETHANE

All of the above results point clearly to the conclusion that at pressures of a few hundred millimeters of mercury and at temperatures of 400°C and above the methyl radical recombination is essentially a third-order reaction. It is therefore necessary to reconsider Quinn's conclusion that it is a second-order reaction.

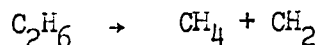
Quinn's conclusion is based on the result that the methane formation in this reaction is first-order in ethane, and involves the assumption that methane is produced solely by the processes





This assumption must be in error. In an earlier investigation Danby, Spall, Stubbs and Hinshelwood (51) also studied the rate of methane production in the ethane pyrolysis, and also noted that it was first-order in ethane. They obtained the significant result that the methane production was not inhibited by nitric oxide. This clearly eliminates the possibility that the main source of methane is abstraction by  $\text{CH}_3$ , since nitric oxide will certainly reduce markedly the concentration of methyl radicals.

In view of this it seems necessary to conclude with Danby et al (51) that methane production occurs by the reaction



This reaction, involving a much less symmetrical breakdown of the ethane molecule, may well be first order (52). The occurrence of this reaction provides an explanation for the hitherto unexplained result of Wall and Moore (53, 54) that in the pyrolysis of  $\text{C}_2\text{H}_6 - \text{C}_2\text{D}_6$  mixtures the product  $\text{CH}_2\text{D}_2$  was formed in much larger amounts than could be explained in terms of the conventional mechanism.

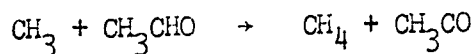
Further evidence against Quinn's mechanism for the ethane pyrolysis, and in favor of that of K $\ddot{u}$ chler and Theile, is provided by the result of K $\ddot{u}$ chler and Theile (38) that inert gases have hardly any effect on the rate of the decomposition of ethane maximally inhibited by

Part III

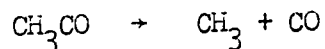
THE UNINHIBITED DECOMPOSITION OF ACETALDEHYDE

INTRODUCTION

Steacie (55) commented that "the acetaldehyde decomposition is remarkable for the lack of agreement on both mechanism and experimental fact, and for the complications involved". There is, however, general agreement that the chain propagating steps are



and



The nature of the chain initiating and terminating processes is, however, still a matter of great controversy.

Review of the Earlier Work

Hinshelwood and his co-workers (56-58), studying the thermal decomposition of acetaldehyde in the temperature range 490 - 570°C, found no evidence of any appreciable heterogeneous reaction. They suggested that different modes of activation within the molecule were involved.

Letort (59, 60) made an extensive study of this reaction and found that the reaction was completely homogeneous and that the over-all order was approximately three-halves. The rate constant can be expressed as

$$k_{3/2} = 2.4 \times 10^{12} e^{-\frac{46000}{RT}} \text{ cc}^{1/2} \text{ mole}^{-1/2} \text{ sec}^{-1}$$

Inert gases like carbon monoxide and methane were found to inhibit the reaction slightly.

From a study of this reaction, Boyer, Niclause and Letort (61) concluded that the reaction was of three-halves order and that the rate constant could be expressed as

$$k_{3/2} = 2.3 \times 10^{12} e^{-\frac{48000}{RT}} \text{ cc}^{1/2} \text{ mole}^{-1/2} \text{ sec}^{-1}$$

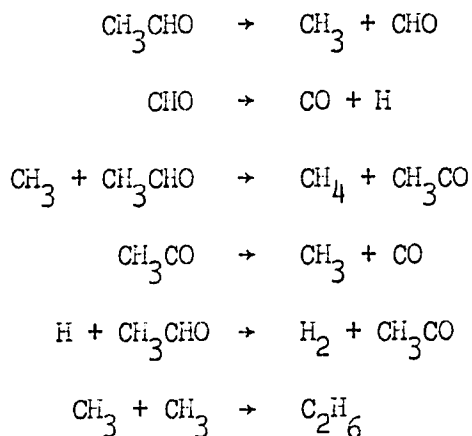
In 1958, Freeman, Danby, and Hinshelwood (62), reinvestigating this decomposition over the pressure range 21 - 1190 mm and temperature range 504 - 525°C, concluded that the over-all order was approximately three-halves. They also detected trace amounts of  $\text{C}_2\text{H}_6$ ,  $\text{H}_2$  and  $\text{C}_2\text{H}_4$  by mass spectrometry. It was suggested that both molecular and chain reactions were operative in the system. However, the suggestion that a molecular reaction was present was not based on firm grounds.

Imai, Yoshida and Toyama (63), studying at somewhat lower temperatures (380 - 460°C), found that the order of the reaction was three-halves and that the rate constant could be represented as

$$k_{3/2} = 1.2 \times 10^{12} e^{-\frac{43300}{RT}} \text{ cc}^{1/2} \text{ mole}^{-1/2} \text{ sec}^{-1}$$

The above activation energy is somewhat lower than that obtained by previous workers.

In all the above cases, attempts have been made to explain the results by using the following simple Rice-Herzfeld (37) mechanism:



As will be described later, the above simple mechanism is inconsistent with the results obtained in the presence of inert gases and with the recent work of Trenwith (44).

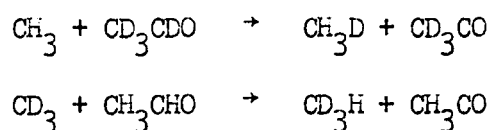
#### Evidence for Free Radicals

In 1932, Rice, Johnston and Evering (64) detected methyl radicals in the temperature range 800 - 1000°C by using the Paneth technique. Burton, Ricci and Davis (65) showed the presence of radicals at 500°C by using radioactive lead mirrors.

Patat and Sachsse (66-69), using the para-ortho hydrogen method, demonstrated the presence of radicals at 550°C. The hydrogen atom concentration was, however, found to be about  $10^2$  times less than that

predicted by the Rice-Herzfeld mechanism. Since the values of the activation energies were assumed, this calculation may not be considered to be very accurate.

Morris (70, 71) studied the pyrolysis of a mixture of  $\text{CH}_3\text{CHO}$  and  $\text{CD}_3\text{CDO}$  at about  $500^\circ\text{C}$  with a view to establishing the nature of the decomposition. In the case of a free-radical mechanism, mixed methanes such as  $\text{CH}_3\text{D}$  and  $\text{CD}_3\text{H}$  are expected to be formed by the following reactions:

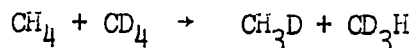


However, analysing the products by infrared absorption, Morris, could not find the mixed methanes in appreciable amounts when the ordinary and deuterated aldehydes were purified by treatment with hydroquinone followed by distillation. But when the mixture of aldehydes was purified in the usual way, the amounts of mixed methanes produced were such that about one-half of the reaction could be attributed to a chain reaction. It was suggested that hydroquinone removed some oxidising impurity which was responsible for the initiation of chain processes. This conclusion has, however, been contradicted by later investigations.

Zemany and Burton (72), investigating the photolysis and pyrolysis of a mixture of  $\text{CH}_3\text{CHO}$  and  $\text{CD}_3\text{CDO}$ , found that the results obtained with aldehydes purified in the usual way were identical with those obtained by treatment with hydroquinone. Hydroquinone itself was, however, found to inhibit the reaction. From the observed ratios of  $\text{CD}_3\text{H}$  to  $\text{CD}_4$  at different temperatures they concluded that about 25% of the reaction proceeded by a

molecular reaction. The evidence is not, however, particularly strong.

Wall and Moore (59) made an extensive study of the isotopic mixing in the pyrolysis of a mixture of ordinary and deuterated aldehydes. Like Zeman and Burton, they also observed extensive isotopic mixing. Treatment of the sample with hydroquinone had no effect on the extent of mixing. It was shown that the following exchange reaction



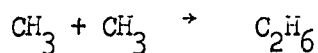
was very slow under their experimental conditions.

Rice and Varnerin (73), decomposing a 50 - 50 mixture of  $\text{CH}_3\text{CHO} - \text{C}_2\text{D}_6$  or  $\text{CD}_3\text{CDO} - \text{C}_2\text{H}_6$  at  $500^\circ\text{C}$  and analysing the products of the reaction by mass spectrometry, found that the measured  $\text{CH}_3\text{D}/\text{CH}_4$  or  $\text{CD}_3\text{H}/\text{CD}_4$  ratio was proportional to the percentage of aldehyde decomposed. From the observed values of the above ratios, it was concluded that the thermal decomposition of  $\text{CH}_3\text{CHO}$  and  $\text{CD}_3\text{CDO}$  was similar and that the contribution of a molecular process was quite insignificant.

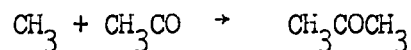
The fact that free radicals can induce the decomposition of acetaldehyde at temperatures where thermal decomposition does not occur is strong evidence of the chain character of the reaction. Allen and Sickman (74, 75) showed that azomethane induces the decomposition of acetaldehyde at  $300^\circ\text{C}$  and chain lengths up to 500 were obtained. That methyl radicals from azomethane can sensitize the acetaldehyde decomposition even at room temperature has been observed by Blacet and Taurog (76).

Calvert and Gruver (77), studying the azomethane sensitized decomposition of acetaldehyde found that the rate of acetone formation was unimportant in comparison with that of ethane formation. This observation

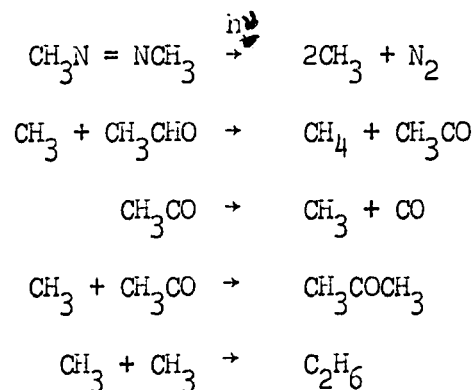
is worth noting in that according to the suggested mechanism even below 127°C the reaction



is 8 - 10 times faster than the reaction



The following mechanism was found to be consistent with their results



From a mercury photosensitized decomposition of a mixture of  $\text{CH}_3\text{CHO}$  and  $\text{CD}_3\text{CDO}$  at 55°C, Lossing (78) concluded that the reaction proceeded mainly by a free radical process and that the contribution of a molecular process was less than 5%.

The decomposition of acetaldehyde was also found to be sensitized by ethylene oxide (79, 80) and by biacetyl (81). It was shown by Letort and Niclause (82, 83) that an amount of oxygen as small as 0.04% could induce this decomposition to an appreciable degree at temperatures as low

as 150°C.

Strong evidence in favour of the chain character of this reaction also came from the study of the effect of inhibitors. This will be described in detail in Part 4 of this dissertation.

#### Inhibition by Inert Gases

The Rice-Herzfeld mechanism, involving first-order initiation and second-order termination ( $\text{CH}_3 + \text{CH}_3$ ), as described before, is a straightforward example of a mechanism leading to three-halves-order kinetics, and has commonly been regarded as giving a correct interpretation of the acetaldehyde decomposition.

On the other hand, Brill, Goldfinger, Letort, Mattys and Niclause (43, 84) have proposed an alternative explanation, based largely on the results of experiments in which foreign gases were added to the reaction system: their conclusion was that the termination step, the combination of methyl radicals, is in its third-order region and that the initiation reaction is hardly affected by inert gases. The work of Laidler and Wojciechowski (40) on the ethane decomposition also led to the conclusion that under the usual conditions of pyrolysis experiments the methyl radical combination reaction is third-order. A difficulty still remains, however, since a third-order termination reaction requires a second-order initiation reaction in order for the over-all order to be three-halves; this, however, appears to be inconsistent with the conclusion that the initiation reaction is hardly influenced by the addition of several foreign gases. The fact that initiation is second-order has received support from a recent investigation by Trenwith (44), who found that the rate of hydrogen production

(which should be a good measure of the rate of initiation) is second-order in acetaldehyde.

Further doubt about the mechanism has arisen as a result of Quinn's work (41) on the ethane decomposition. This appeared at first sight to require that the methyl radical recombination is second order, which is inconsistent with conclusions from the acetaldehyde work. As shown in Part 2., however, Quinn's results are not compelling, and an alternative explanation is possible.

In view of these various difficulties it was decided to reinvestigate the reaction, both uninhibited and inhibited by nitric oxide (see Part 4). Since a very large amount of reliable experimental work has been done on this problem it was not thought necessary, in the present investigation of the uninhibited reaction, to carry out a great deal of additional experimental work. The work has, in fact, been confined to checking the over-all order, to studying the kinetics of formation of the minor product ethane, and to obtaining some specific quantitative information about the effect of added foreign gases; in particular, the effect of foreign gases ( $\text{CO}_2$ ,  $\text{CH}_4$ ,  $\text{N}_2$ ,  $\text{CO}$  and  $\text{C}_2\text{H}_6$ ) on the order of the reaction has been carefully studied. On the basis of these results a mechanism is proposed for the over-all reaction.

#### EXPERIMENTAL

##### Apparatus

Figure 4 is a schematic representation of the all-glass static system used in the present investigation. A photograph of the arrangement

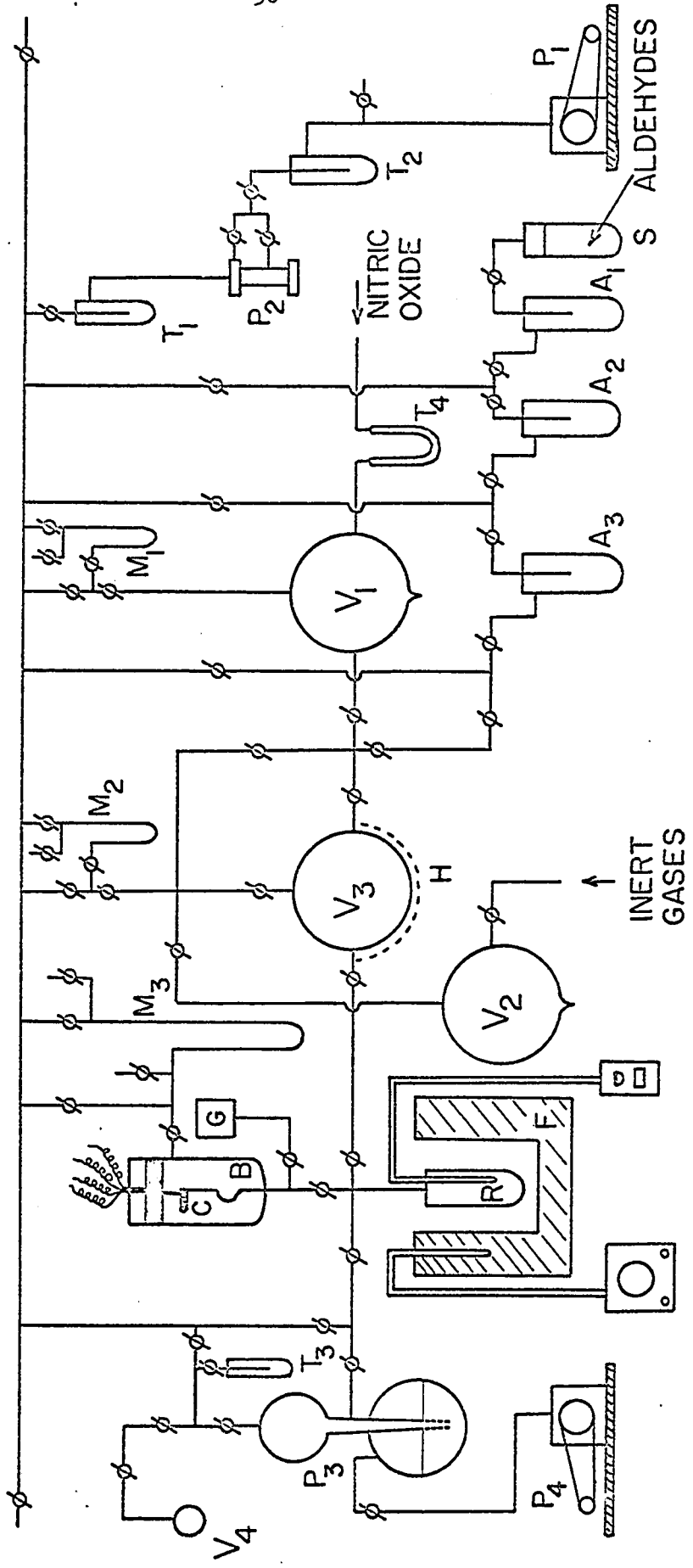


Figure 4. Schematic diagram of the apparatus.

is shown in Plate 1.

Acetaldehyde dried with calcium sulphate was stored in the cylindrical vessel S. After several back and forth distillations from 0 to 70°C using traps A<sub>1</sub> and A<sub>2</sub> pure acetaldehyde was collected in A<sub>3</sub> kept at 0°C. In all distillations, head and tail fractions were rejected and the middle fraction was collected for further purification or for storage. Nitric oxide and the inert gases were stored in the vessels V<sub>1</sub> and V<sub>2</sub> respectively. The U-tube packed with high activity silica gel, placed before the storage vessel V<sub>1</sub>, was used to remove NO<sub>2</sub> from nitric oxide. The storage vessels V<sub>1</sub> and V<sub>2</sub> were provided with nipples at the bottom to freeze out the condensable gases. All the storage vessels lead to the spherical mixing vessel V<sub>3</sub> which was partially wrapped with the heating mantle H in order to provide a slight temperature gradient in the mixing vessel and to speed up the mixing. Gas pressures inside the vessels were read on the manometers M<sub>1</sub> and M<sub>2</sub>. Gases from the mixing vessel V<sub>3</sub>, were led to the reaction vessel R which was a pyrex cylindrical vessel 21 cm long and 4 cm in diameter. All the outlets from the reaction vessel were made from 1 mm diameter capillary tube so that the dead space was about 3 c.c.

Gases from the reaction vessel were led either to the common manifold for evacuation or to the Töepler pump P<sub>3</sub>, to be pushed into the sampling bulb V<sub>4</sub> for analysis. Trap T<sub>3</sub> was meant for condensing out condensable gases. The Pirani gauge head G was placed between the reaction vessel and the Bourdon gauge, in order that the pressure inside the reaction vessel would be read while evacuating.

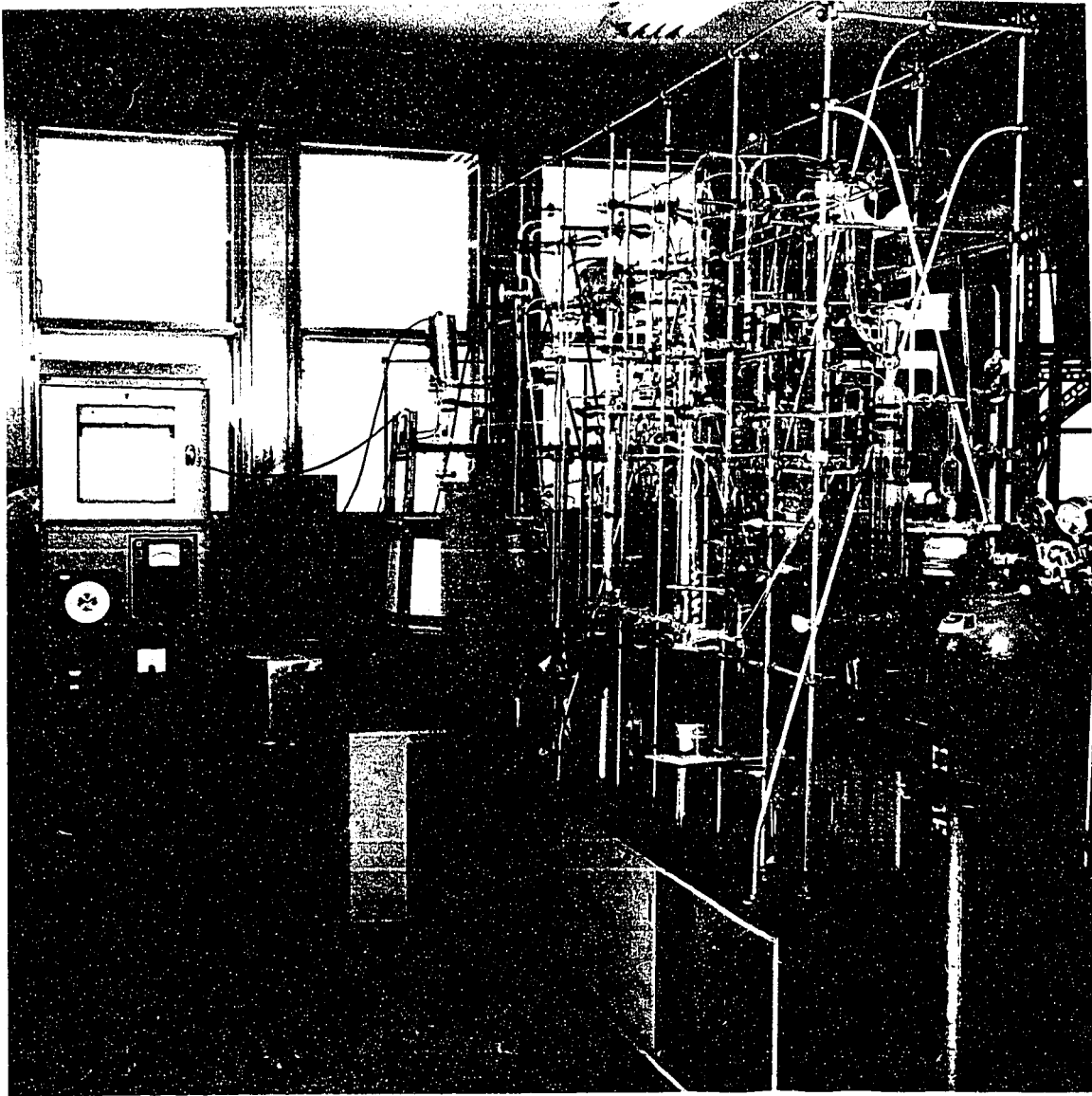


Plate I. View of the apparatus.

The reaction vessel was confined in a copper block which had two concentric windings of nichrome wire around it. The voltage across the inner winding, which had a resistance of 22 ohms, was so adjusted with the help of a Variac that the temperature was slightly below the desired point. The 31 ohm-outer winding was controlled with a Thermo-Electric on-off Signalling Controller. The sensing element of the controller was placed in a hole drilled in the copper block. The voltage across the outer winding was adjusted with a Variac in such a way that the times on both halves of the on-off cycle were equal. In this way the temperature was controlled to within  $\pm 0.2^{\circ}\text{C}$ .

The temperature of the reaction vessel was measured with the help of a Thermo Electric "Minimite" potentiometer, using a chromel alumel thermocouple calibrated at the melting point of zinc, lead and tin. The thermocouple was kept in a hole in the reaction vessel, as shown in Figure 4.

The Pressure increase in the reaction vessel R was followed with the help of the quartz spoon Bourdon gauze B the arm of which was attached, through the screw arrangement C, to the armature of a Statham pressure transducer which was under some strain. The transducer consisted of 4 strain-sensitive resistance wires disposed in the form of a Wheatstone Bridge (Figure 5A) in such a way that any displacement of the armature from its equilibrium position would cause two of the wires to increase in length and the other two to decrease in length. The resistance change of the wires due to the change in their lengths would alter the electrical balance of the bridge and produce an electric signal in the output circuit.

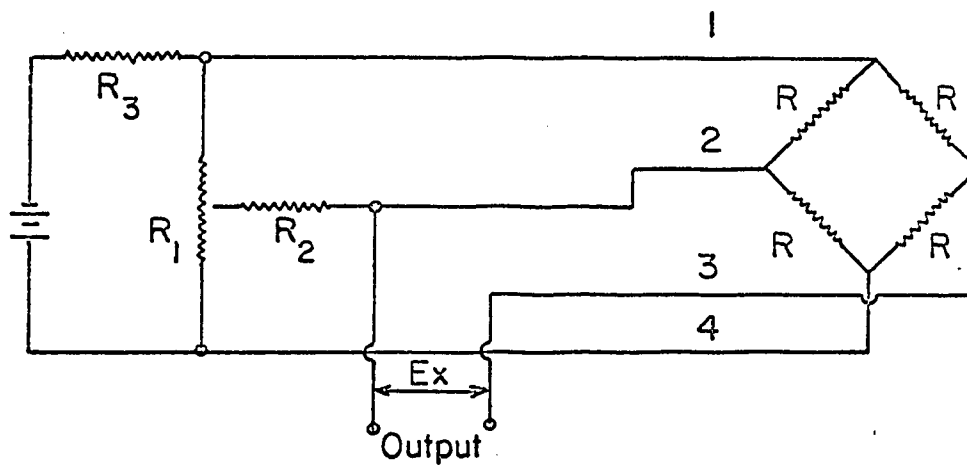


Figure 5A. Schematic circuit of the transducer.

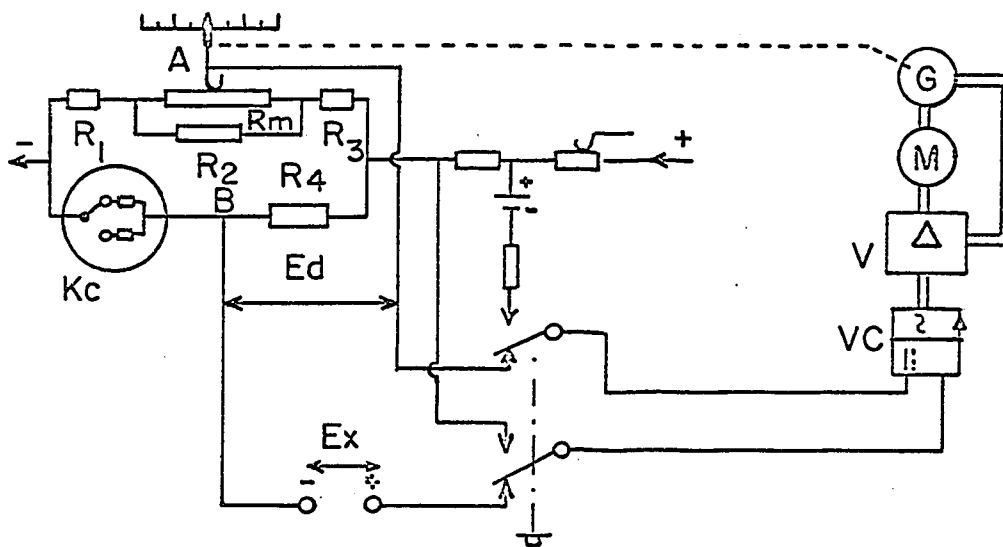


Figure 5B. Schematic diagram of the measuring part of the recorder.

The wire-wound rheostat  $R_3$  controlled the power supply to the transducer. The wire wound potentiometer  $R_1$ , together with the high resistor  $R_2$ , was used for zero adjustment. The output from the transducer was fed to a Philips pen-and-ink recorder the measuring principle of which is shown schematically in Figure 5B. The wire-wound measuring potentiometer  $R_m$  was supplied with a known stabilised direct current. The voltage  $E_d$  (compensation voltage) across A and B was, therefore, known. If the output  $E_x$  was not equal to  $E_d$ , the voltage difference was fed to the amplifier V via the vibrator converter VC. The amplified alternating voltage drove a servomotor M which, in turn, caused the sliding contact A of the measuring potentiometer to move in such a way that  $|E_x - E_d| = 0$ . The size and the initial value of the measuring range could be adjusted with the resistances  $R_1$ ,  $R_2$ ,  $R_3$  and  $R_4$ .

The apparatus was calibrated from time to time and was found to be very stable; the displacement on the recorder varied exactly linearly with the pressure difference. The maximum sensitivity of the particular arrangement used was 0.5 inch displacement per mm Hg. All of the runs, were, however, done at 1/10 or 1/20 of the maximum sensitivity, in order to give higher stability. Higher sensitivities could readily be obtained by modifications of the Bourdon gauze, and in other ways, but only at the expense of a decrease in stability.

All the vessels were connected to a common manifold. The system could be evacuated to less than  $10^{-5}$  mm with the Edwards type 203 oil diffusion pump  $P_2$  backed by the Welch rotary pump  $P_1$ .

### Method

Acetaldehyde used was Eastman product. It was purified by following the procedure described before and found to be completely free from oxygen. Inert gases used were Matheson C.P. grade chemicals and were further purified by trap to trap distillations.

Before a run was carried out the reaction vessel was evacuated to about 1  $\mu$ . Acetaldehyde was then introduced into the reaction vessel. The pressure outside the reaction vessel, as read on the manometer  $M_3$ , was maintained at a value that was slightly less than the initial pressure of the decomposing gas; as the reaction proceeded the differential pressure increased and could be followed on the recorder.

After following the pressure change for the desired amount of time, the reactants and the products were led either to the manifold for evacuation or to the Töpler pump for analysis. This procedure was repeated over the whole range of temperature and pressure studied. Initial rates were obtained from the initial slopes of the records. The rates were initially not very reproducible, but after several runs had been carried out in the same vessel a high degree of reproducibility was achieved. Residual pressures of 1 to 10  $\mu$  in the reaction vessel had little effect on the reproducibility.

Acetaldehyde and the inert gas were mixed in the spherical flask  $V_3$  in appropriate proportions, and complete mixing was ensured by producing a slight temperature gradient and allowing the gases to stand together for at least 30 mins.

Analysis of the minor product ethane was carried out using gas-phase chromatography. After a certain residence time in the furnace the reaction was stopped by allowing the gas to expand. Acetaldehyde was removed from the expanded gas using a dry ice-acetone mixture, and ethane was condensed in a small evacuated bulb surrounded by liquid nitrogen. Using helium as carrier gas, ethane was passed through the chromatographic analysis unit containing a two-metre column packed with silica gel and maintained at 30°C.

### Results

It has been well established by previous work (56, 58, 85-88) that the only major products of the acetaldehyde decomposition are  $\text{CH}_4$  and  $\text{CO}$ , and that a pressure increase of 1 mm corresponds to the decomposition of 1 mm of acetaldehyde within the experimental error of 2%. The pressure technique has therefore been used entirely in the present investigation for the measurement of the over-all rates.

The decomposition was studied from 480 to 525°C and over the pressure range 30 mm to 579 mm Hg. A typical  $\Delta P-t$  curve recorded automatically is shown in Figure 6. As mentioned before, rates were always obtained from the slopes at the initial points. Figure 7 shows a double-logarithmic plot of rate against pressure, and shows that the reaction is accurately of three-halves-order over the whole range of temperature and pressure; this agrees with the work of Boyer, Niclaude and Letort (61), Freeman, Danby and Hinshelwood (62) and Imai, Yoshida and Toyama (63). Figure 8 shows an Arrhenius plot, from it the following rate

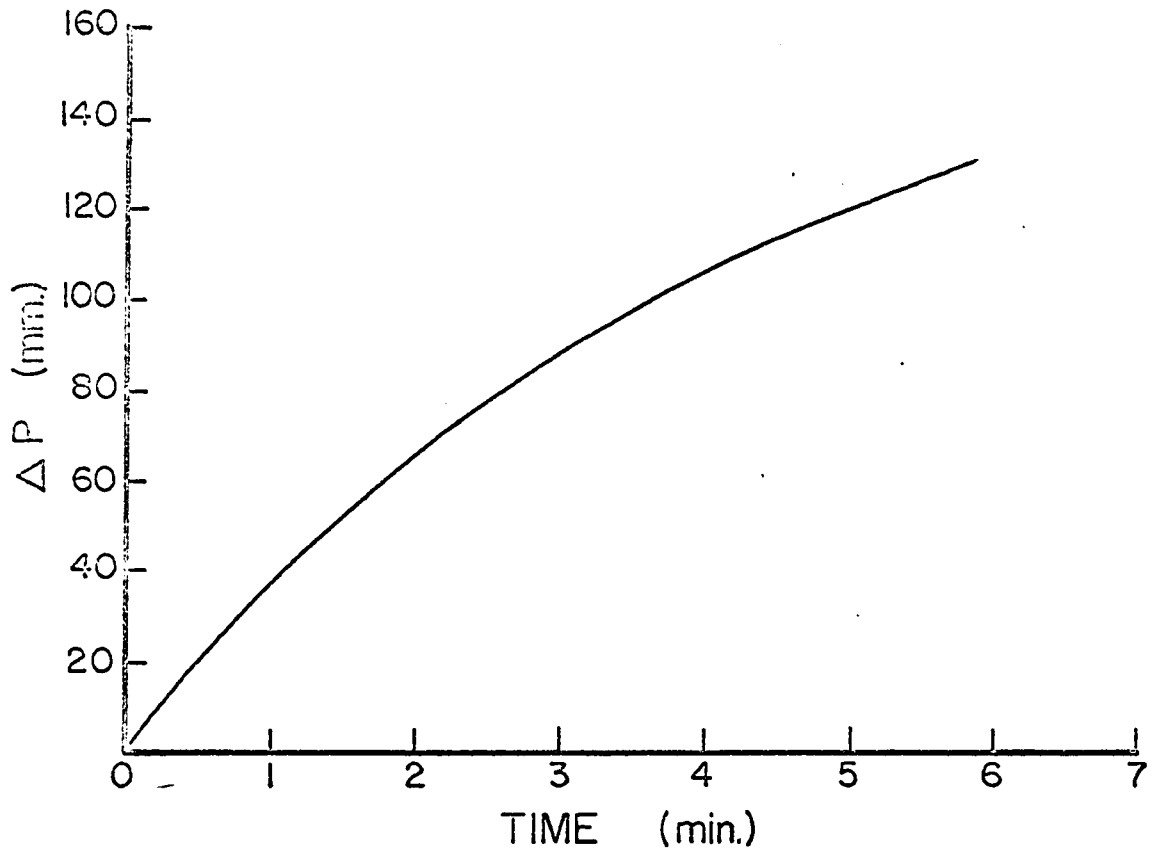


Figure 6. Typical pressure-time curve for the uninhibited decomposition of acetaldehyde.

Initial pressure of acetaldehyde = 311 mm Hg.

Temperature = 525°C.

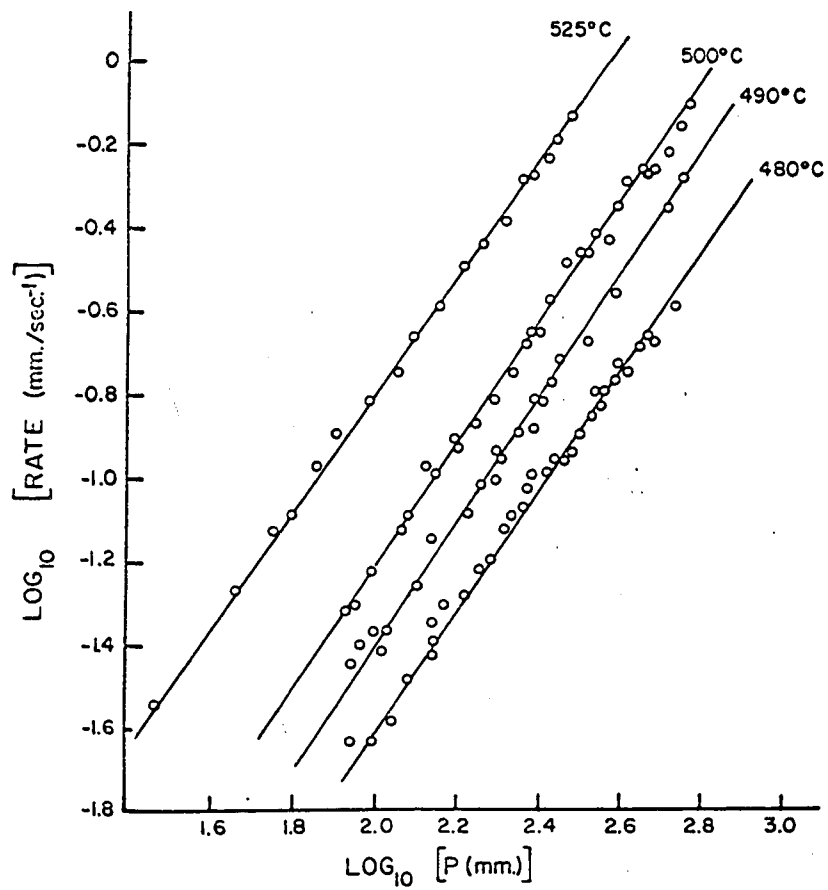


Figure 7. Plots of log rate against log pressure of acetaldehyde at different temperatures.

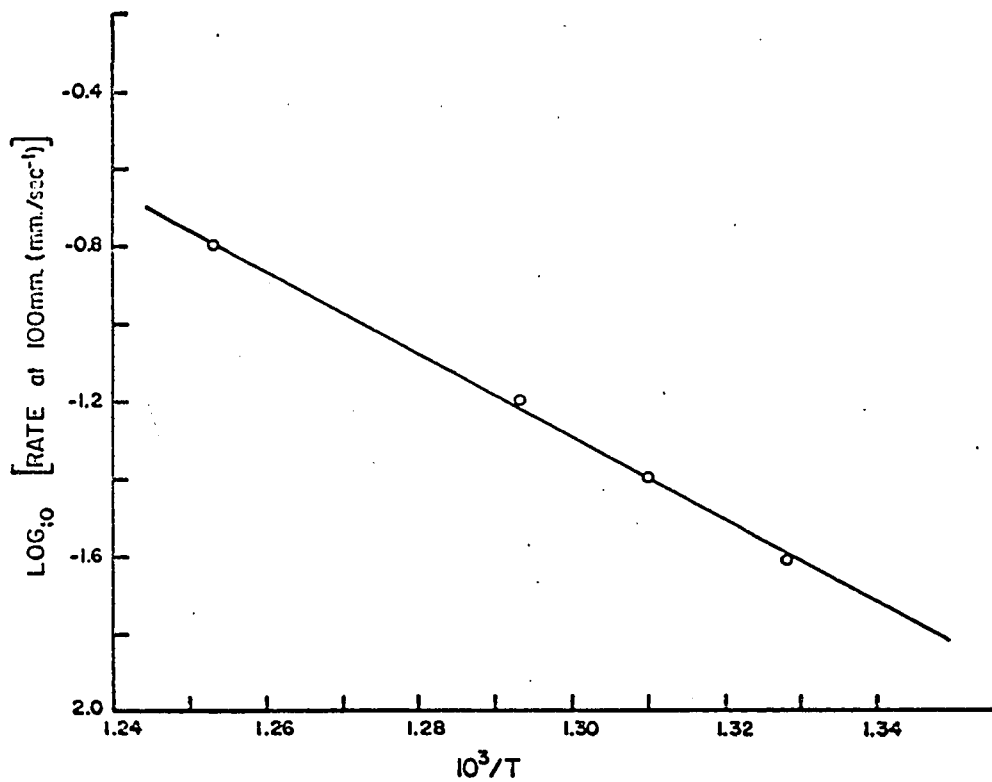


Figure 8. Arrhenius plot for the uninhibited reaction.

expression is derived:

$$k = 1.16 \times 10^{-13} e^{-47,600/RT} \text{ cc}^{1/2} \text{ mole}^{-1/2} \text{ sec}^{-1}$$

The activation energy agrees satisfactorily with the value of 48.0 kcal. per mole obtained by Boyer, Niclause and Letort (61) and of 47.7 kcal per mole at high pressure by Fletcher and Hinshelwood (56).

Added foreign gases were found to bring about a decrease in the rate of the reaction, over the entire pressure range investigated, and to increase the order significantly. Figure 9 shows the effect of adding 100 mm of various foreign gases at 525°C. The order of the reaction has been increased from 1.5 to about 1.60. The Figure further shows that essentially the same effect is brought about by adding the same pressure of carbon dioxide, methane, nitrogen, carbon monoxide and ethane.

Figure 10 shows a plot of the amount of ethane formed as a function of time. In Figure 11 the logarithms of the initial slopes are plotted against the logarithms of the initial acetaldehyde pressure; the slope is close to 2. Figure 10 also shows that the rate of ethane formation is increased by the addition of nitrogen.

## DISCUSSION

### The Reaction Mechanism

The principal difficulty that exists with regard to the mechanism of the acetaldehyde pyrolysis may be formulated as follows. Using the

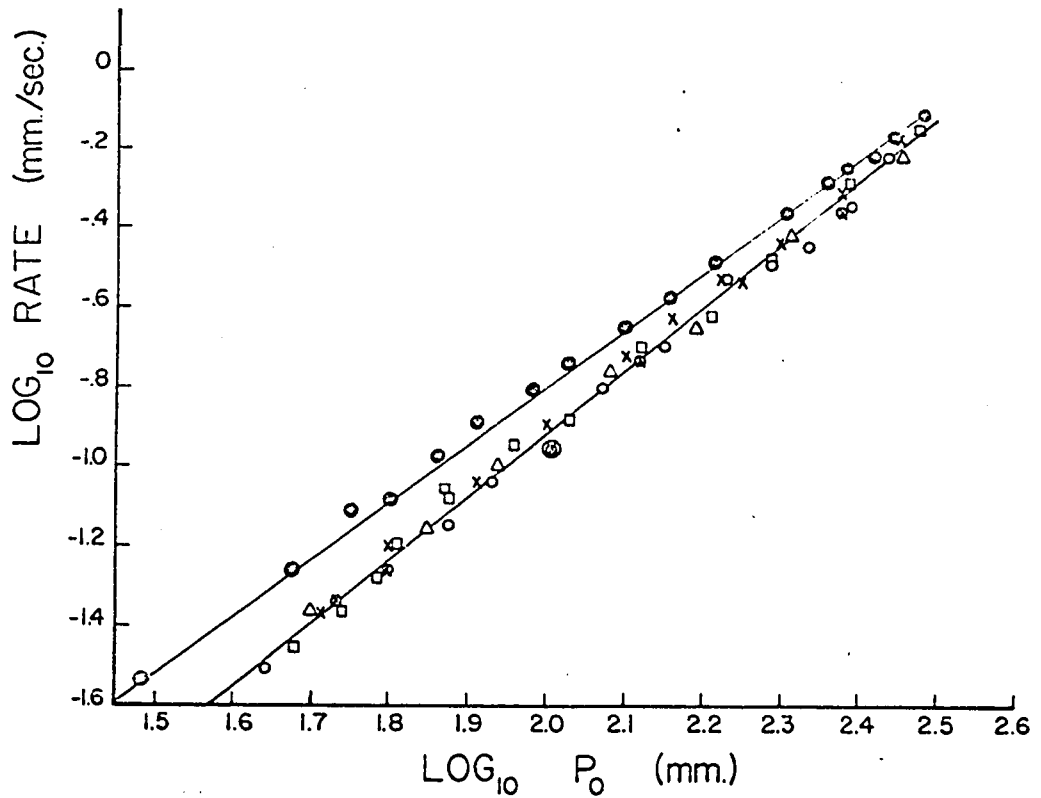


Figure 9. Plots of log rate against log pressure showing the effects of 100 mm of added foreign gases at 525°C. The black circles denote rates with no added foreign gases. Rates with added CO<sub>2</sub> are shown as O, those with CH<sub>4</sub> as □, those with N<sub>2</sub> as Δ, those with CO as ⊗, and those with C<sub>2</sub>H<sub>6</sub> as X.

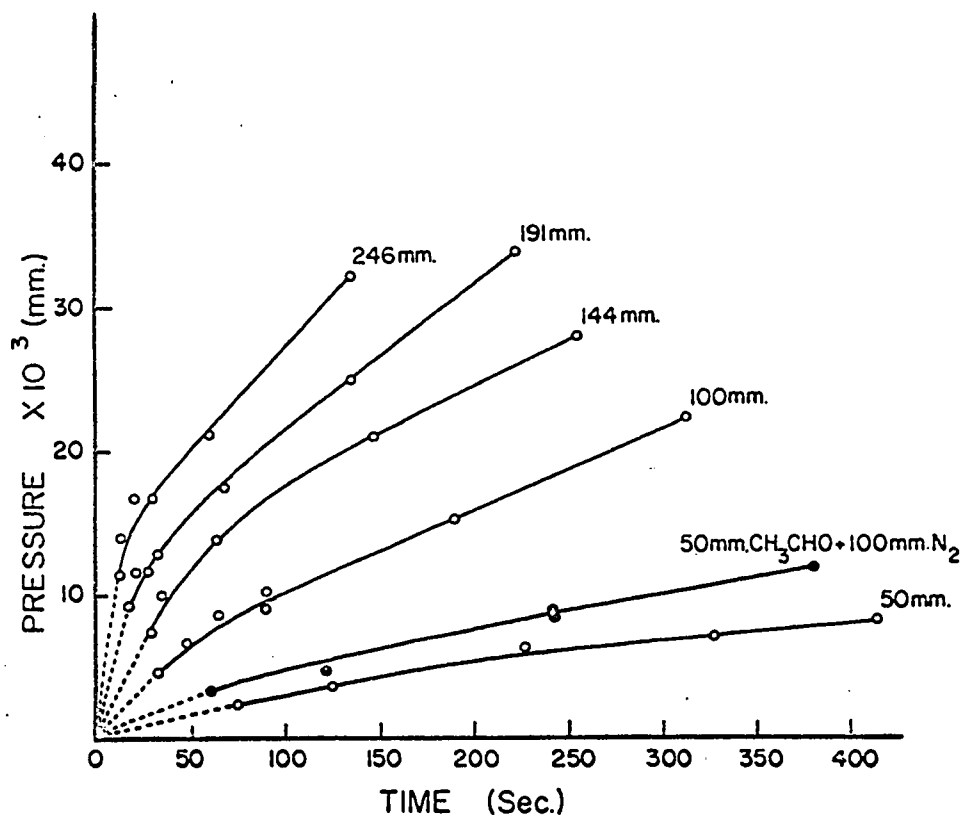


Figure 10. Plots of the amount of ethane formed as a function of time with different initial pressures of acetaldehyde at  $525^\circ\text{C}$ .

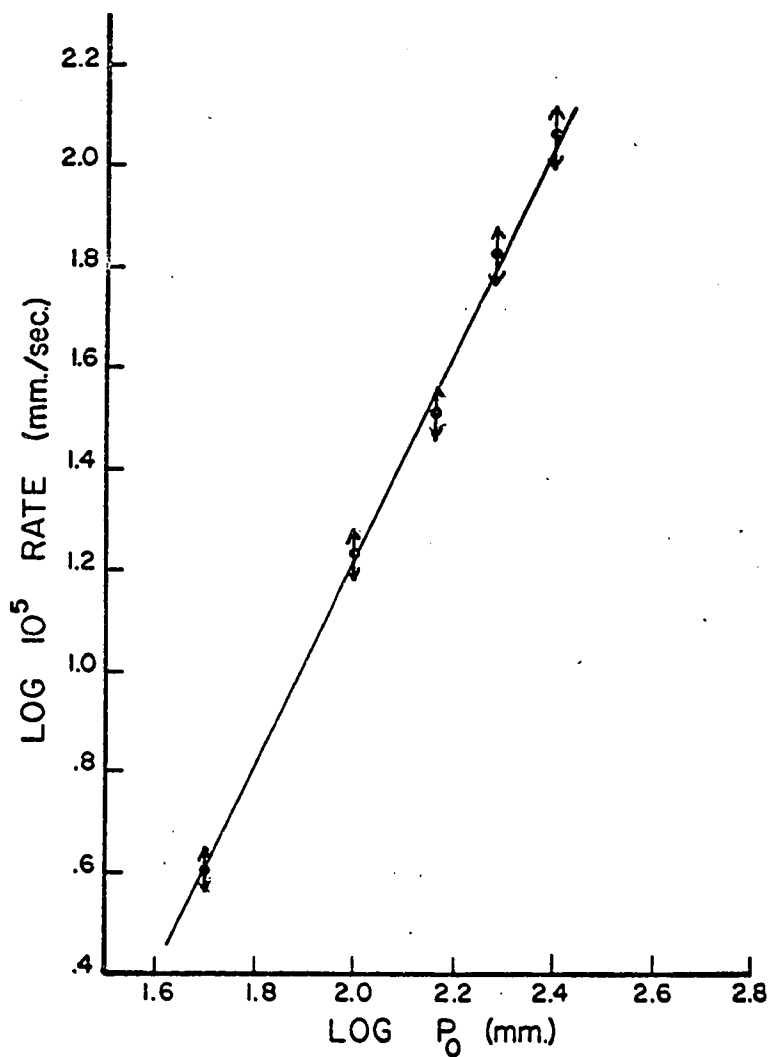
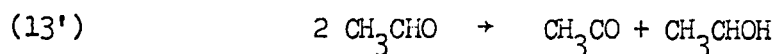


Figure 11. Plot of log initial rate of formation of ethane against log initial pressure of acetaldehyde at 525°C.

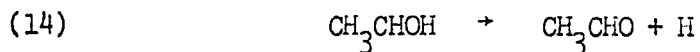
terminology introduced by Laidler, Sagert and Wojciechowski (39) the possible mechanism leading to 3/2-order kinetics are  $^1\beta\beta_{3/2}$ ,  $^2\beta u_{3/2}$  and  $^2\beta\beta M_{3/2}$ . The first of these,  $^1\beta\beta_{3/2}$ , is the original Rice-Herzfeld scheme; it can be rejected as predicting no inert-gas effect, and because it seems clear that the  $\beta$  radicals, being methyl radicals, must combine by third-order processes (40, 89). The second possibility must be rejected as predicting acceleration by inert gases. The third possibility in its simplest form leads to little or no inert-gas effect; it will now be shown, however, that a modification of the  $^2\beta\beta M_{3/2}$  mechanism can be made to explain the results in a quantitative fashion.

What is needed is a mechanism that involves third-order termination - and in this way explains the inhibition by inert-gases - and an initiation reaction that, as found in particular by Brill, Goldfinger, Letort, Mattys and Niclause (43), is only slightly affected by inert gas. The initiation reaction must, however, be in its second-order region, and acceleration by inert gas is normally to be expected. Since a variety of inert gases ( $\text{CO}_2$ ,  $\text{CO}$ ,  $\text{CH}_4$ ,  $\text{N}_2$  and  $\text{C}_2\text{H}_6$ ) give the same effect it would seem unreasonable to postulate that the gases involved are abnormally ineffective in transferring energy on collision to an acetaldehyde molecule. If, however, one postulates that an acetaldehyde molecule plays a very specific role in bringing about the decomposition of another acetaldehyde molecule, the difficulty disappears. The suggestion that is here made is that the initial step in the acetaldehyde decomposition occurs predominantly by the reverse of the "complex" mechanism for radical-combination reactions that has been proposed by Rabinowitch (35) and emphasized by Porter (17) on the basis of experimental

results; this mechanism has recently been considered theoretically by Eusuf and Laidler (90). Specifically, it is suggested that the acetaldehyde initiation occurs as the hydrogen-atom transfer reaction

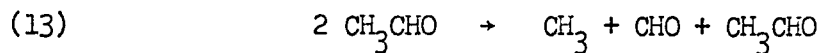


followed by



The over-all process is the split of  $\text{CH}_3\text{CHO}$  into  $\text{CH}_3\text{CO} + \text{H}$ ; the  $\text{CH}_3\text{CHOH}$  radical may also abstract a hydrogen atom from an acetaldehyde molecule or combine with the most abundant radical  $\text{CH}_3$ . The consequences of these reactions will be considered in a later section. The initiation reaction is second-order, but is unaffected by inert gases, since one of the acetaldehyde molecules plays a specific role in bringing about dissociation of the other.

The contribution of the proposed initiation reaction by hydrogen transfer may be compared with that of the corresponding splitting reaction



in the following way. According to Benson (91) reaction (13) is more endothermic by about 27 kcal. per mole than reaction (13') and the entropy changes of reactions (13) and (13') are  $28.5 \text{ cal. mole}^{-1} \text{ deg.}^{-1}$  and  $4.5 \text{ cal. mole}^{-1} \text{ deg.}^{-1}$  respectively (for the standard state of 1 mole per litre).

The ratio of equilibrium constants of the two reactions is then calculated to be, at 800°K,

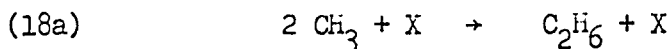
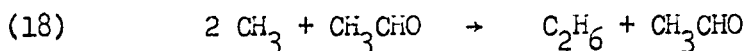
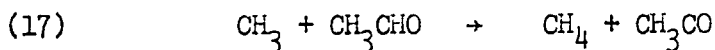
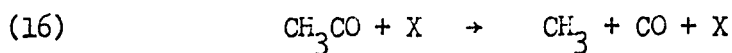
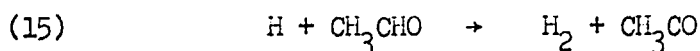
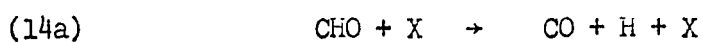
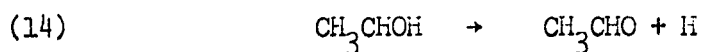
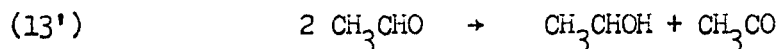
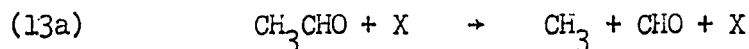
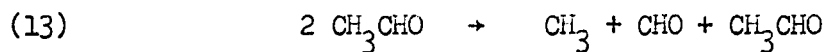
$$\frac{K'_{13}}{K_{13}} = \frac{k'_{13}}{k_{13}} \frac{k_{-13}}{k'_{-13}} = 1.4 \times 10^5 \text{ ml mole}^{-1}$$

The value of  $k'_{-13}$  may be predicted to a reasonable approximation by simple collision theory and is estimated at  $1 \times 10^{14} \text{ cc. mole}^{-1} \text{ sec.}^{-1}$  at 800°K. The rate of combination of  $\text{CH}_3$  and  $\text{CHO}$  radicals to form  $\text{CH}_3\text{CHO}$  is smaller than that of two  $\text{CH}_3$  radicals by a factor of at least 10 (91). The third-order rate constant for the combination of methyl radicals has been estimated at  $3.5 \times 10^{18} \text{ cc.}^2 \text{ mole}^{-2} \text{ sec}^{-2}$  at 800°K (92). The maximum value of  $k_{-13}$  at 800°K is, therefore,  $3.5 \times 10^{17} \text{ ml.}^2 \text{ mole}^{-2} \text{ s}^{-1}$ . From this it follows that

$$\frac{k'_{13}}{k_{13}} = 40$$

Even if one allows an uncertainty of 4 kcal. per mole in the value of  $\Delta H_i$ , and of one power of ten in the value of  $k'_{-13}$ , the contribution of reaction (13') is at least one-third of that of reaction (13) at 800°K and more at lower temperatures. The fact that foreign gases have only a small effect on the initiation reaction indicates that reaction (13') is probably much more important than reaction (13). However, both types of initiation will be included in the present scheme of reactions for the sake of completeness.

The reaction mechanism to which these considerations lead is



Application of the steady-state treatment to this scheme leads to the following expressions for the radical concentration:

$$[\text{CH}_3] = \left\{ \frac{k_{13} [\text{CH}_3\text{CHO}]^2 + k'_{13} [\text{CH}_3\text{CHO}]^2 + k_{13a} [\text{CH}_3\text{CHO}] [\text{X}]}{k_{18} [\text{CH}_3\text{CHO}] + k_{18a} [\text{X}]} \right\}^{1/2} \dots (32)$$

$$[\text{CH}_3\text{CO}] = \frac{k_{17} [\text{CH}_3\text{CHO}]}{k_{16} [\text{X}]} \left\{ \frac{k_{13} [\text{CH}_3\text{CHO}]^2 + k'_{13} [\text{CH}_3\text{CHO}]^2 + k_{13a} [\text{CH}_3\text{CHO}] [\text{X}]}{k_{18} [\text{CH}_3\text{CHO}] + k_{18a} [\text{X}]} \right\}^{1/2} \dots (33)$$

$$[\text{CH}_3\text{CHOH}] = \frac{k'_{13}}{k_{14}} [\text{CH}_3\text{CHO}]^2 \quad \dots (34)$$

$$[\text{H}] = \left(\frac{k_{13}}{k_{15}}\right) [\text{CH}_3\text{CHO}] + \left(\frac{k'_{13}}{k_{15}}\right) [\text{CH}_3\text{CHO}] + \left(\frac{k_{13a}}{k_{15}}\right) [\text{X}] \quad \dots (35)$$

$$[\text{CHO}] = \frac{k_{13}}{k_{14a}} \frac{[\text{CH}_3\text{CHO}]^2}{[\text{X}]} + \frac{k_{13a}}{k_{14a}} [\text{CH}_3\text{CHO}] \quad \dots (36)$$

The rate of disappearance of acetaldehyde is given by

$$= k_{17} \left\{ \frac{(k_{13} + k'_{13}) [\text{CH}_3\text{CHO}] + k_{13a} [\text{X}]}{k_{18} [\text{CH}_3\text{CHO}] + k_{18a} [\text{X}]} \right\}^{1/2} [\text{CH}_3\text{CHO}]^{3/2} \quad \dots (37)$$

The rate of disappearance of pure acetaldehyde is therefore

$$= k_{17} \left\{ \frac{k_{13} + k'_{13}}{k_{18}} \right\}^{1/2} [\text{CH}_3\text{CHO}]^{3/2} \quad \dots (38)$$

This rate equation is in agreement with the experimental order of three-halves for the decomposition of pure acetaldehyde.

Influence of Foreign Gases

Foreign gases such as  $\text{CO}_2$ ,  $\text{CH}_4$ ,  $\text{CO}$ ,  $\text{N}_2$  and  $\text{C}_2\text{H}_6$  inhibit the decomposition of acetaldehyde and increase the order of reaction. The general rate equation (37) accounts for the observed increase in order as the inert gas concentration is increased provided that  $k_{13a}$  is small and  $k_{18a}$  large.

On the basis of the observed inert-gas effect it is now possible to arrive at a conclusion as to the importance of reaction (13a) as the initiation reaction in comparison with reactions (13) and (13'), and that of reaction (18a) as the termination reaction in comparison with reaction (18). With the use of equations (37) and (38), the ratio of rates in the presence ( $v_x$ ) and absence ( $v_o$ ) of inert gas X can be written as

$$\frac{v_x}{v_o} = \frac{\left\{ \frac{[\text{CH}_3\text{CHO}] + \frac{k_{13a}}{k_{13} + k_{13'}} [\text{X}]}{[\text{CH}_3\text{CHO}] + \frac{k_{18a}}{k_{18}} [\text{X}]} \right\}^{1/2}}{\left\{ \frac{[\text{CH}_3\text{CHO}] + r_i [\text{X}]}{[\text{CH}_3\text{CHO}] + r_t [\text{X}]} \right\}^{1/2}} \dots (39)$$

An equation similar to (39) has been employed by Brill et al (43). The values of  $r_i$  and  $r_t$  thus obtained from Figure 9 are as follows

$$r_i = 0.19$$

$$r_t = 1.02$$

However, these values are highly sensitive to the slopes of the lines in Figure 9; the  $r_i$  value might, for example, be as high as 0.3.

The above results show that reaction (13a) plays a smaller part than (13) and (13') in the initiation reaction and that the efficiencies of  $\text{CO}_2$ ,  $\text{CH}_4$ ,  $\text{N}_2$ ,  $\text{CO}$  and  $\text{C}_2\text{H}_6$  and  $\text{CH}_3\text{CHO}$  in bringing about recombination of methyl radicals are approximately the same. The values of  $r_i$  and  $r_t$  are slightly higher than those obtained by Brill *et al.* (43, 84). Traces of oxygen may have a significant effect on the values of  $r_i$  and  $r_t$ .

#### Formation of Ethane

The results given in Figures 10 and 11 show that the rate of formation of ethane is proportional to the square of the acetaldehyde concentration. Reaction (18) is the only reaction that might be expected to produce ethane. According to the ~~pro~~posed mechanism the rate of formation of ethane from pure acetaldehyde is

$$v_{\text{C}_2\text{H}_6} = k_{18}[\text{CH}_3]^{2} [\text{CH}_3\text{CHO}] \quad (40)$$

$$= (k_{13} + k'_{13}) [\text{CH}_3\text{CHO}]^2 \quad (41)$$

in agreement with the experimental result. It is obvious that the square in this rate expression will only arise if the initiation reaction is second-order. The experimental result that the rate of ethane formation is second-order in acetaldehyde is therefore strong evidence that the initiation process is second-order, and for the mechanism proposed.

Formation of Hydrogen

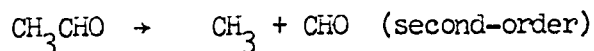
Equally strong evidence is provided by Trenwith's result (44) that the hydrogen production is second-order in acetaldehyde. According to the mechanism

$$v_{H_2} = k_{15} [H] [CH_3CHO] \quad (42)$$

$$= (k_{13} + k'_{13}) [CH_3CHO]^2 \quad (43)$$

Second-order behavior is again only predicted if the initiation reaction is second-order.

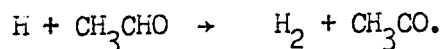
Trenwith (44) has also found that the hydrogen production shows an induction period of a minute or so, the actual value varying with the temperature and surface area of the reaction vessel but being independent of the acetaldehyde pressure. Trenwith explains this in terms of the initiation reaction



followed by



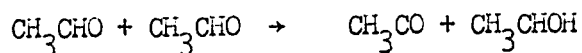
and



To explain an induction period of the order of a minute it is necessary to

postulate that the half-life of the intermediate CHO is of the order of a minute. There is a difficulty, however, about assuming that the dissociation of CHO occurs primarily on the surface with such a half life, since the homogeneous decomposition of CHO almost certainly occurs much more rapidly; from the results of studies of the photolysis of aldehydes, an activation energy of about 14 kcal. per mole has been deduced for the reaction, and this would correspond to a half life of a very small fraction of a second.

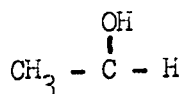
A more plausible interpretation of Trenwith's results on the induction period would seem to be provided in terms of the initiation reaction



followed by



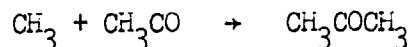
the latter reaction occurring primarily on the surface. The intermediate  $\text{CH}_3\text{CHOH}$ , which probably has the structure



may well have a stability of over 40 kcal., so that its dissociation in the gas phase may be slow; there is therefore no difficulty in assuming that it mainly decomposes on the surface. Trenwith's results on the variation of induction period with temperature indicate a frequency factor of  $10^{5.3} \text{ sec}^{-1}$  and an activation energy of 26.3 kcal. ; the very low frequency factor is understandable if it is a surface reaction.

Formation of Acetone

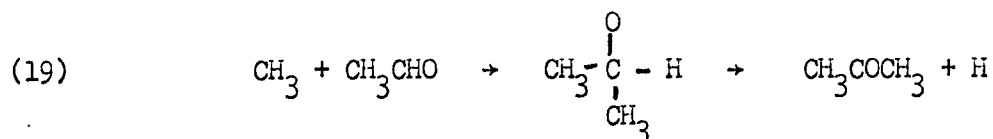
In a private communication Trenwith (93) has informed us of his results on the formation of acetone, the rate of which is greater than the rate of formation of ethane. At first sight it might be thought that acetone would <sup>be</sup> formed by the reaction



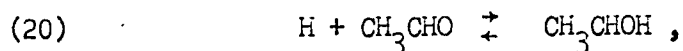
and that this termination reaction is more important than the methyl radical recombination. There are, however, two serious objections to this :

1) This reaction is a termination reaction of the Bu type, and to obtain three-halves order kinetics the initiation reaction must be second-order. This type of mechanism cannot, however, explain the fact that foreign gases reduce the rate of reaction

2) If  $\text{CH}_3 + \text{CH}_3\text{CO}$  is an important termination reaction in the thermal decomposition of acetaldehyde, it should be so a fortiori in the photochemical decomposition where the temperatures are lower and the radical concentrations, especially of  $\text{CH}_3\text{CO}$ , may be higher. Calvert and Gruver (77; cf. also Steacie, ref. 55), however, find that acetone formation is unimportant in the photochemical decomposition of acetaldehyde. This difference between the thermal and photochemical results suggests that the acetone formation is controlled by some process that is temperature dependent. The most plausible reaction would seem to be



Several other reactions of this type, involving initial addition of a radical to a double bond, have been proposed (94-96). The hydrogen atoms produced will come to equilibrium with acetaldehyde molecules

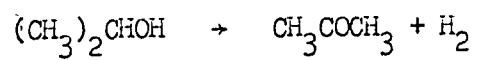
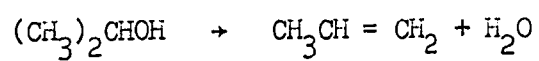
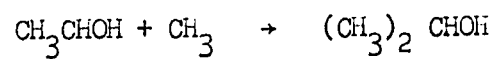
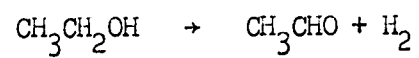
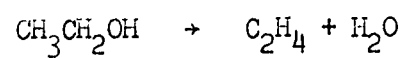


and owing to the slowness of the dissociation of the radical  $\text{CH}_3\text{CHOH}$  there will be an induction period for the production of hydrogen molecules.

The point of view that has been arrived at is therefore that hydrogen production is due to the two reactions (14) and (19) with the equilibrium (20) leading to an induction period. The maximum rate of hydrogen production by reaction (19) will be roughly equal to the rate of production of acetone. Since hydrogen is also produced as a result of reaction (14) the maximum rate of its production will be somewhat greater than that of acetone, which is what Trenwith (93) found.

#### Formation of Other Minor Products

Other minor products which have been found in the acetaldehyde pyrolysis are propylene and water (86), and ethylene (62, 93). These products are readily explained as arising through the intermediate  $\text{CH}_3\text{CHOH}$ , as follows:



Part IV

THE DECOMPOSITION OF ACETALDEHYDE IN THE  
PRESENCE OF NITRIC OXIDE

INTRODUCTION

The thermal decomposition of acetaldehyde in the presence of nitric oxide has been the subject of a number of studies for the last thirty years. The reaction has usually been discussed on the basis of its occurring by a combination of molecular and free radical mechanisms, the sole function of the nitric oxide being to remove radicals. No satisfactory mechanism has yet been put forward to explain the behaviour of acetaldehyde at high temperatures in the presence of nitric oxide.

Review of the Earlier Work

The first investigation on the effect of nitric oxide on the thermal decomposition of acetaldehyde was made by Verhoek (97) who found that the decomposition was catalysed by large amounts of nitric oxide.

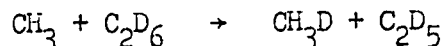
This study was then taken up by Hinshelwood and co-workers. In 1936, Staveley and Hinshelwood (98, 99) made a brief study of the effect of small amounts of nitric oxide on this decomposition. The reaction was followed by measuring the time of half change i.e. the time required for the 50% of the acetaldehyde to decompose. At 559°C with 150 mm of acetal-

dehyde no change in the time of half-change was observed up to 0.53 mm nitric oxide; higher amounts showed positive catalysis. From this observation they concluded that the reaction was purely a molecular process unaccompanied by any chain process. This conclusion is, as shown below, now unacceptable.

In 1942, Smith and Hinshelwood (100), reinvestigating this reaction, made an important modification of the earlier view of Staveley and Hinshelwood (98). They found that with 50 mm acetaldehyde the reaction was inhibited to 90% of the uninhibited one by about 0.8 mm of nitric oxide. Higher amounts caused positive catalysis. At higher pressures of acetaldehyde (above 150 mm) the first one mm or two had little effect on the rate, but larger amounts showed strong catalysis. It was thought that the lack of appreciable inhibition might be due to the rapid removal of nitric oxide by acetaldehyde. 0.72 mm of nitric oxide was, however, found to reduce the rate of a mixture of 150 mm ether and 50 mm acetaldehyde by about 55% at 540°C. This is strong evidence that rapid removal of nitric oxide does not occur in the pyrolysis of acetaldehyde. In the same investigation propylene was found to cause strong inhibition at all acetaldehyde pressures studied (50 - 400 mm), the degree of inhibition being dependent on the initial pressures of acetaldehyde. The conclusion was drawn that the decomposition took place by the concurrent occurrence of both molecular and chain reactions and that the lack of inhibition by nitric oxide was due to its strong catalytic effect masking its inhibitory action. No suggestion was, however, made as to the nature of the catalytic action of nitric oxide. The conclusion that some molecular decomposition was occurring was not based on any firm

grounds.

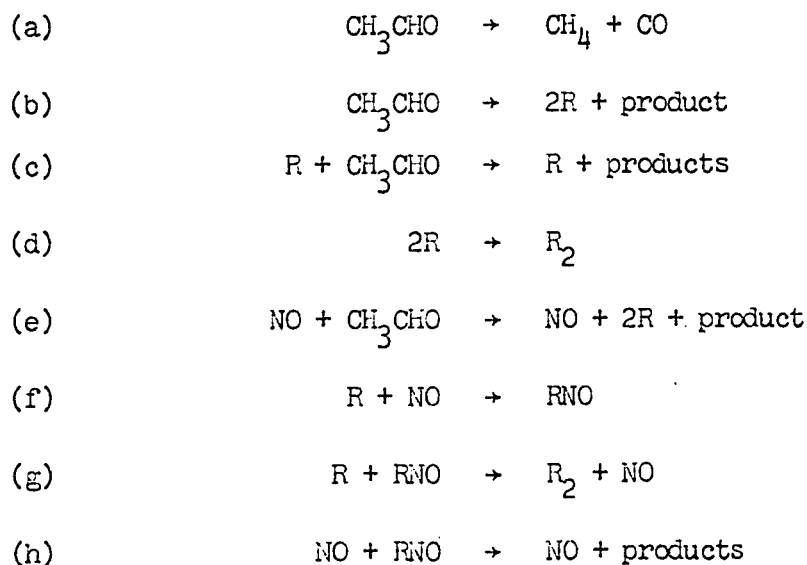
Isotopic mixing in the pyrolysis of a mixture of acetaldehyde and hexadeutero ethane was studied by Rice and Varnerin (73) at 500°C. If the reaction is a molecular one, no CH<sub>3</sub>D is expected to be formed; but in the presence of a chain reaction some CH<sub>3</sub>D must be formed by the following reaction



With a 50 - 50 mixture of acetaldehyde and hexadeutero ethane at 500°C, the ratio CH<sub>3</sub>D/CH<sub>4</sub>, obtained by mass spectrometry, was approximately the same in the presence and absence of nitric oxide at low conversions and was proportional to the percentage of acetaldehyde decomposed. With higher nitric oxide pressures and at higher conversions the mixing was found to be greater than in the absence of nitric oxide. Nitric oxide was found to show great accelerating effect under the same conditions of temperature and pressure. If the acceleration is due to the catalysis of the molecular reaction by nitric oxide, the ratio CH<sub>3</sub>D/CH<sub>4</sub>, is expected to be lower in the presence than in the absence of nitric oxide. The above observations lend quite strong support to the conclusion that nitric oxide catalyses through a chain reaction only.

In 1958, Freeman, Danby and Hinshelwood (62) reinvestigated this reaction from the analytical and kinetic points of view. Analyses were made by mass spectrometry and vapour-phase chromatography. For 50% decomposition the ratio of aldehyde reacted to nitric oxide consumed was found to be

greater than 100 if the ratio of the initial pressure of nitric oxide to that of acetaldehyde was less than 0.13. An increase of the latter ratio led to a decrease of the former one. These observations are consistent with the previous conclusion that the nitric oxide consumption is unimportant in the pyrolysis of acetaldehyde. The rates of formation of the minor products  $C_2H_6$ ,  $C_2H_4$  and  $H_2$  were significantly increased by nitric oxide. The initial rates of decomposition, obtained from pressure measurements, were found to be approximately three-halves with respect to acetaldehyde and one-half with respect to nitric oxide at high nitric oxide pressures. More propylene was necessary in the presence than in the absence of nitric oxide for maximum inhibition. The following mechanism was suggested .



In order for the overall order given by the above mechanism to be consistent with the experimental one, some very drastic assumptions like  $k_e \gg k_f$  have to be made. It was also suggested that about one quarter of the total rate

represented the molecular reaction (a). This suggestion was not, however, based on any firm experimental grounds.

Wojciechowski and Laidler (101, 102) have recently proposed that when organic decompositions are inhibited by nitric oxide an important role is played by a reaction in which the nitric oxide molecule abstracts a hydrogen atom from the substrate molecule; in addition, they have proposed that chain termination may occur by reaction between radicals and species such as HNO and  $\text{CH}_3\text{NO}$ . These proposals have been successful in leading to a quantitative interpretation of a number of organic decompositions (103 - 107). The acetaldehyde behaviour is a good deal more complicated than the cases previously investigated, and its study therefore provides a valuable test of the validity of the proposed mechanisms. The present work describes the results of an experimental reinvestigation of the reaction, and presents a free-radical mechanism, based on the ideas previously put forward in this laboratory, that appear to be consistent with the results.

#### EXPERIMENTAL

The apparatus and procedures were the same as described in Part 3. The nitric oxide used was Matheson Research Grade and was purified by the method of Hughes (109): the distillate collected was completely colourless. Acetaldehyde and nitric oxide were mixed in a spherical flask in appropriate proportions, and complete mixing was ensured by producing a temperature gradient and allowing the gases to stand together for at least 30 minutes.

## Results

Figure 12 shows a typical  $\Delta P - t$  record in presence of nitric oxide. Initial rates were obtained from the initial slopes. Figure 13, 14 and 15 show the effects of nitric oxide on the rate under various conditions. Figure 13 shows that at a relatively low acetaldehyde pressure (52 mm) there is inhibition followed by catalysis; the degree of inhibition decreases with increasing temperature, there being very little inhibition at 525°C. The degree of inhibition with acetaldehyde is always very much less than that with the hydrocarbons. Figure 14 shows how the inhibition curves vary with the acetaldehyde concentration, there being no inhibition at the higher pressures. It will be seen later that at higher acetaldehyde pressures and lower nitric oxide pressures the rate is equal to

$$v = 2 k_{13i} [\text{CH}_3\text{CHO}] [\text{NO}] + k' [\text{CH}_3\text{CHO}]^n \quad (44)$$

where  $3/2 < n < 2$  and  $k_{13i}$  is the rate constant for the reaction  $\text{CH}_3\text{CHO} + \text{NO} \rightarrow \text{CH}_3\text{CO} + \text{HNO}$ . From the initial slopes of the curves in Figure 14, values of  $k_{13i}$  have been calculated and are approximately constant.

Figure 15 shows plots of rate against nitric oxide concentration at two acetaldehyde pressures (70 and 152 mm) and at various temperatures. From the  $k_{13i}$  values calculated from the initial slopes the Arrhenius plot shown in Figure 16 has been obtained; the activation energy is 38.9 kcal. per mole, and the rate constant can be represented by

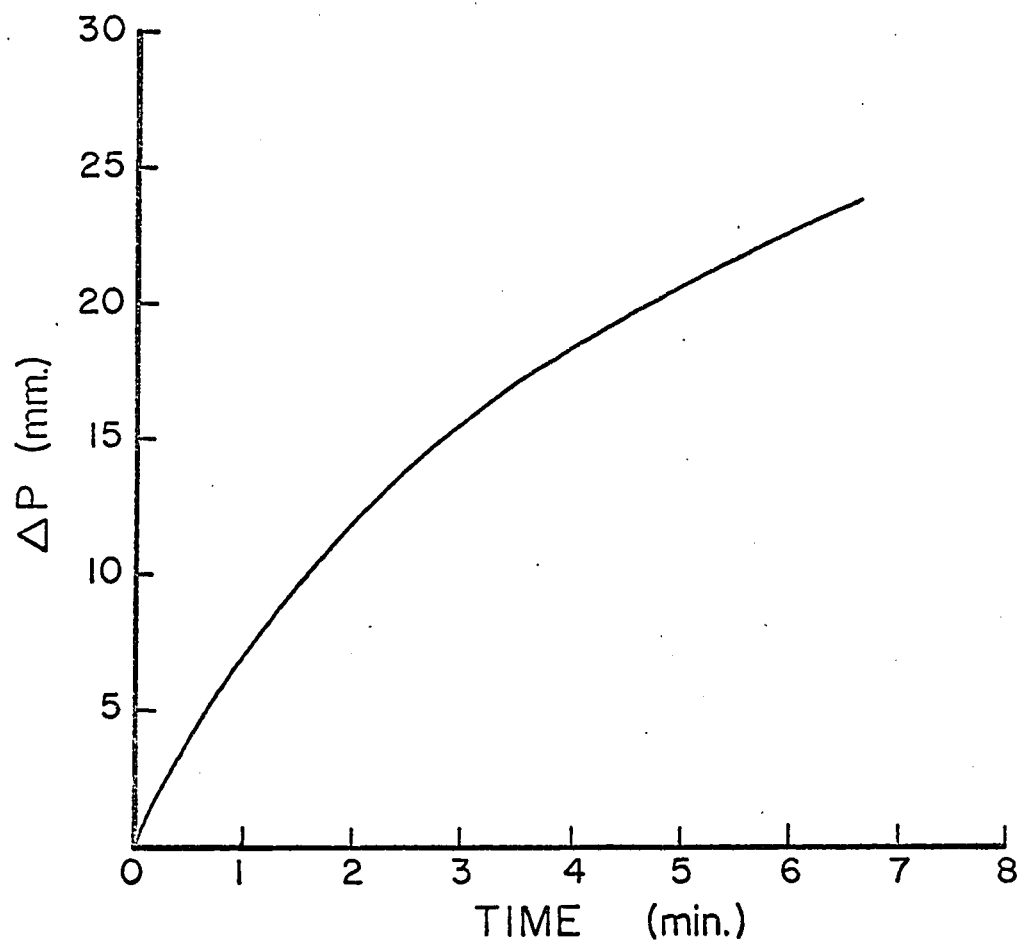


Figure 12. Typical  $\Delta P$ - $t$  curve for the decomposition of acetaldehyde in the presence of nitric oxide

$P_{\text{CH}_3\text{CHO}} = 51 \text{ mm Hg}$

$P_{\text{NO}} = 50 \text{ mm Hg}$

Temperature =  $515^\circ\text{C}$

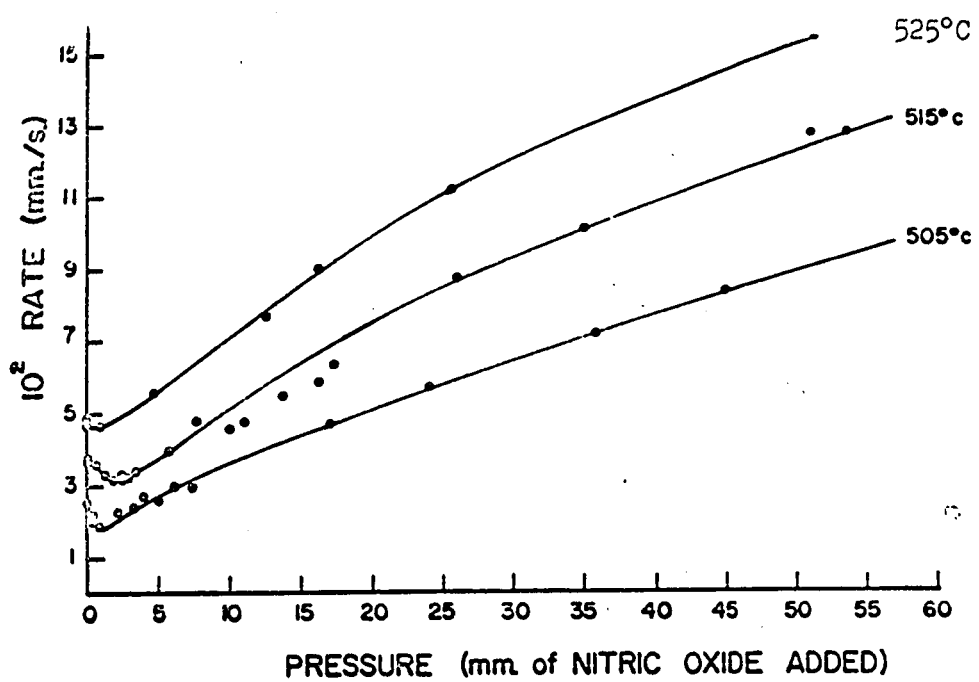


Figure 13. Effect of temperature on the inhibition by nitric oxide

Pressure of acetaldehyde = 52 mm Hg.

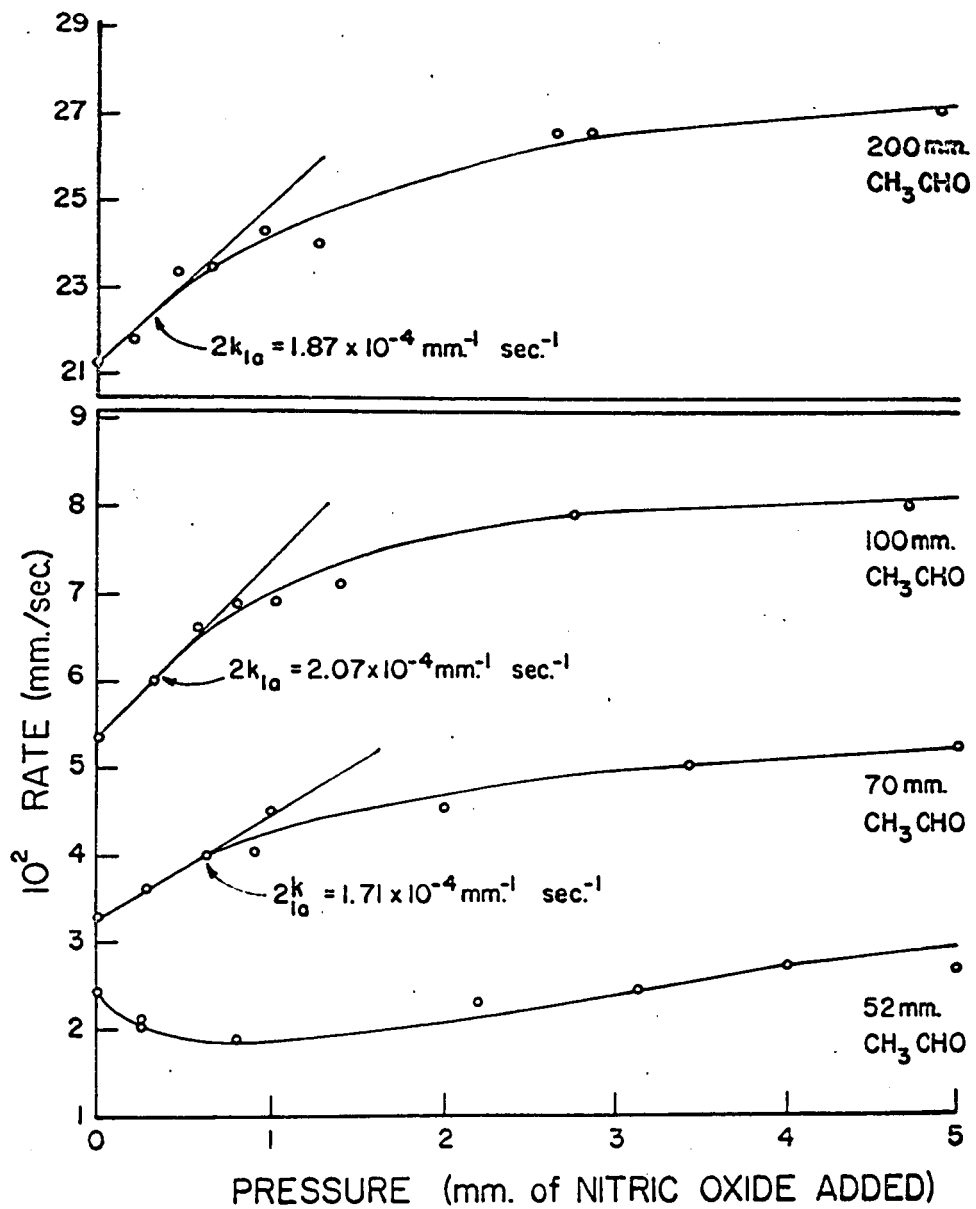


Figure 14. Plots of rates against the pressures of nitric oxide added at various acetaldehyde pressures.

Temperature = 505°C.

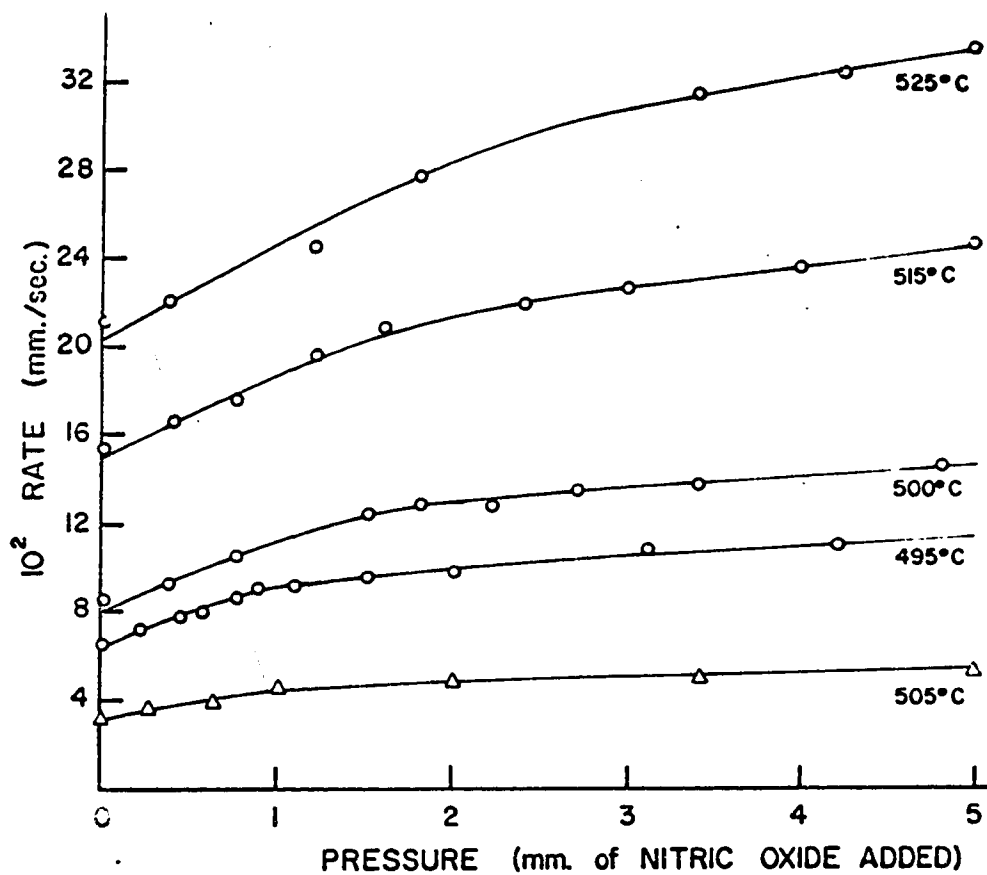


Figure 15. Plots of rates against the pressures of nitric oxide at different temperatures. The circles denote rates with, 152 mm of acetaldehyde and the triangles with 70 mm of acetaldehyde.

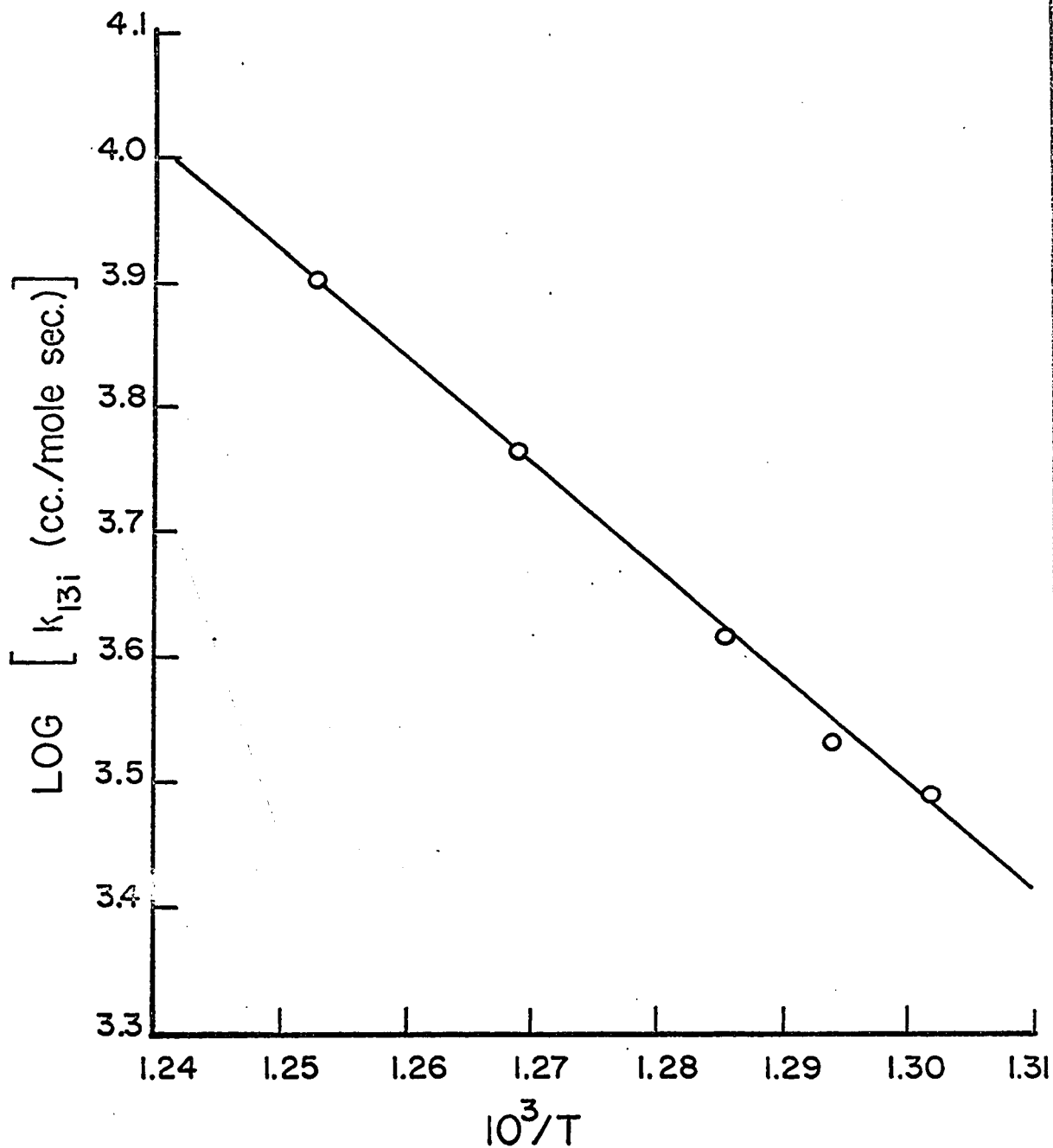


Figure 16. Arrhenius plot, the rate constants being those obtained by dividing the initial slopes (Figure 15) by twice the acetaldehyde concentrations.

$$k_{13i} = 3.46 \times 10^{14} e^{-38900/RT} \text{ cc mole}^{-1} \text{ sec}^{-1}$$

The results indicate that the order of the reaction with respect to acetaldehyde is 3/2 when the ratio  $[\text{NO}]/[\text{CH}_3\text{CHO}]$  is high, but is greater than 3/2 when the ratio is low. This effect is shown in Figure 17; when the pressure of nitric oxide was 50 mm the order was 3/2 over the entire range of acetaldehyde pressures, but the order is approximately 1.8 at higher acetaldehyde pressures when the nitric oxide pressure is 5 mm. Figure 18 confirms the 3/2 order at the higher nitric oxide pressure and at four temperatures; the results of Freeman, Danby and Hinshelwood (62) are added for comparison and are seen to be in excellent agreement.

At higher acetaldehyde pressures the rate varies not only with  $[\text{CH}_3\text{CHO}]^{3/2}$  but with  $[\text{NO}]^{1/2}$ ; this result, which was reported by Freeman, Danby and Hinshelwood (62) is illustrated by Figure 19. Figure 20 shows an Arrhenius plot for this region in which the rate varies with  $[\text{CH}_3\text{CHO}]^{3/2}$ , and leads to the rate constant

$$k = 2.2 \times 10^{15} e^{-43,500/RT} \text{ cc mole}^{-1} \text{ sec}^{-1}$$

The main results as far as orders of reaction are concerned are summarized in Figure 21.

#### THE REACTION MECHANISM

In treating the decompositions of hydrocarbons and of ether it has proved expedient to consider, as a separate problem, the situation at maximal

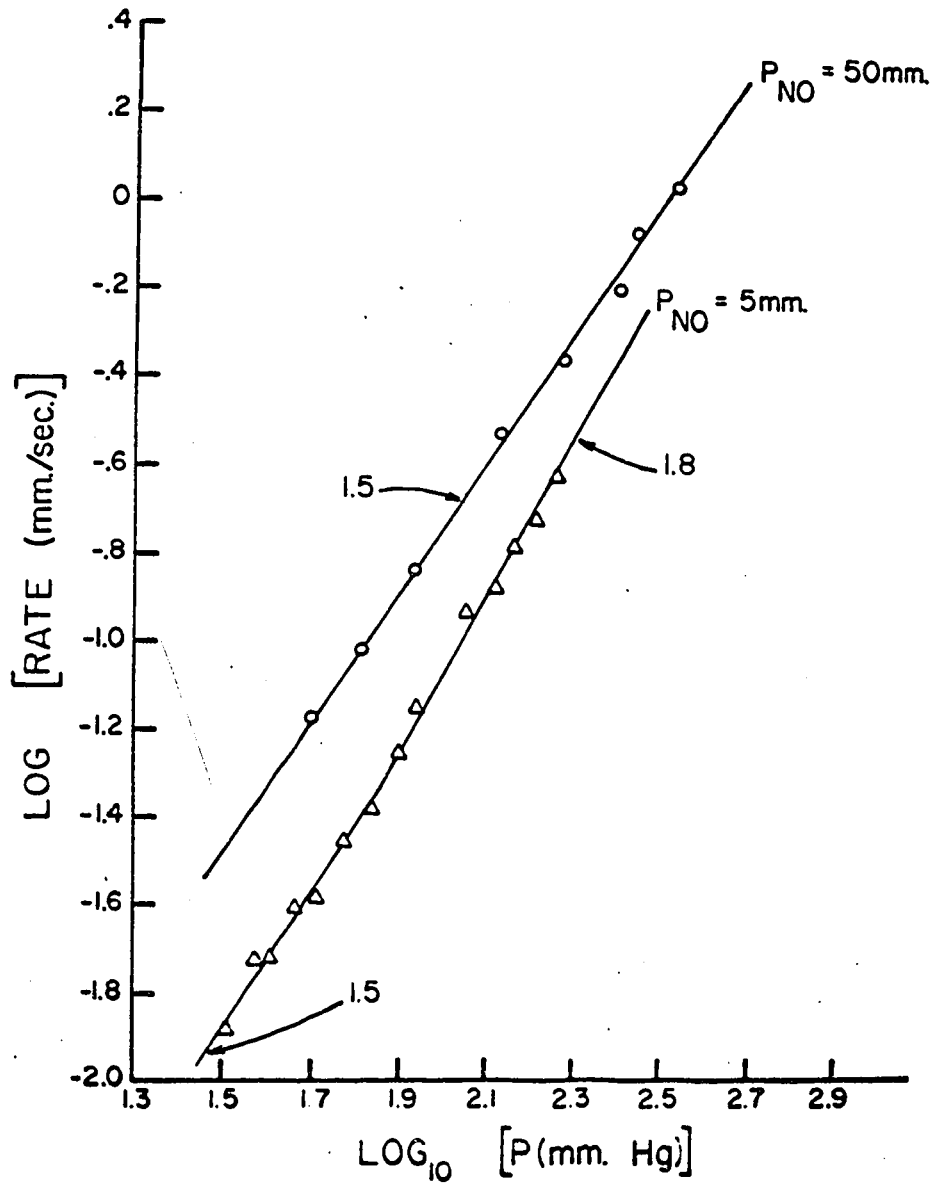


Figure 17. Plots of log rate against log pressure of acetaldehyde, showing the effects of nitric oxide on the order with respect to acetaldehyde.

Temperature = 505°C.

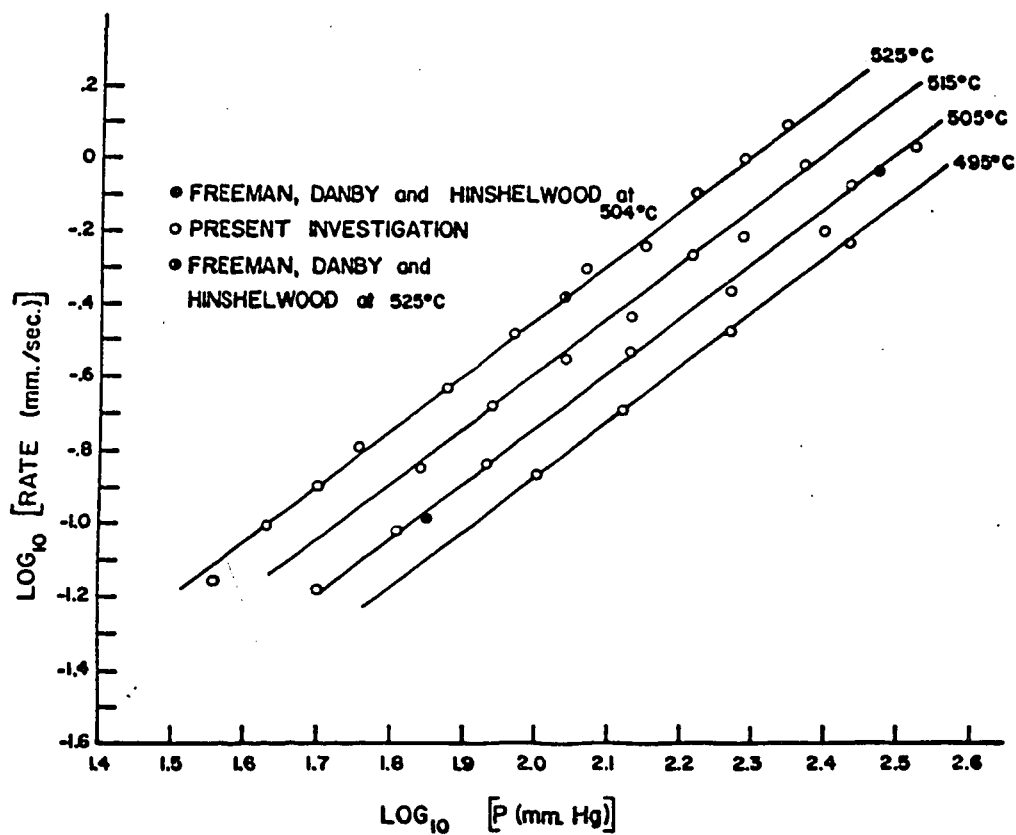


Figure 18. Plots of log rate against log pressure of acetaldehyde at different temperatures with 50 mm of nitric oxide added. The results of Freeman, Danby and Hinshelwood (62) are also shown for comparison.

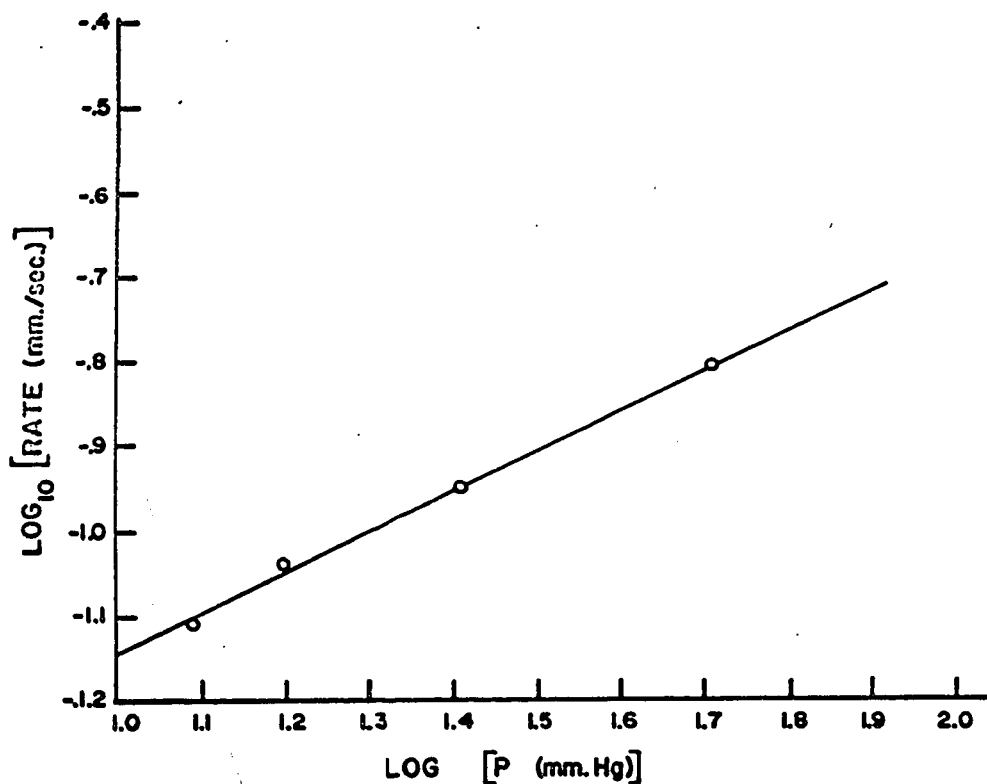


Figure 19. Plot of log rate against log pressure of nitric oxide added to 52 mm of acetaldehyde.

Temperature = 525°C.

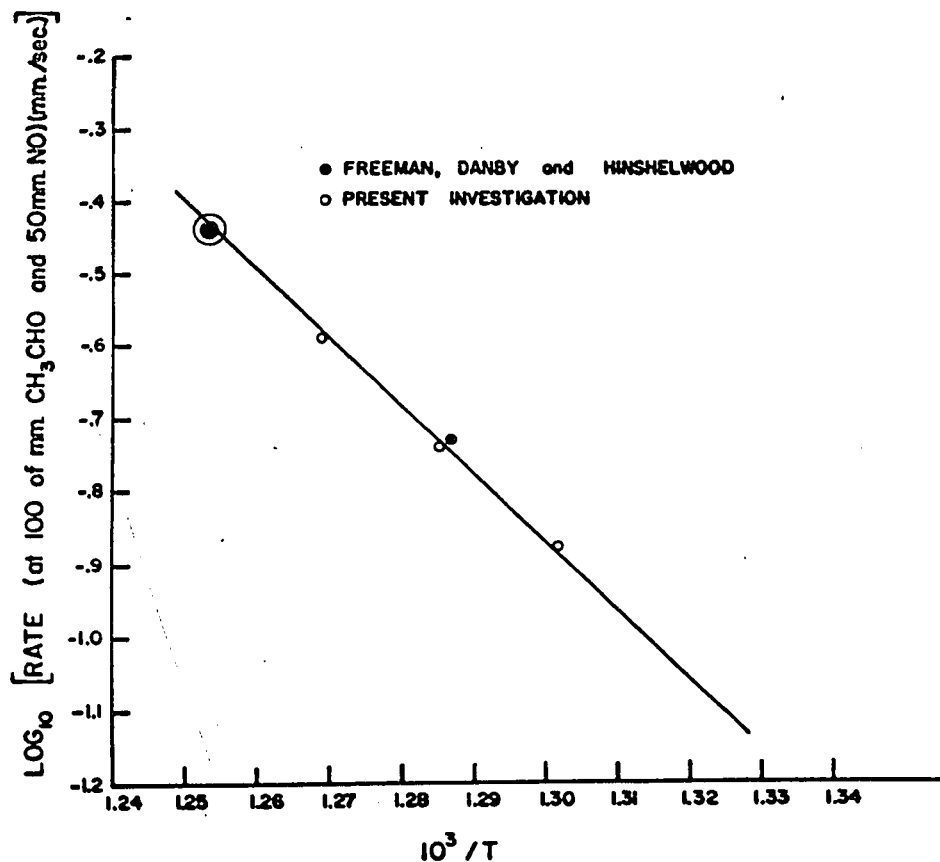


Figure 20. Arrhenius plot in the region of three-halves order with respect to acetaldehyde and one-half order with respect to nitric oxide. The results of Freeman, Danby and Hinshelwood (62) are also shown for comparison.

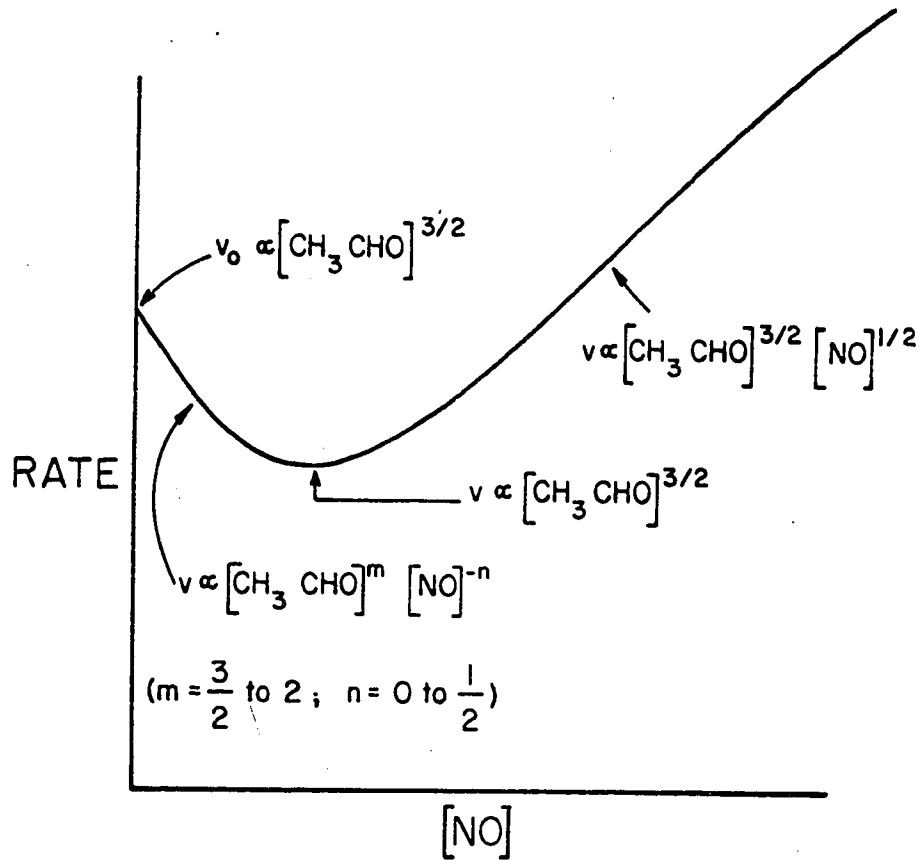
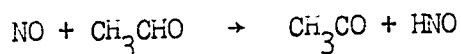
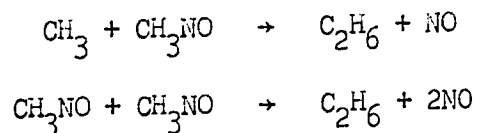


Figure 21. Schematic diagram showing the reaction orders at various concentrations of nitric oxide.

inhibition; under these conditions the nitric oxide-induced initiation reaction can be shown to be much more important than the other initiation processes. In the acetaldehyde decomposition, however, there is no flat region when velocity is plotted against nitric oxide concentration. The situation is therefore more complicated, in that one must take into account the initiation processes that occur in the absence of nitric oxide (cf. Part 3) together with the reaction

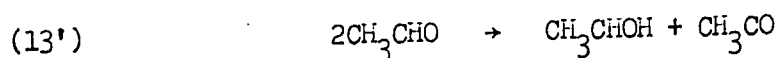
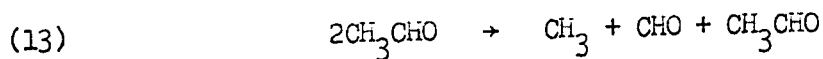


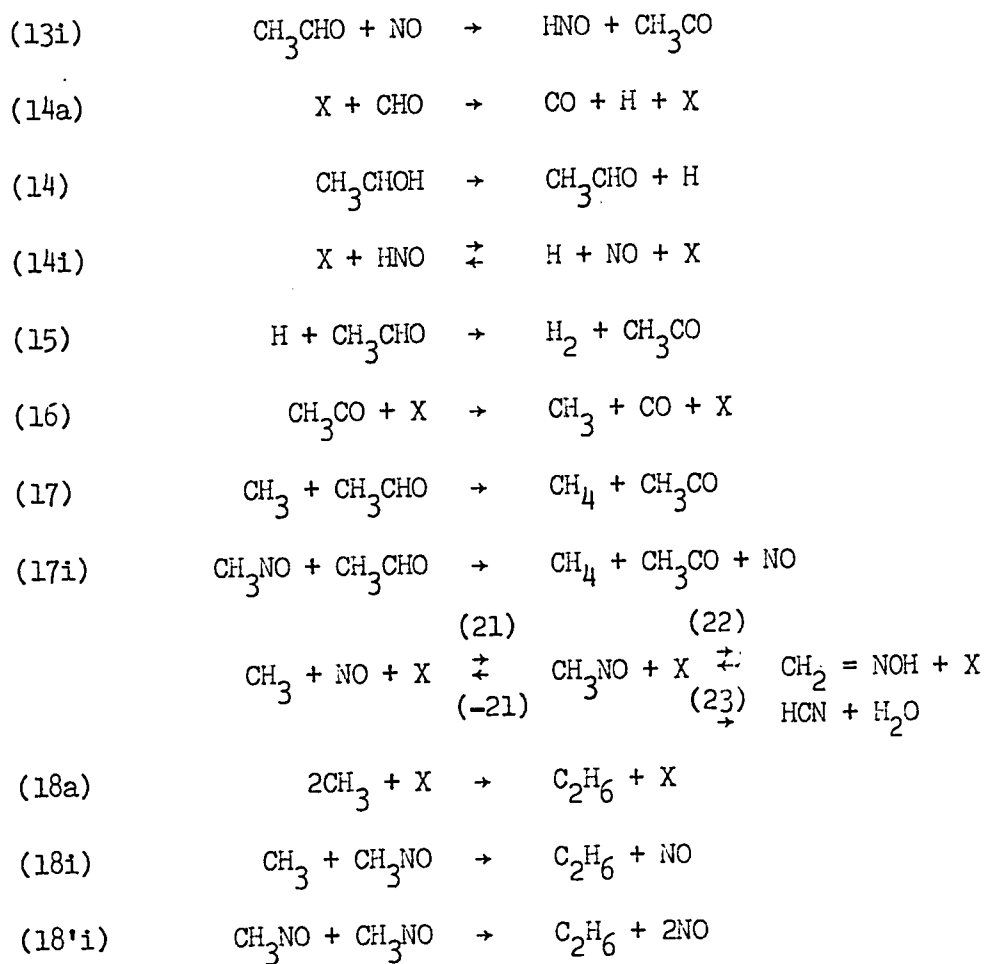
In the same way one must include the termination process for the uninhibited reaction (cf. Part 3) together with the termination reactions that become important after nitric oxide is added;



The last reaction has been omitted in previous schemes, but must be included here on account of the higher  $\text{CH}_3\text{NO}$  concentrations - resulting from the somewhat lower temperatures employed.

The complete scheme may be written as:





The numbering is consistent with the mechanism of Part 3. X represents a third body, which may be acetaldehyde itself.

Application of the steady-state treatment, with the usual approximations, leads to the following expressions for the concentrations of  $\text{CH}_3\text{CO}$ ,  $\text{CH}_3$  and  $\text{CH}_3\text{NO}$  and for the rate of decomposition:

$$[\text{CH}_3\text{CO}] = \frac{\{(k_{13} + 2k'_{13})[\text{CH}_3\text{CHO}] + 2k_{13i}[\text{NO}] + k_{17}[\text{CH}_3] + k_{17i}[\text{CH}_3\text{NO}]\}[\text{CH}_3\text{CHO}]}{k_{16}[\text{X}]} \quad (45)$$

$$[\text{CH}_3] = \left( \frac{(k_{13} + k'_{13})[\text{CH}_3\text{CHO}] + k_{13i}[\text{NO}]}{k_{18a}[\text{X}] + k_{18i} k_{21}[\text{NO}] + k'_{18i} k_{21}^2[\text{NO}]} \right)^{1/2} [\text{CH}_3\text{CHO}]^{1/2} \quad (46)$$

$$[\text{CH}_3\text{NO}] = k_{21}[\text{CH}_3][\text{NO}] \quad (k_{21} = k_{21}/k_{-21}) \quad (47)$$

$$\begin{aligned} v &= 2(k_{13} + k'_{13})[\text{CH}_3\text{CHO}]^2 + 2k_{13i}[\text{CH}_3\text{CHO}][\text{NO}] \\ &= k_{17}[\text{CH}_3][\text{CH}_3\text{CHO}] + k_{17i}[\text{CH}_3\text{NO}][\text{CH}_3\text{CHO}] \end{aligned} \quad (48)$$

$$= 2 k_{13i} [\text{CH}_3\text{CHO}][\text{NO}] +$$

$$\frac{k_{17} \left( \frac{k_{13} + k'_{13}}{k_{18}} \right)^{1/2} \left( 1 + \frac{k_{17i} k_{21}[\text{NO}]}{k_{17}} \right) \left( [\text{CH}_3\text{CHO}] + \frac{k_{13i}}{k_{13} + k'_{13}} [\text{NO}] \right)^{1/2}}{\left( [\text{CH}_3\text{CHO}] + \frac{k_{18i} k_{21}[\text{NO}]}{k_{18}} + \frac{k'_{18i} k_{21}^2[\text{NO}]^2}{k_{18}} \right)^{1/2}} [\text{CH}_3\text{CHO}]^{3/2} \quad (49)$$

A number of important special cases of this rate equation are as follows:

(1) If  $[\text{NO}]$  is zero the equation reduces to

$$v = k_{17} \left( \frac{k_{13} + k'_{13}}{k_{18}} \right)^{1/2} [\text{CH}_3\text{CHO}]^{3/2}$$

This is merely a check that in the absence of nitric oxide the equation reduces to equation (38) of Part 3.

(2) It can be shown by conventional methods that the second term in equation (49) passes through a minimum only if

$$[\text{CH}_3\text{CHO}] < \frac{\frac{k_{18i}}{k_{18}} K_{21} - \frac{k_{13i}}{(k_{13} + k'_{13})}}{2 \frac{k_{17i}}{k_{17}}}$$

This explains why there is inhibition only at low concentrations of acetaldehyde; at higher concentrations the rate increases steadily with increasing nitric oxide concentration.

(3) If [NO] is sufficiently small that

$$\frac{k_{17i}}{k_{17}} K_{21} [\text{NO}] \ll 1, \quad \frac{k'_{18i}}{k_{18}} K_{21}^2 [\text{NO}]^2 \ll \frac{k_{18i}}{k_{18}} K_{21} [\text{NO}]$$

and

$$\frac{k_{13i}}{(k_{13} + k'_{13})} [\text{NO}] \ll [\text{CH}_3\text{CHO}],$$

the rate equation reduces to

$$v = 2 k_{13i} [\text{CH}_3\text{CHO}][\text{NO}] + k_{17} \left( \frac{(k_{13} + k'_{13})^{1/2}}{k_{18}} \right) \frac{[\text{CH}_3\text{CHO}]^2}{\left( [\text{CH}_3\text{CHO}] + \frac{k_{18i} k_{21}}{k_{18}} [\text{NO}] \right)^{1/2}}$$

(50)

of which the first term is usually smaller than the second. Two sub-cases are of particular interest:

(a) If  $[\text{CH}_3\text{CHO}]$  is also sufficiently small there will be inhibition by nitric oxide and the order with respect to acetaldehyde is between 3/2 and 2; this is exactly the behaviour observed. In the limit of very low acetaldehyde concentrations the order will be 2, and the rate will vary with  $1/[\text{NO}]^{1/2}$ .

(b) If  $[\text{CH}_3\text{CHO}]$  is not small the term  $(k_{18i}/k_{18})k_{21}[\text{NO}]$  in equation (50) will be negligible and there will be no appreciable inhibition. Instead there will be acceleration at all concentrations of nitric oxide, owing to the increase in the term  $2k_{13i}[\text{CH}_3\text{CHO}][\text{NO}]$ . It was on this basis that the value of  $k_{13i}$ , and that of the corresponding activation energy  $E$ , was calculated.

(3) If  $[\text{CH}_3\text{CHO}]$  is small but  $[\text{NO}]$  is not particularly small the dominant terms in equation (49) are

$$\frac{k_{17i} k_{21}}{k_{17}} [\text{NO}], \quad \frac{k_{13i}}{k_{13} + k'_{13}} [\text{NO}] \quad \text{and} \quad \frac{k_{18i}^2 k_{21}}{k_{18}} [\text{NO}]^2$$

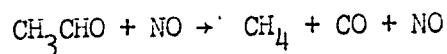
Under these circumstances the rate equation reduces to

$$v = 2 k_{13i} [\text{CH}_3\text{CHO}][\text{NO}] + k_{17i} \left( \frac{k_{13i}}{k'_{18i}} \right)^{1/2} [\text{CH}_3\text{CHO}]^{3/2} [\text{NO}]^{1/2} \quad (51)$$

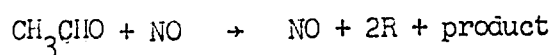
If [NO] is not too high the second term is dominant and the orders with respect to acetaldehyde and nitric oxide will therefore be 3/2 and 1/2 respectively, in agreement with experiment.

#### THE ELEMENTARY REACTIONS

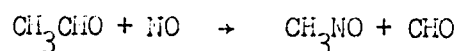
Some of the postulated elementary reaction may now be considered in more detail; those occurring in the uninhibited reaction were dealt with in Part 3, and only the reactions involving nitric oxide are discussed here. The fact that the experimental results show that under certain conditions the reaction is 1/2 order in nitric oxide is a very strong indication that nitric oxide is involved in the initiation of a chain reaction. On this basis one can exclude, as an important reaction, the process



postulated by Freeman, Danby and Hinshelwood (62). Freeman et al. also suggested the reaction



but this would have a higher activation energy than the experimental value of 38.9 kcal. Reaction (13i), on the other hand, is endothermic by 36.4 kcal. (on the basis of  $D(\text{HNO}) = 48.6$  kcal (110) and  $D(\text{CH}_3\text{CO-H}) = 85$  kcal. per mole); the activation energy is entirely consistent with this and provides good support for the proposed reaction. Initiation might alternatively occur as



but there is nothing to support this suggestion.

Reaction (17i), the abstraction of a hydrogen atom by  $\text{CH}_3\text{NO}$ , is an important reaction in the present scheme, since it explains why the degree of inhibition of the acetaldehyde decomposition is much smaller than with hydrocarbon decompositions in which the analogous reaction has a higher activation energy and therefore occurs more slowly. A reaction analogous to (17i) has been postulated by Szabó and Márta (111, 112) as playing a role in the propionaldehyde decomposition. Ree, Yang and Eyring (113) have also considered reactions of the same type, and have described the action of nitric oxide as a "saloon effect"; the nitric oxide molecule is playing the role of a "chaperon" but acts as a negative catalyst by making the radical less reactive. Ree et al. have suggested a method for estimating the activation energies for reactions such as (17i); for this reaction their method leads to a value of 26 kcal. per mole, to be compared with 39.5 in the case of abstraction from a hydrocarbon molecule.

The disappearance of  $\text{CH}_3\text{NO}$  by reactions [22] and [23] has been suggested by Mitchell and Hinshelwood (114). Reaction [23] has been demonstrated by Taylor and Bender (115), and the occurrence of reaction [22] is suggested by the work of Gowenlock and Trotman (116), and Lüttke (117). Some evidence for reaction [-22] is obtained from the work of Taylor and Bender (115), who found that ethane is formed in the decomposition of

formaldoxime  $\text{CH}_2 = \text{NOH}$ .

Reaction [18i] was suggested by Freeman, Danby and Hinshelwood (62) in the acetaldehyde decomposition induced by nitric oxide, and McKenney, Wojciechowski and Laidler (106) postulate it in the dimethyl ether decomposition, Hoare (118) has also found evidence for reaction between nitrosomethane and methyl radicals in the photolysis of acetone at 200°C; at this lower temperature he found that an average of between 2 and 3 methyl radicals were used up per nitric oxide molecule. Reaction [18'i] was first postulated by Taylor and Vesselowsky (119) in the decomposition of nitromethane, and Szabó and Márta (111, 112) have postulated the analogous reaction involving  $\text{C}_2\text{H}_5\text{NO}$  in the propionaldehyde decomposition. An attempt to detect the chain-ending products in the absence and presence of nitric oxide has been made by Freeman, Danby and Hinshelwood (62), who found that the ratio  $\text{C}_2\text{H}_6/\text{CH}_4$  is increased by the addition of nitric oxide. That nitric oxide reduces markedly the concentration of  $\text{CH}_3$  radicals is now beyond question. The increase of ethane production in the presence of nitric oxide must, therefore, be attributed to the occurrence of reactions [18i] and [18'i]; in other words, nitric oxide acts as a 'chaperon' in the combination of methyl radicals. This is an example of the radical-molecule complex mechanism which has recently been considered theoretically by Eusuf and Laidler (90).

An estimate of the activation energy for reaction [18'i] can be made on the basis of the experimental activation energy of 43.5 kcal. for the reaction in which the rate varies with  $[\text{CH}_3\text{CHO}]^{3/2}[\text{NO}]^{1/2}$ . This activation energy is seen from equation (51) to be  $E_{17i} + 1/2 (E_{13i} - E'_{18i})$ .  $E_{13i}$  has been seen to be 38.9 kcal., and  $E_{17i}$  was estimated above to be 26 kcal. These figures leads to a value of 3.9 kcal. per mole for  $E'_{18i}$  which seems reasonable.

Part V

THE UNINHIBITED DECOMPOSITION OF PROPIONALDEHYDE

INTRODUCTION

Since 1926, there have been a number of investigations on the thermal decomposition of propionaldehyde. Though there is evidence that free radicals are present in the system, not too much can be said with certainty about the details of the mechanisms. Some striking disagreements on important experimental facts are also found in the earlier work, a review of which is given below.

Review of the Earlier Work

In 1926, Hinshelwood and Thompson (120), studying the pyrolysis of propionaldehyde in the temperature range 450-600°C, found that the contribution of any heterogeneous reaction was not more than 1% of the total reaction. From the approximately constant value 2 for the ratio  $t_{75}/t_{50}$  where  $t_{75}$  is the time for 75% decomposition and  $t_{50}$  that for 50% decomposition, they suggested that the reaction was approximately first order with respect to propionaldehyde over 100 mm Hg. The activation energy corresponding to the first-order rate constant was calculated to be 55.0 kcal per mole. The first-order rate constant was, however, found to fall off monotonously with the decrease of pressure showing that the order of the reaction was greater than unity.

Winkler, Fletcher and Hinshelwood (121), reinvestigating the reaction at 549°C confirmed the previous results that the reaction was completely homogeneous and of approximately first order. Above 35 mm propionaldehyde pressures 1 mm pressure increase was found to correspond to the decomposition of approximately 1 mm of propionaldehyde. The activation energy varied from 63.5 kcal at 30 mm to 56.0 kcal at 350 mm propionaldehyde pressure. Analysis of the products was made by using the conventional chemical methods. The major products were CO, C<sub>2</sub>H<sub>6</sub>, C<sub>2</sub>H<sub>4</sub>, H<sub>2</sub> and CH<sub>4</sub>. C<sub>2</sub>H<sub>4</sub> and H<sub>2</sub> were produced in equal amounts and found to increase with decrease of propionaldehyde pressures. From the segmented nature of the  $1/t_{1/2} - P_0$  curve where  $P_0$  is the initial pressure of propionaldehyde, it was concluded that several "quasi-unimolecular" reactions contributed to the over-all rate. A closer scrutiny of their data, however, reveals that above 40 mm propionaldehyde pressure the over-all order of the reaction is between 1.2 and 1.3.

Patat and Sachsse (66-69) detected free radicals by the para-ortho hydrogen method. The radical concentration was calculated to be about  $10^{1.3}$  less than that predicted by the Rice-Herzfeld mechanism. In view of the various assumptions involved, this calculated result may not be considered very reliable.

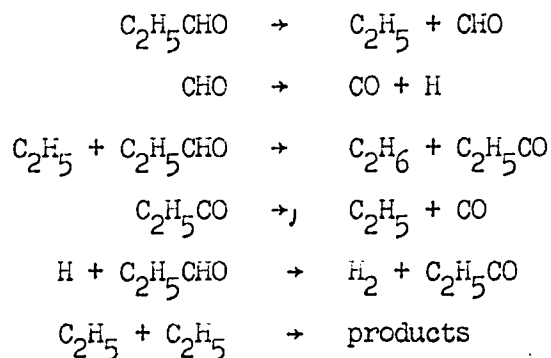
Sworski and Burton (122), using the mirror technique, could detect both CH<sub>3</sub> and C<sub>2</sub>H<sub>5</sub> radicals in the temperature range 850 - 950°C. Detection of ethyl radicals, in spite of their apparent instability in the above temperature range, leads to the conclusion that the ethyl radical is the principal chain carrier in this decomposition.

Boyer and Niclause (123) investigated the pyrolysis of propionaldehyde at somewhat lower temperatures (427 - 486°C) and found that the overall order of the reaction was three-halves with respect to propionaldehyde.

The rate was expressed as

$$v = 1.45 \times 10^{13} [\text{C}_2\text{H}_5\text{CHO}]^{3/2} e^{-\frac{50300}{RT}} \text{ min.}^{-1}$$

the units being moles per gram molecular volume. The reaction was found to be sensitized by biacetyl and di-tert-butyl peroxide. In addition to the major products CO and C<sub>2</sub>H<sub>6</sub> small amounts of C<sub>2</sub>H<sub>4</sub>, H<sub>2</sub> and CH<sub>4</sub> were formed over the whole range of temperature studied. The following Rice-Herzfeld mechanism is consistent with their results



In a recent investigation by Márta (128) the over all rate was reported to be three halves in the temperature range 515 - 565°C and pressure range 100 - 250 mm Hg. Inert gases were found to have no effect on the rate. An attempt was made to explain the results by the Rice-Herzfeld

mechanism described above. This mechanism does not, however, explain the formation of the significant amount of ethylene observed by Winkler et al (121).

Recently HO (125) made a brief study of the pyrolysis of propionaldehyde at 522.5°C. He confirmed the previous result that 1 mm pressure increase corresponds to the decomposition of 1 mm of propionaldehyde and that the reaction is essentially homogeneous. Analysis of his graphical data shows that the over-all order of the reaction is about 1.35, significantly lower than that of acetaldehyde (Part 3).

The presence of appreciable amounts of  $C_2H_4$  and  $H_2$  (121) indicates that the  $C_2H_5$  radical is not as stable as suggested by Márta (124), and if that be so, the order of the propionaldehyde decomposition is expected to be lower than that of acetaldehyde; the reason is that in the latter case the stable  $CH_3$  radical is the principal chain carrier.

Previous work in these laboratories has shown that the thermal decomposition of a number of organic compounds can be satisfactorily explained by free radical mechanisms. The present work describes an experimental study of the pyrolysis of propionaldehyde, the object being to establish the disputed facts and to elucidate the details of the mechanism.

#### EXPERIMENTAL

The apparatus used was essentially the same as described in Part 3. The reaction was carried out in a quartz vessel 20 cms long and 4 cms wide with a dead space of about 1% of the total volume. It was confined in a metal

block the temperature of which was controlled to within  $0.2^{\circ}\text{C}$ . Analyses were made by using the technique of gas-phase chromatography. A Perkin-Elmer Vapor Fractometer containing a 4-metre silica gel column maintained at  $30^{\circ}\text{C}$  was used. Dry helium was used as a carrier gas.

The propionaldehyde used was an Eastman Kodak product. It was purified by following the same technique employed in the case of acetaldehyde (Part 3) and stored in a dark place. Inert gases used were Matheson Research Grade Chemicals and were purified by several distillations.

### Results

The reaction was studied in the temperature range  $520$  to  $560^{\circ}\text{C}$  and pressure range  $21$  to  $362$  mm Hg. Figure 22 shows a typical  $\Delta P$ -  $t$  record at  $550^{\circ}\text{C}$ . At lower temperatures and lower pressures a short induction period was observed. Rates were obtained from the maximum slopes.

It has been shown by several investigations (120, 121, 123, 125) that the ratio of pressure increase to the amount of propionaldehyde decomposed is approximately unity. Figure 23 confirms the above fact. This figure shows a plot of the pressure of CO formed against time at  $540^{\circ}\text{C}$  and  $100$  mm pressure. The rate of formation of CO obtained from Figure 23 agrees with the rate obtained from pressure increase (Figure 24) within 6%. All of the rate measurements were, therefore, made from the pressure increase recorded automatically.

Figure 24 shows double logarithmic plots of initial rates against initial pressures of propionaldehyde at different temperatures. The order

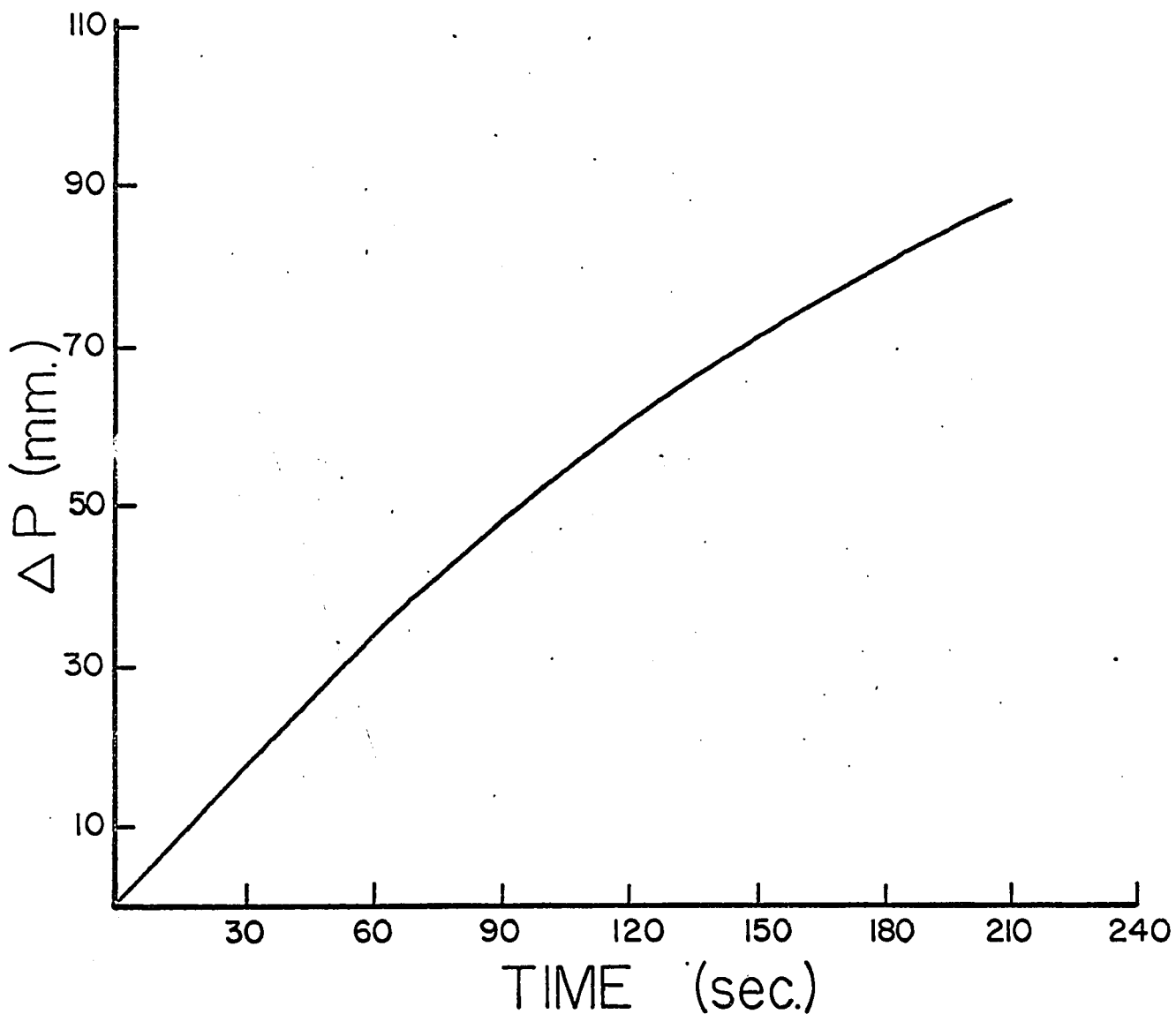
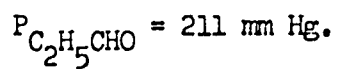


Figure 22. Typical pressure-time curve for the uninhibited decomposition of propionaldehyde



Temperature = 550°C.

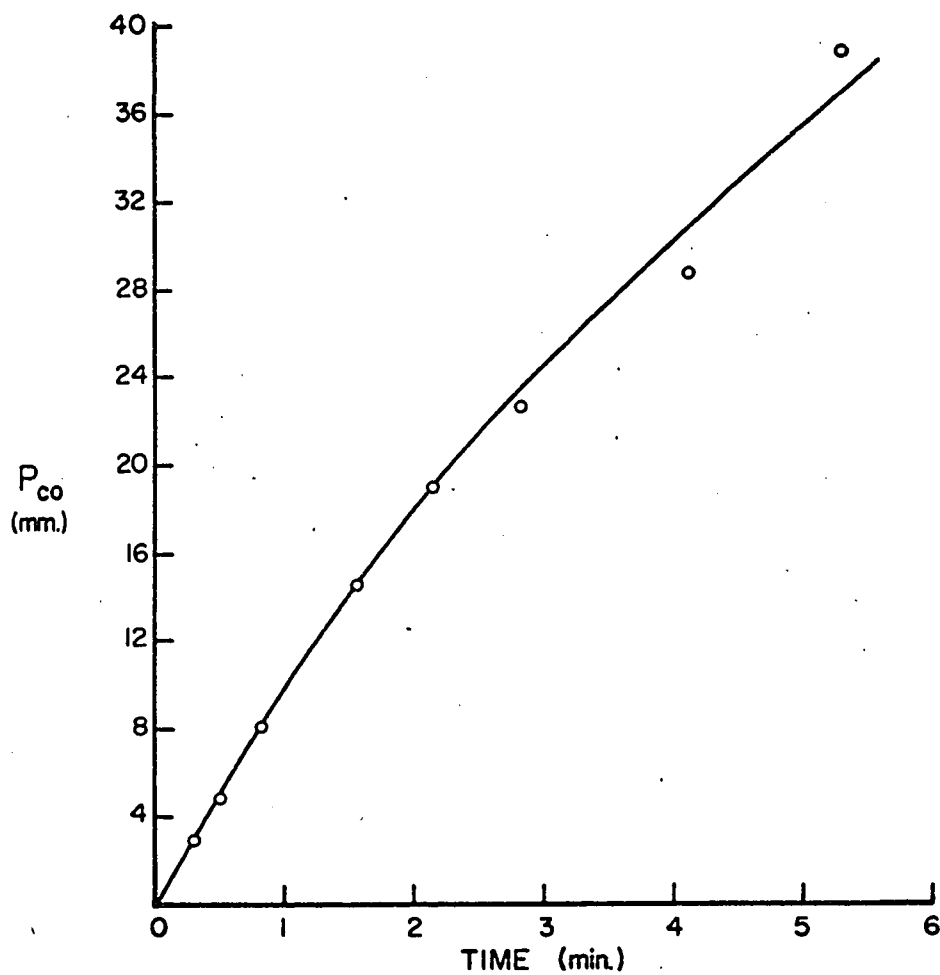


Figure 23. Plot of the pressure of carbon monoxide formed against time with 100 mm of propionaldehyde at 540°C.

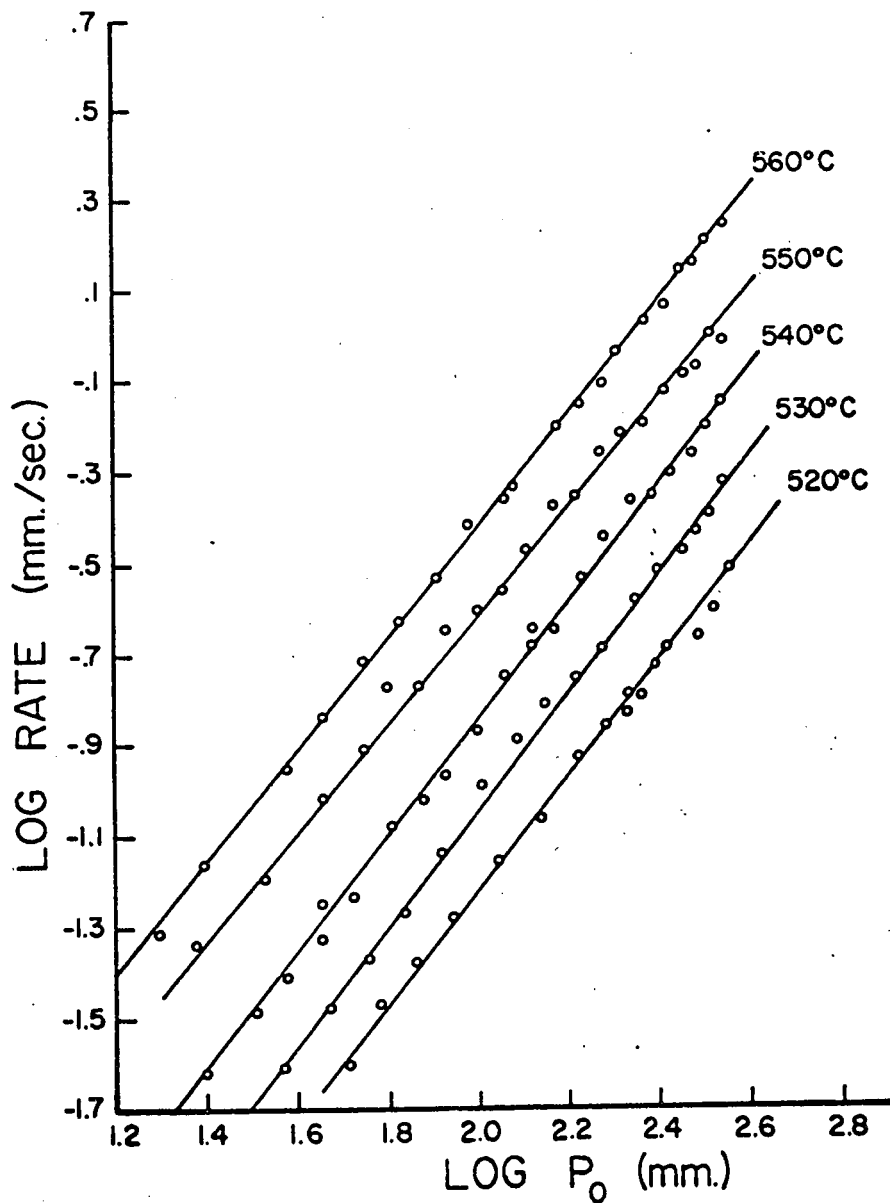


Figure 24. Double logarithmic plots of initial rate against initial pressure of propionaldehyde at different temperatures.

is seen to be between 1.25 and 1.30. This result is in apparent disagreement with the results of Márta (124), but in close agreement with those of Hinsherwood and co-workers (120, 121) and of HO (125). The results of the present investigation are not directly comparable with those of Boyer and Niclause (123) because of the much lower temperature used by the latter.

Figure 25 shows that excess of added  $\text{CO}_2$  and  $\text{C}_2\text{H}_6$  has no effect on the reaction at  $520^\circ\text{C}$ . This is in agreement with the high pressure results of Hinshelwood and Thompson (120). The same effect has been observed by Márta (124) in the presence of a variety of inert gases. Figure 26 shows the effect of 100 mm  $\text{CO}_2$  added to 100 mm propionaldehyde on the rate of formation of ethylene and ethane. It is clear that the added inert gas has little effect on the rates of formation of ethylene and ethane. In this connection it may be mentioned that in a study of the pyrolysis of n-butane by Purnell and Quinn (126) the ratio  $v_{\text{C}_2\text{H}_4}/v_{\text{C}_2\text{H}_6}$  has been found to increase with the addition of an inert gas at n-butane pressures below 24 mm Hg.

Figure 27 shows a plot of  $P_{\text{C}_2\text{H}_6}/P_{\text{C}_2\text{H}_4}$  against  $P_{\text{C}_2\text{H}_5\text{CHO}}$  at  $540^\circ\text{C}$  at 6% decomposition. The curve shows a slight negative curvature. In Figure 28 is shown a plot of  $v_{\text{C}_2\text{H}_6}/v_{\text{C}_2\text{H}_4} [\text{C}_2\text{H}_5\text{CHO}]^{1/2}$  against  $[\text{C}_2\text{H}_5\text{CHO}]^{1/2}$ . At the initial stage of decomposition  $P_{\text{C}_2\text{H}_6}/P_{\text{C}_2\text{H}_4}$  will be equal to  $v_{\text{C}_2\text{H}_6}/v_{\text{C}_2\text{H}_4}$ .

As will be shown later, the over-all rate can be divided into two parts - one part varying as  $[\text{C}_2\text{H}_5\text{CHO}]^{1/2}$  and the other as  $[\text{C}_2\text{H}_5\text{CHO}]^{3/2}$ . Figure 29 shows a plot of  $v_0/P_{\text{C}_2\text{H}_5\text{CHO}}^{1/2}$  against  $P_{\text{C}_2\text{H}_5\text{CHO}}$  at different temperatures. The one-half order rate constants are given by the intercepts and the three-halves order ones by the slopes. The rate constants thus

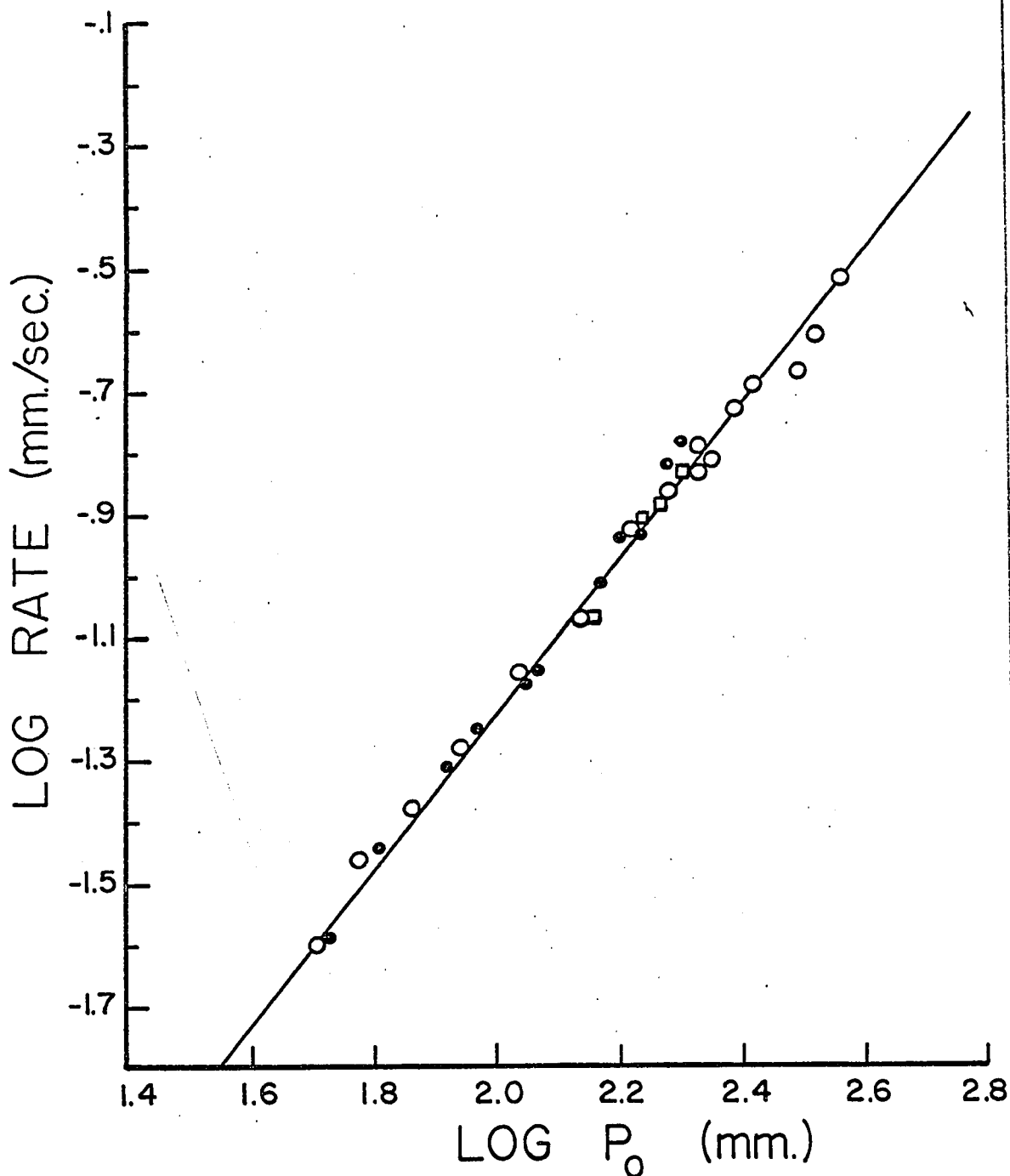


Figure 25. Plot of log rate against log pressure of propionaldehyde showing the effect adding  $\text{CO}_2$  and  $\text{C}_2\text{H}_6$ . Rates with no inert gas are shown as  $\text{O}$ , those with added  $\text{CO}_2$  ( $\frac{\text{CO}_2}{\text{C}_2\text{H}_5\text{CHO}} = 0.5$ ) as  $\square$ , and those with added  $\text{C}_2\text{H}_6$  ( $\frac{\text{C}_2\text{H}_6}{\text{C}_2\text{H}_5\text{CHO}} = 0.5 - 2.0$ ) as  $\bullet$ . Temperature =  $520^\circ\text{C}$ .

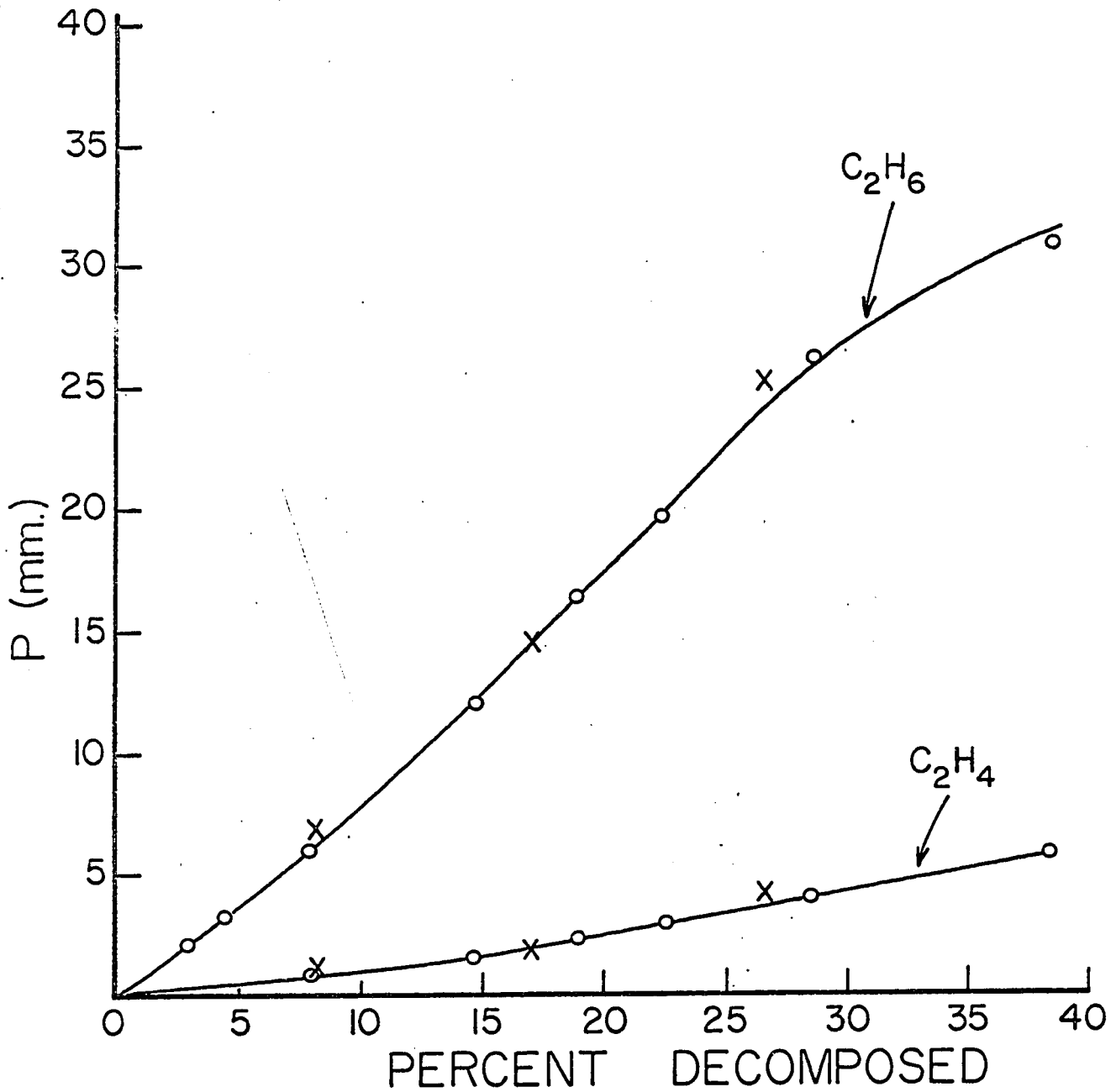


Figure 26. Plots of the pressures of  $C_2H_6$  and  $C_2H_4$  formed against the percentage of propionaldehyde decomposed showing the effect of adding 100 mm of  $CO_2$  to 100 mm of propionaldehyde without  $CO_2$ , O; with  $CO_2$ , X.

Temperature =  $540^\circ C$ .

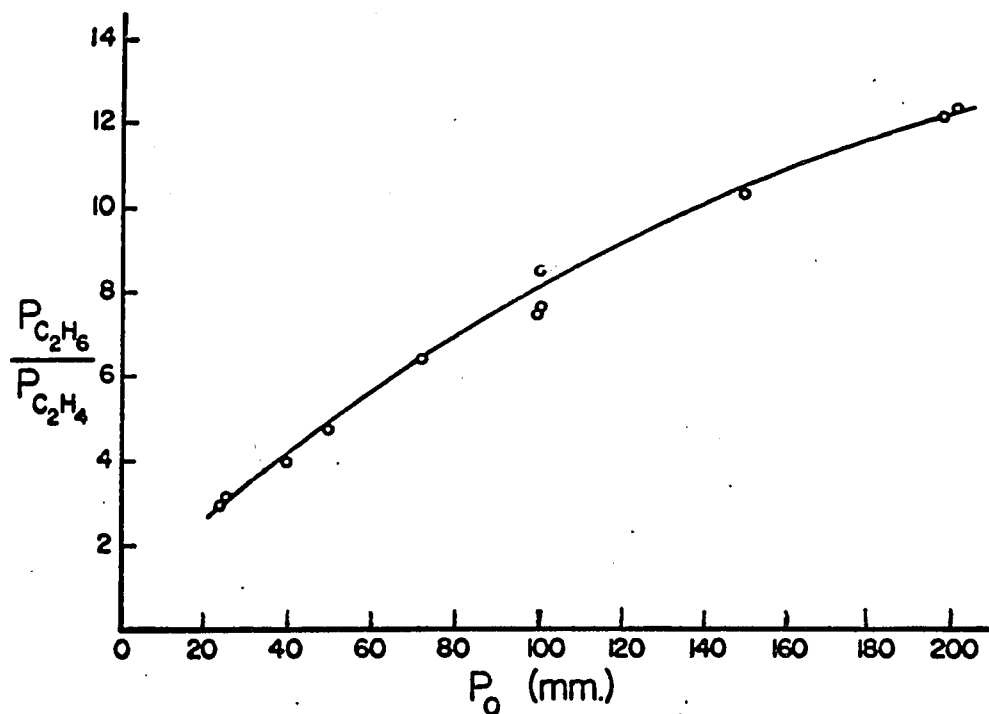


Figure 27. Plot of the ratio  $\frac{P_{C_2H_6}}{P_{C_2H_4}}$  against the initial pressure of propionaldehyde for 6 percent decomposition.

Temperature = 540°C.

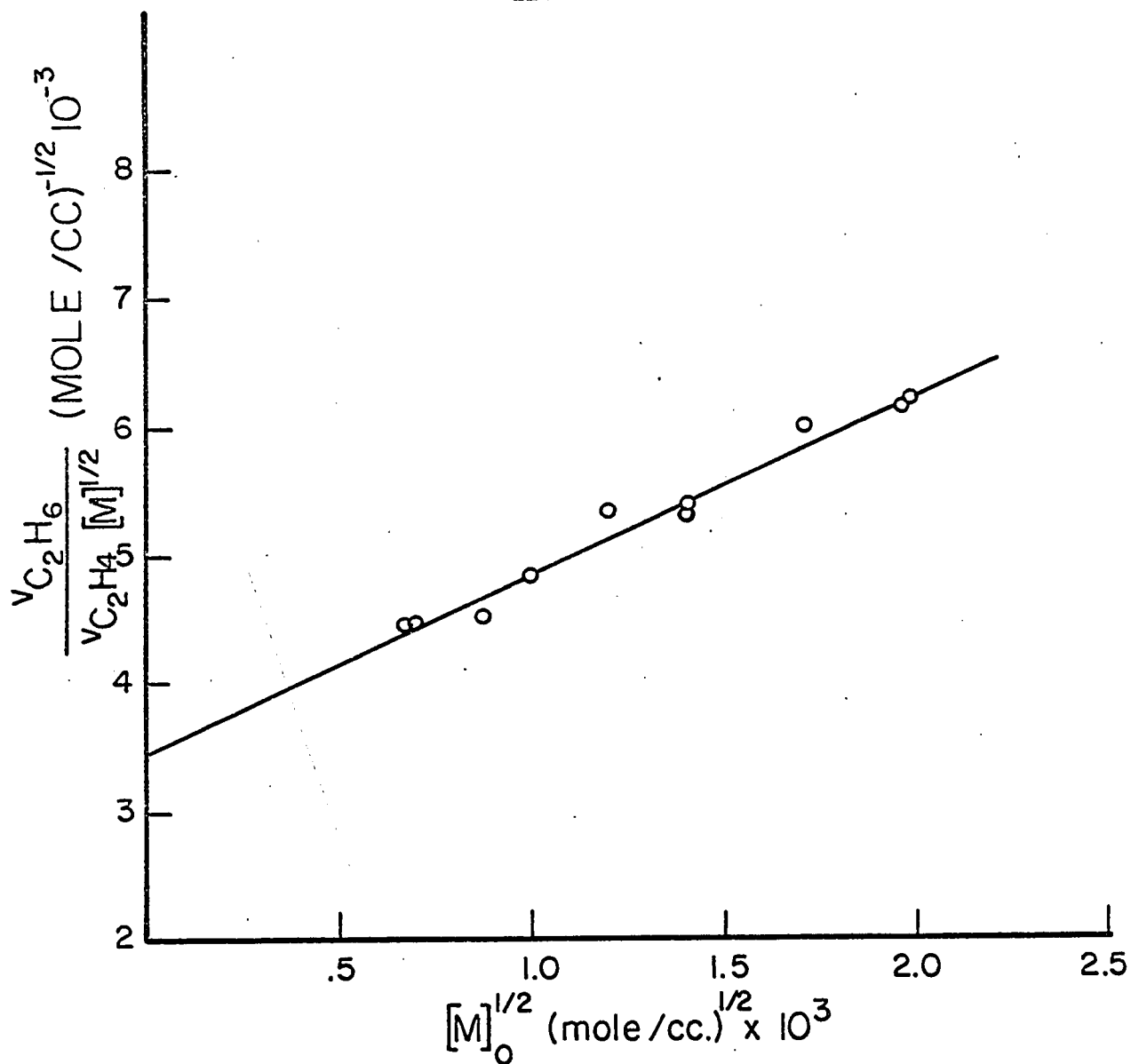


Figure 28. Plot of  $v_{C_2H_6} / v_{C_2H_4} [C_2H_5CHO]^{1/2}$  against  $[C_2H_5CHO]^{1/2}$  at 540°C.

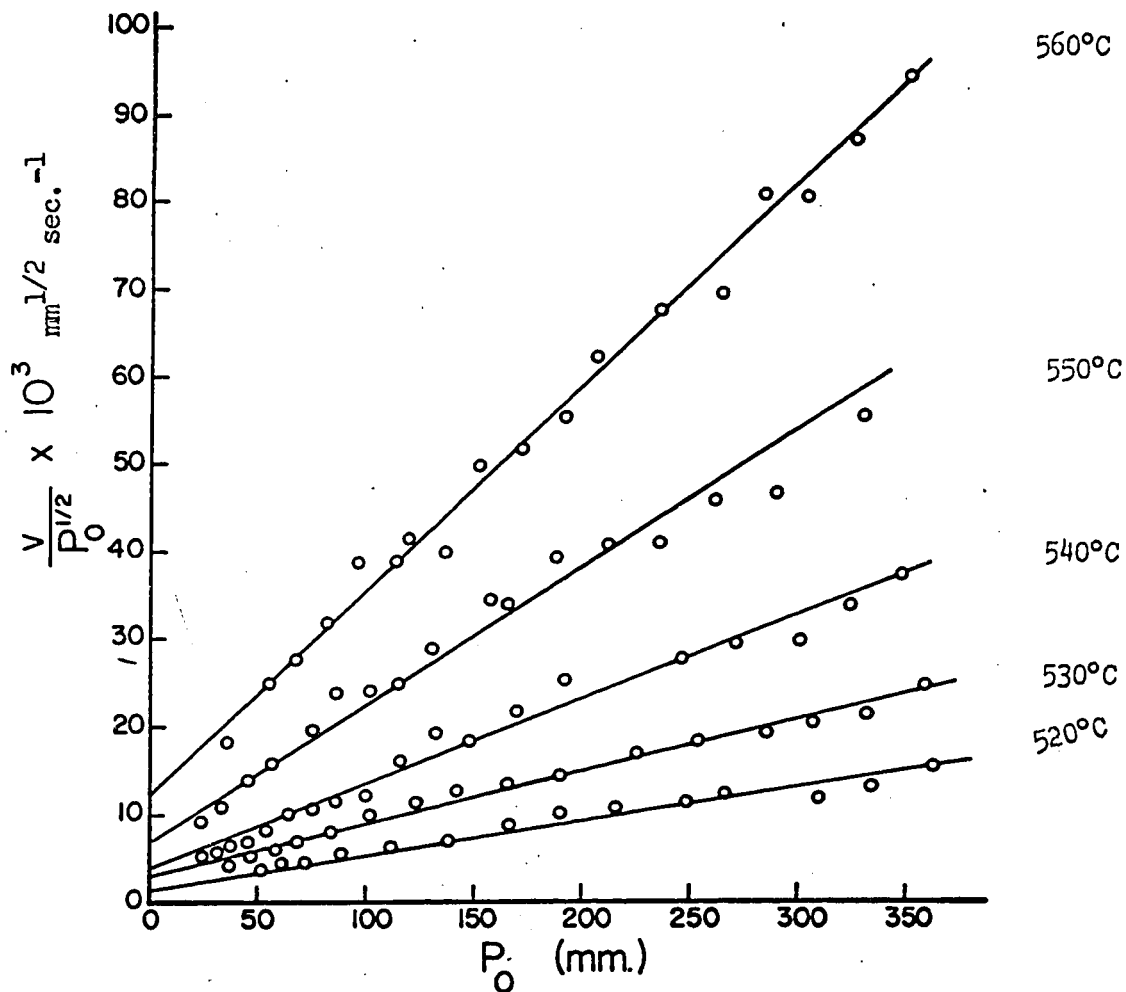


Figure 29. Plots of  $v/P_{C_2H_5CHO}^{1/2}$  against  $P_{C_2H_5CHO}$  at different temperatures.

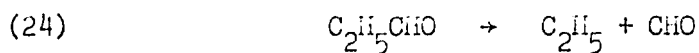
obtained are listed in Table 6.

These rate constants are plotted against the reciprocals of temperatures in Figure 30. The lower curve which shows the plot of one-half order rate constants gives an activation energy of 70.8 kcal per mole. The activation energy of the three-halves order process is given by the upper curve and calculated to be 57.1 kcal per mole.

### DISCUSSION

#### Overall Reaction Mechanism

It is now generally agreed (122-125) that in the thermal decomposition of propionaldehyde  $C_2H_5$  is the most abundant radical and that the combination of  $C_2H_5$  radicals is the predominant chain ending process. The fact that significantly more ethane than ethylene is produced (Figure 27) indicates that the concentration of H atoms is much lower than that of  $C_2H_5$  radicals. It will be shown later that the molecular decomposition producing ethane is of minor importance under the conditions of the present investigations. Since the combination of  $C_2H_5$  radicals is a pressure independent process under ordinary pyrolytic conditions (40, 127), and inert gases have no effect on the rate of decomposition (Figures 25 and 26), chain initiation must be a first order process. In line with other work (123-125), this process can be suggested as



on the basis of the energetics of the reaction.

Table 6

ONE-HALF ORDER AND THREE-HALVES ORDER RATE  
CONSTANTS FOR THE UNINHIBITED DECOMPOSITION OF  
PROPIONALDEHYDE

Temperature (°C)	$k_{1/2} \times 10^3$ ( $\text{mm}^{1/2} \text{sec}^{-1}$ )	$k_{3/2} \times 10^5$ ( $\text{mm}^{-1/2} \text{sec}^{-1}$ )
520	1.48	3.75
530	2.75	6.23
540	4.02	10.10
550	6.50	15.63
560	12.10	23.75

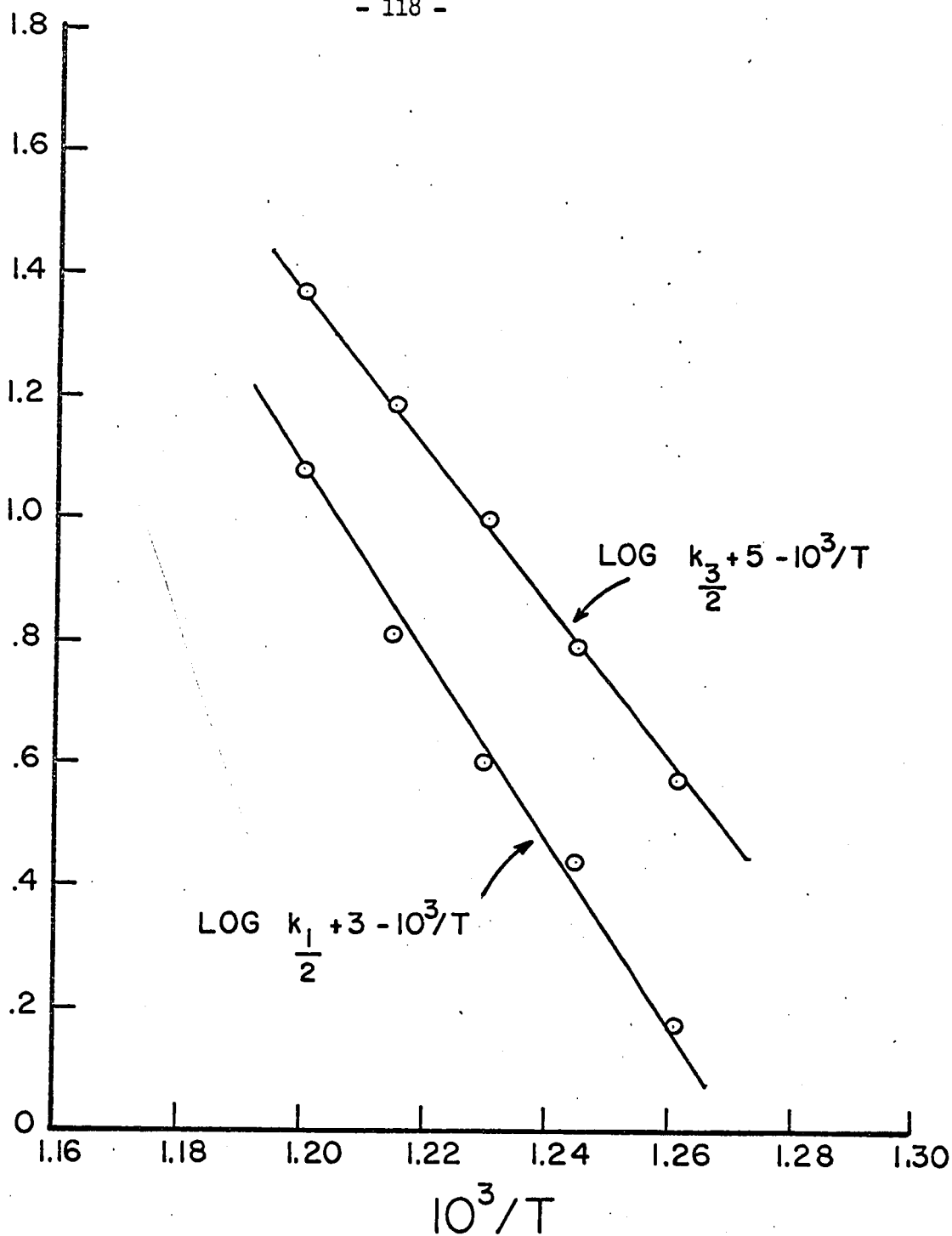
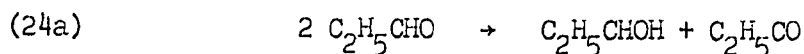


Figure 30. Arrhenius plots. The lower curve shows the plot of  $10^3 k_{1/2} \text{ mm}^{1/2} \text{ sec}^{-1}$  and the upper one that of  $10^5 k_{3/2} \text{ mm}^{-1/2} \text{ sec}^{-1}$ ,  $k_{1/2}$  and  $k_{3/2}$  being the one-half and the three-halves order rate constants respectively.

It can easily be shown that, unlike the situation with acetaldehyde (Part 3), the above splitting reaction (24) is more favourable thermodynamically than the following abstraction reaction



$\Delta H_{24}$  and  $\Delta S_{24}$  are calculated to be 81.6 kcal per mole and 34.4 cal. per mole per deg. respectively.  $\Delta H_{24a}$  and  $\Delta S_{24a}$  are estimated at  $\sim 54.7$  kcal per mole and  $\sim 4.7$  cal. per mole per deg. respectively. The value for  $D(\text{C}_2\text{H}_5\text{CHOH} - \text{H})$  is estimated at 90.0 kcal per mole by comparison with iso- $\text{C}_3\text{H}_7 - \text{H}$  and  $t - \text{C}_4\text{H}_9 - \text{H}$  (55) and that for  $D(\text{C}_2\text{H}_5\text{CO} - \text{H})$  is taken to be 85 kcal per mole by comparison with  $D(\text{CH}_3\text{CO} - \text{H})$  (55). Other thermal data have been taken from Szwarc (128) and from Benson (129). Entropies (for the standard state of 1 mole per litre at 25°C) have been calculated following Benson (129). Assuming comparable frequency factors for reactions (24) and (24a)

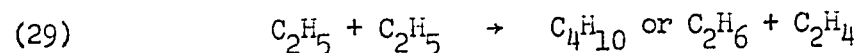
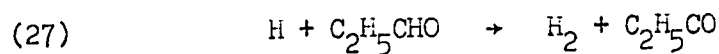
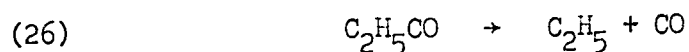
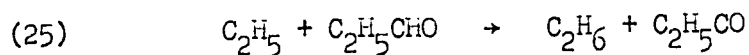
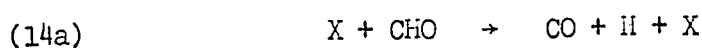
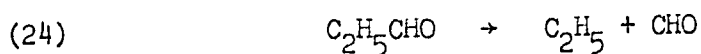
$$\frac{v_{24}}{v_{24a}} = \frac{e^{29.6/R} e^{-\frac{27000}{RT}}}{[\text{C}_2\text{H}_5\text{CHO}]} = 8.6 \text{ at } 800^\circ\text{K and } 1 \text{ atm pressure. At } 362 \text{ mm}$$

pressure (the highest pressure studied) this ratio is 18.1 at 800°K and higher at temperatures. The abstraction reaction (24a) is, therefore, probably unimportant in comparison with the splitting reaction (24) in the pyrolysis of propionaldehyde.

Since the ratio  $\frac{P_{\text{C}_2\text{H}_6}}{P_{\text{C}_2\text{H}_4}}$  decreases with decrease of pressure

(Figure 27) but increases with decrease of temperature (Table 7), the two reactions producing ethane and ethylene must be in competition with each other. The same conclusion has been drawn by Purnell and Quinn (126) from their experimental results in the pyrolysis of n-butane.

The mechanisms to which the above considerations lead is



This mechanism without reaction (28) is very similar to that proposed by Boyer and Niclause (123) and by Márta (124). Application of the steady-state treatment to the above mechanism gives rise to the following expressions for the radical concentrations:

$$[\text{C}_2\text{H}_5] = \left( \frac{k_{24}}{k_{29}} \right)^{1/2} [\text{C}_2\text{H}_5\text{CHO}]^{1/2} \quad (52)$$

$$[\text{H}] = \frac{k_{24}}{k_{27}} + \frac{k_{28}}{k_{27}} \left( \frac{k_{24}}{k_{29}} \right)^{1/2} [\text{C}_2\text{H}_5\text{CHO}]^{1/2} \quad (53)$$

Table 7

RATIOS OF DECOMPOSITION PRODUCTS

Initial Pressure = 100 mm Hg.

Temperature °C	$\frac{C_2H_6}{C_2H_4}$	$\frac{H_2}{C_2H_4}$
560	5.86	1.80
560	5.73	1.80
540	7.47	1.33
540	7.56	1.50
540	8.50	1.50
520	10.25	1.25
520	10.62	1.30

Assuming large chain lengths, the rate of disappearance of propionaldehyde can be written as

$$v = k_{25} \left( \frac{k_{24}}{k_{29}} \right)^{1/2} [C_2H_5CHO]^{3/2} + k_{28} \left( \frac{k_{24}}{k_{29}} \right)^{1/2} [C_2H_5CHO]^{1/2} \quad (54)$$

A similar rate equation has been suggested by HO (125) to fit his experimental results of the pyrolysis of iso-butylaldehyde.

---

Comparison of the Experimental and Predicted Values of the Ratio  $v_{C_2H_6}/v_{C_2H_4}$

---

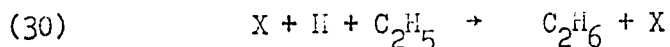
In equation (54) the first term represents the rate of formation of ethane and the second term that of ethylene. The ratio of the two terms at 540°C and 100 mm pressure is

$$\frac{v_{C_2H_6}}{v_{C_2H_4}} = \frac{k_{25}}{k_{28}} [C_2H_5CHO] = 2.9$$

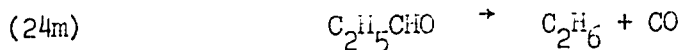
the values for the rate constants  $k_{25}$  and  $k_{28}$  being taken from Table 8. The agreement of this calculated value with the experimental result 8.1 (Figure 27) within a factor of less than 3 must be considered satisfactory in view of the fact that an uncertainty of 1 kcal per mole in the value of E changes this ratio by a factor of about 2. This agreement lends support to the suggested mechanism.

Contribution of the Molecular Process  $C_2H_5CHO \rightarrow C_2H_6 + CO$

The predominance of the chain termination reaction



over reaction (29) at low pressures does not affect the order of ethane formation. Reaction (30) is placed in its pressure dependent region, because the excited species  $C_2H_6^*$  has at least 12 kcal more than required to split up into two  $CH_3$  radicals. If the decomposition of  $C_2H_5$  radicals is a pressure dependent process, the order of ethylene formation will tend to 3/2 as the pressure is lowered and a plot of  $P_{C_2H_6}/P_{C_2H_4}$  against  $P_{C_2H_5CHO}$  should show a positive curvature. The reverse character of the above plot (Figure 27) is attributed to the formation of some ethane by the molecular process.



and to reaction (28) being in its first-order high-pressure region. This latter conclusion is also supported by Figure 26.

The contribution of reaction (24m) to the overall rate may be estimated in the following way.

$$v_{C_2H_6} = k_{24m}[C_2H_5CHO] + k_{25} \left( \frac{k_{24}}{k_{29}} \right)^{1/2} [C_2H_5CHO]^{3/2} \quad (55)$$

$$v_{C_2H_4} = k_{28} \left( \frac{k_{24}}{k_{29}} \right)^{1/2} [C_2H_5CHO]^{1/2} \quad (56)$$

$$v_{C_2H_6}/v_{C_2H_4} = \frac{k_{24m}}{k_{28}} \left( \frac{k_{29}}{k_{24}} \right)^{1/2} [C_2H_5CHO]^{1/2} + \frac{k_{25}}{k_{28}} [C_2H_5CHO] \quad (57)$$

$$\frac{v_{C_2H_6}}{v_{C_2H_4}} \left( \frac{1}{[C_2H_5CHO]} \right)^{1/2} = \frac{k_{24m}}{k_{28}} \left( \frac{k_{29}}{k_{24}} \right)^{1/2} + \frac{k_{25}}{k_{28}} [C_2H_5CHO]^{1/2} \quad (58)$$

From Figure 28

$$\frac{k_{24m}}{k_{28}} \left( \frac{k_{29}}{k_{24}} \right)^{1/2} = 3.4 \times 10^3 \text{ cc}^{1/2} \text{ mole}^{-1/2} \text{ at } 540^\circ\text{C.}$$

Inserting the values of  $k_{24}$ ,  $k_{28}$  and  $k_{29}$  from Table 8, the value of  $k_{24m}$  calculated to be  $0.53 \times 10^{-5} \text{ sec}^{-1}$ . A comparison of the rate calculated from the above rate constant with the overall rate (Figures 23 and 24) shows that the molecular process constitutes less than 4% of the overall process. In view of uncertainties in the various parameters, it is, however, felt that this contribution may not be greater than 10% of the total rate.

#### Activation Energies

The predicted activation energies for the one-half and three-halves order reactions are given by the expressions

Table 8

KINETIC PARAMETERS FOR ELEMENTARY REACTIONS

Reaction	Frequency factor*	Activation energy (kcal mole <sup>-1</sup> )	References
(24)	$1.7 \times 10^{15}$	82.8	Márta (124)
(25)	$2.36 \times 10^{11}$	7.6	Volman and Brinton (130)
(28)	$6.3 \times 10^{13}$	39.5	Bywater and Steacie (131) and Trotman-Dickenson (132)
(29)	$1.6 \times 10^{13}$	0	Ivin and Steacie (133) and Shepp and Kutsckke (134)

\* sec.<sup>-1</sup> or cc mole<sup>-1</sup> sec.<sup>-1</sup>

$$E_{1/2} = E_{28} + \frac{1}{2} (E_{24} - E_{29}) \quad (59)$$

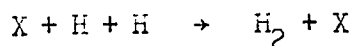
and

$$E_{3/2} = E_{25} + \frac{1}{2} (E_{24} - E_{29}) \quad (60)$$

respectively. Insertion of the values for  $E_{24}$ ,  $E_{28}$  and  $E_{29}$  from Table 8 leads to 80.9 kcal per mole for  $E_{1/2}$  and 49.0 kcal per mole for  $E_{3/2}$ . Agreement of these two values with the respective experimental results 70.8 kcal and 57.1 kcal is not very good. This can probably be attributed to other chain ending steps such as



and

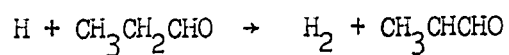
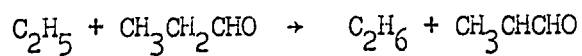


becoming important at low pressures.

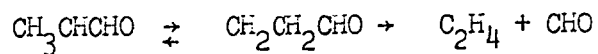
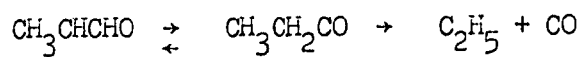
The overall rate of decomposition of propionaldehyde is significantly lower than that of acetaldehyde (125, Part 3) probably because of shorter chain lengths in the former. The activation energy of the over all rate of the former is about 7 kcal higher than that of the latter. The above facts may be explained as follows:

(1) The chain termination process in acetaldehyde is a third-order process, whereas that in propionaldehyde is a second-order one.

(2) H atoms and  $C_2H_5$  radicals may abstract H atoms other than those attached to the carbonyl groups.



The  $\text{CH}_3\dot{\text{C}}\text{HCHO}$  radical will mainly be involved in a chain-ending step because of its higher stability. Higher temperatures may, however, favour the following reactions



giving rise to a larger chain lengths and consequently a higher activation energy than predicted.

Part VI

THE DECOMPOSITION OF PROPIONALDEHYDE IN THE  
PRESENCE OF NITRIC OXIDE

INTRODUCTION

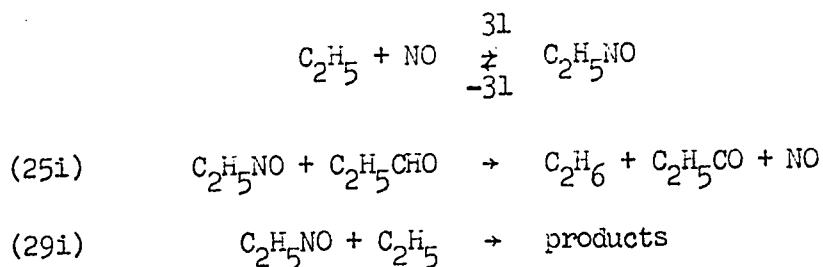
The mechanism of the pyrolysis of propionaldehyde in the presence of nitric oxide has been a matter of more uncertainty than that in the absence of nitric oxide. The nature of the maximally inhibited reaction has been a matter of great dispute, and not much has been discovered about the catalytic action of nitric oxide on this reaction. There have been disagreements on many experimental facts, and further careful study is called for.

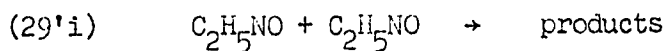
Review of the Earlier Work

In 1936, Staveley and Hinshelwood (98, 99) studying the pyrolysis of propionaldehyde in the temperature range 489°C - 606°C, found that the reaction was inhibited by small amounts of nitric oxide and that there was catalysis at high nitric oxide pressures. The values for the activation energies of the maximally inhibited reaction varied from 58.5 kcal per mole at 30 mm to 51.0 kcal per mole at 350 mm pressure of propionaldehyde. It was suggested that the maximally inhibited reaction was a molecular process, the chain part being completely suppressed by nitric oxide. This suggestion has no firm experimental basis.

Smith and Hinshelwood (100), reinvestigating this reaction at 550°C, found that both nitric oxide and propylene reduced the rate by the same amount and also concluded that the maximally inhibited reaction was a molecular process. Previous work in these laboratories, and the extensive isotopic mixing observed in the pyrolysis of organic compounds in the presence of inhibitors, show that the reduction to the same limiting rate by different inhibitors is no evidence for the conclusion that the maximally inhibited reaction is a molecular process.

That nitric oxide is not consumed during the course of the reaction has recently been demonstrated by Szabó and Márta (111, 112). The reaction inhibited by nitric oxide was first allowed to go to completion and then a new dose of about the same amount of propionaldehyde as used in the previous experiment was introduced. The reaction was found to be inhibited to the same extent. The reaction was studied in the temperature range 515° - 565°C and the overall order was reported to be three-halves with respect to propionaldehyde at all pressures of nitric oxide used (0 - 60 mm) and approximately one-half order with respect to nitric oxide at high nitric oxide pressures. They attempted to explain these results by adding the following reactions





to the scheme of the uninhibited reactions originally suggested by Boyer and Niclause (123). Figure 31 shows the plots of the logarithms of  $k_{25i}K_{31}/k_{25}$ ,  $k_{29i}K_{31}/k_{29}$  and  $k_{29i}^2K_{31}^2/k_{29}$  against the reciprocals of temperatures. From this Figure the following expressions for the activation energies are obtained:

$$E_{25i} + E_{K_{31}} - E_{25} = -25.1 \text{ kcal per mole}$$

$$E_{29i} + E_{K_{31}} - E_{29} = -15.1 \text{ kcal per mole}$$

and

$$E_{29'i} + 2E_{K_{31}} - E_{29} = -37.9 \text{ kcal per mole}$$

Insertion of the values of  $E_{25}$  and  $E_{29}$  from Table 10 and rearrangement give

$$E_{29i} - E_{25i} = 2.4 \text{ kcal per mole}$$

$$E_{29'i} - 2E_{25i} = -2.9 \text{ kcal per mole}$$

Following Ree, Yang and Eyring (113)  $E_{25i}$  is calculated to be 26.0 kcal per mole. This leads to the values of 28.4 and 49.1 kcal per mole for  $E_{29i}$  and  $E_{29'i}$  respectively. These impossibly high activation energies for the chain-ending steps obviously suggest that the above suggested mechanism does not represent the complete picture.

Recently Ho (125) studying the pyrolysis of different aldehydes in the presence of nitric oxide, propylene and isobutene found that in the

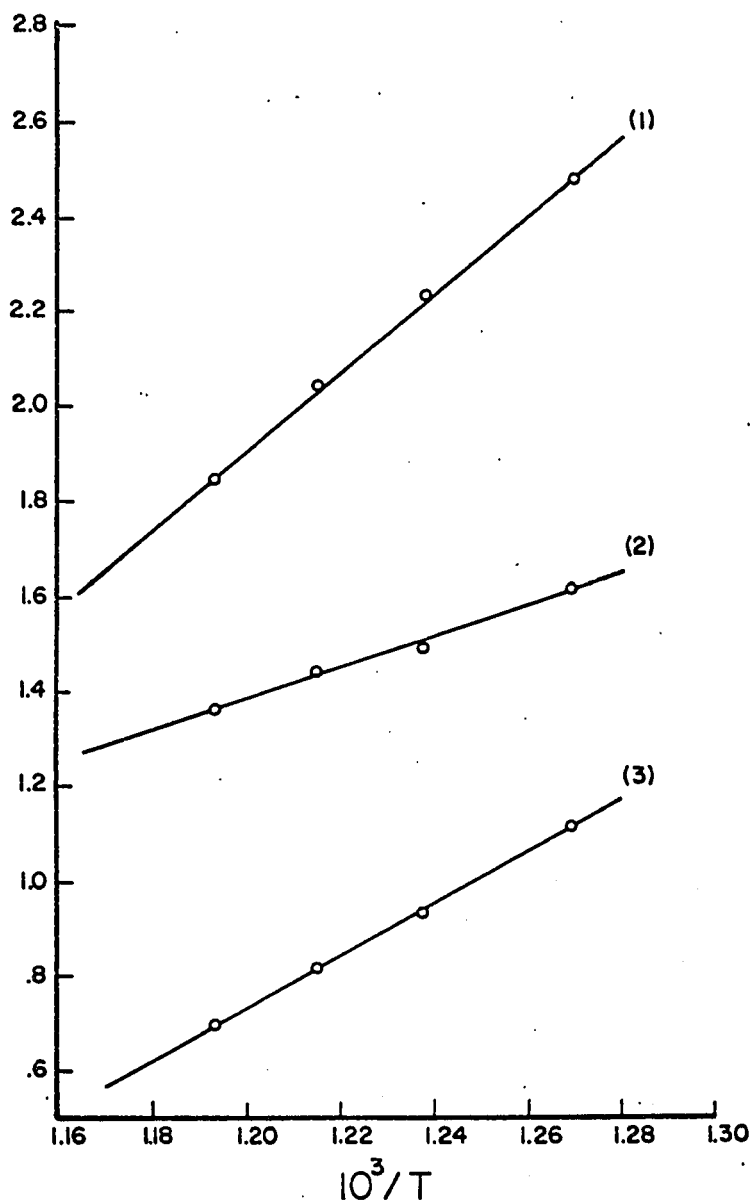
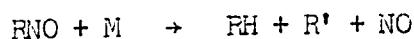


Figure 31. Arrhenius plots. (1) Plot of  $\log 10^5 \frac{k'_{29} K_{31}^2}{k_{29}}$  against  $1/T$   
 (2) plot of  $\log 10 \frac{k_{29} K_{31}}{k_{29}}$  against  $1/T$  (3) plot of  
 $\log 10 \frac{k_{25} K_{31}}{k_{25}}$  against  $1/T$ .

case of propionaldehyde studied at 522.5°C, nitric oxide was more efficient as an inhibitor than propylene and isobutene in disagreement with the work of Smith and Hinshelwood (100). The degree of inhibition was found to decrease with the increase of propionaldehyde pressure in contrast to the conclusion of Szabó and Márta (111, 112) that the degree of inhibition was independent of propionaldehyde pressure.

Previous work (101 - 107) in these laboratories has shown that in the pyrolysis of hydrocarbons and ethers nitric oxide starts chains by abstracting hydrogen atoms and ruptures them by being involved in chain-ending reactions. Aldehydes present an additional interesting feature in that they contain a labile aldehydic hydrogen atom. It has been shown (Part 4) on the basis of experimental results and of calculated activation energies that the following chain-propagating reaction involving a species containing nitric oxide



is significantly more important in acetaldehyde than in hydrocarbons. Though Szabó and Márta (111, 112) have suggested this reaction in the pyrolysis of propionaldehyde the exclusion of the chain initiation by nitric oxide leads, as shown above, to the impossibly high activation energies for the chain-ending steps in order for their mechanism to be consistent with their experimental results.

The present work describes an experimental study of the pyrolysis of propionaldehyde in the presence of nitric oxide. An attempt has been made to explain the results on the basis of the above ideas.

### EXPERIMENTAL

The apparatus used was the same as that described in Part 3. The reaction was carried out in the same vessel as that was used for the uninhibited reaction. The procedure followed to ensure complete mixing of propionaldehyde and nitric oxide was the same as described in Part 4. The analysis of the products was made by a Perkin-Elmer Vapor Fractometer containing a 4-metre silica gel column maintained at 30°C.

### Results

The decomposition was studied in the temperature range 520 - 560°C. A typical pressure - time record of the reaction catalysed by nitric oxide is shown in Figure 32. Rates were obtained from the initial slopes. At low pressures of nitric oxide a short induction period was noticed. It was, however, too small to make any significant difference between the measured inflection rates and the extrapolated initial ones.

It has been shown by Staveley and Hinshelwood (99) and Ho (125) that in the maximally inhibited region 1 mm pressure increase corresponds to the reaction of 1 mm of propionaldehyde. In Figure 33 is shown a plot of the pressure of carbon monoxide formed against time with 100 mm propionaldehyde and 14 mm nitric oxide at 540°C. The rate of formation of carbon monoxide obtained from Figure 33 is found to agree within 4 percent with the overall rate obtained from pressure increase. All of the rate

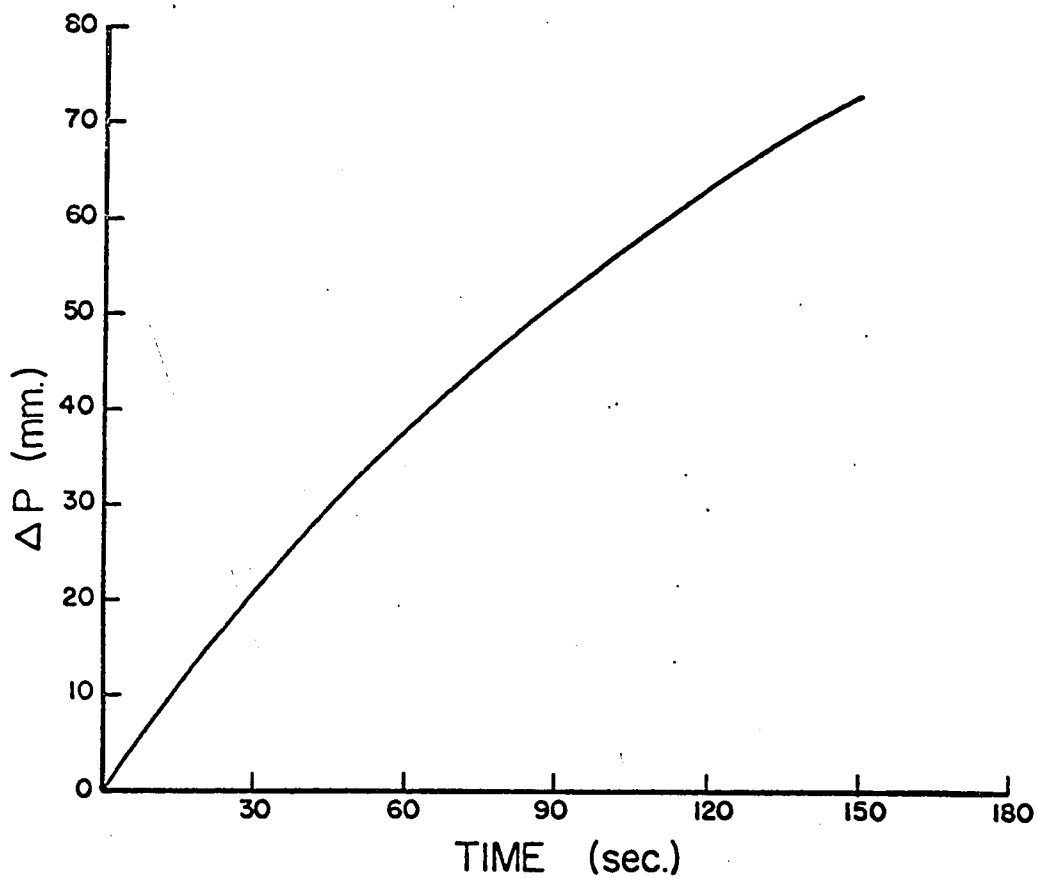


Figure 32. Typical  $\Delta P$ -t curve for the decomposition of propionaldehyde catalysed by nitric oxide.

Propionaldehyde pressure = 200 mm Hg

Nitric oxide " = 55 mm Hg

Temperature = 540°C

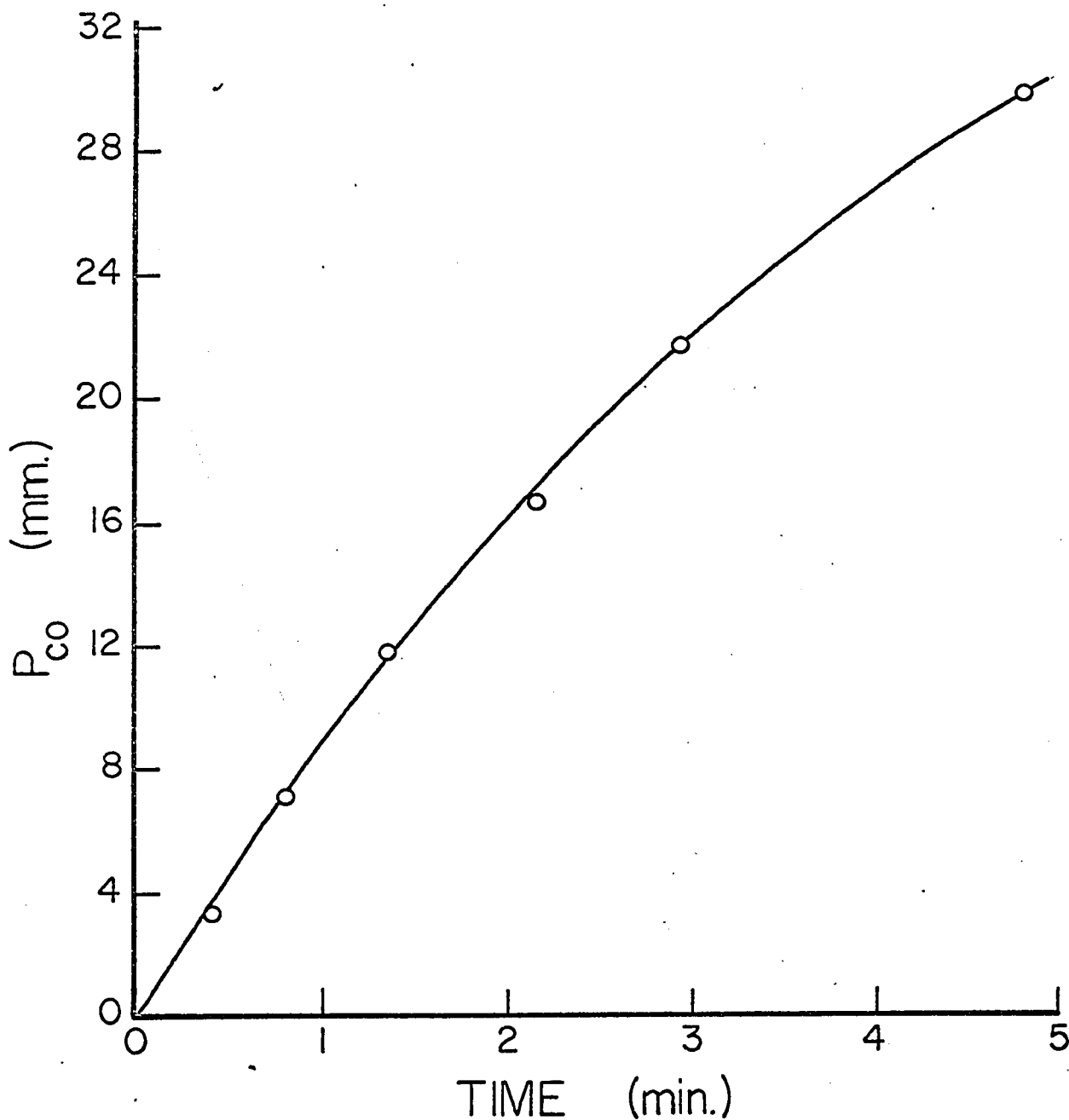


Figure 33. Plot of the pressure of carbon monoxide formed against time with 14 mm nitric oxide added to 100 mm propionaldehyde.

Temperature = 540°C.

measurements were, therefore, made from the pressure increases which were recorded automatically.

Figure 34 shows the effect of nitric oxide on the products of reaction in the catalytic region at 540°C. The overall rate is equal to that in the absence of nitric oxide. Ethylene formation shows marked increase and hydrogen production appears to decrease slightly.

In Figure 35 is shown a plot of relative rate  $v_{NO}/v_{uninhibited}$  against pressure of nitric oxide at different propionaldehyde pressures and at 540°C. It is seen that small amounts of nitric oxide inhibits the reaction but that larger amounts shows strong catalysis. The ratio  $v_{minimum}/v_{uninhibited}$  increases with the increase of propionaldehyde pressure; This result does not agree with the results of Szabó and Márta (111, 112) but is in agreement with those of Ho (125). At higher nitric oxide pressures, the relative rate is approximately independent of the propionaldehyde pressure. This result is in agreement with the results of Szabó and Márta (111, 112) but apparently in disagreement with those of Ho (125).

Figure 36 shows a double logarithmic plot of initial rates against initial pressures of propionaldehyde at 1 mm and 60 mm of nitric oxide at 540°C. The lower curve with 1 mm of nitric oxide represents approximately the maximally inhibited rate and gives an order of 1.5. From the upper curve, with 60 mm nitric oxide, an order of 1.25 is obtained.

Figure 37 shows a double logarithmic plot of initial rates against initial pressures of propionaldehyde with 60 mm nitric oxide. The order of the reaction is seen to be 1.25 with respect to propionaldehyde. Since the orders of the reaction in the absence (Part 5) and presence of large amounts of nitric oxide are the same, the relative rate must be independent of

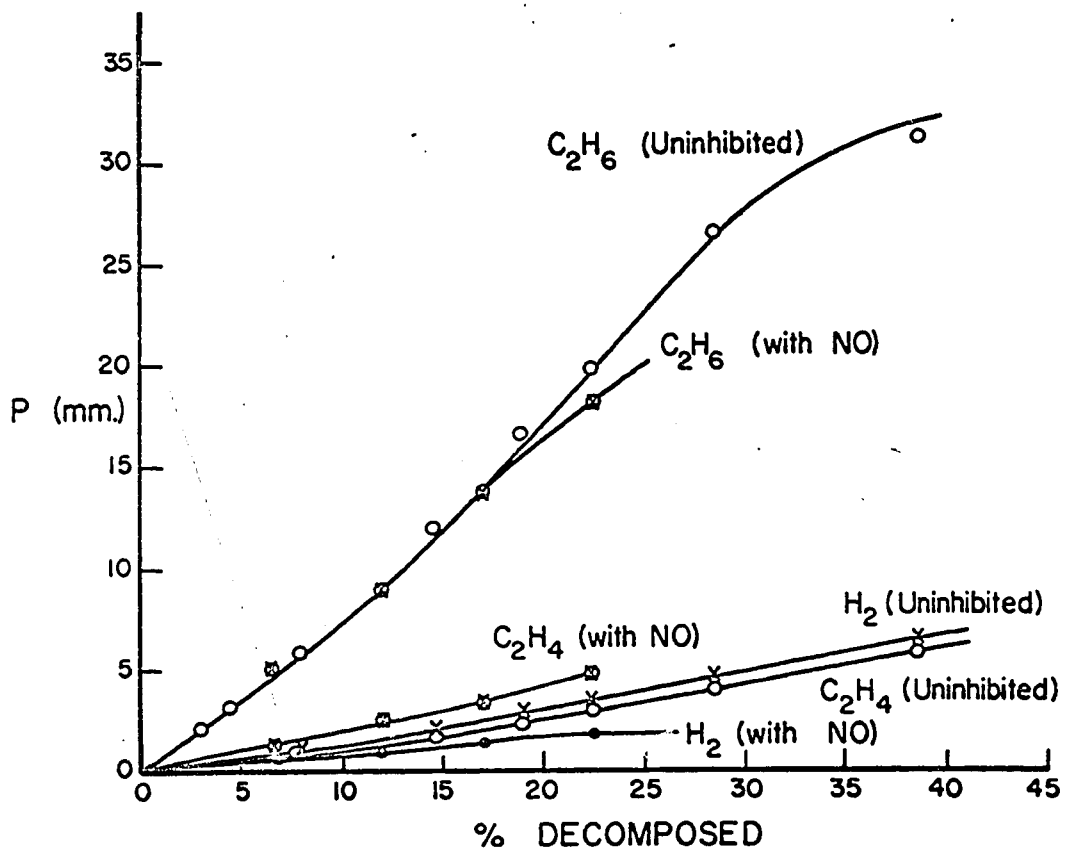


Figure 34. Analytical results for the decomposition of propionaldehyde in the absence and presence of 14 mm of nitric oxide.

Propionaldehyde pressure = 100 mm Hg

Temperature = 540°C.

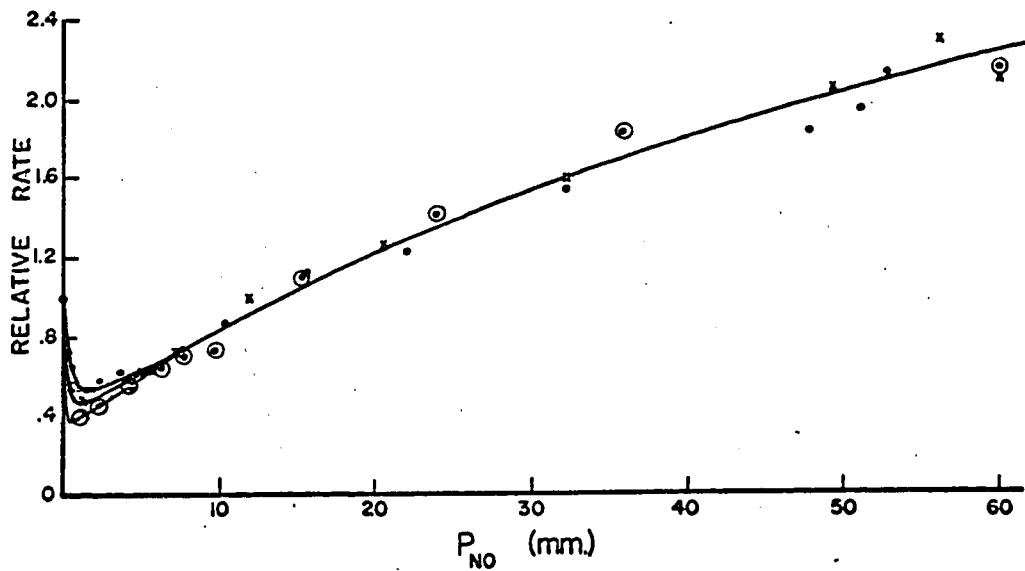


Figure 35. Plots of relative rate against nitric oxide pressure. Relative rates with 50 mm propionaldehyde are shown as  $\odot$ , those *with* /100 mm as X, and those *with* /200 mm as  $\bullet$

Temperature = 540°C.

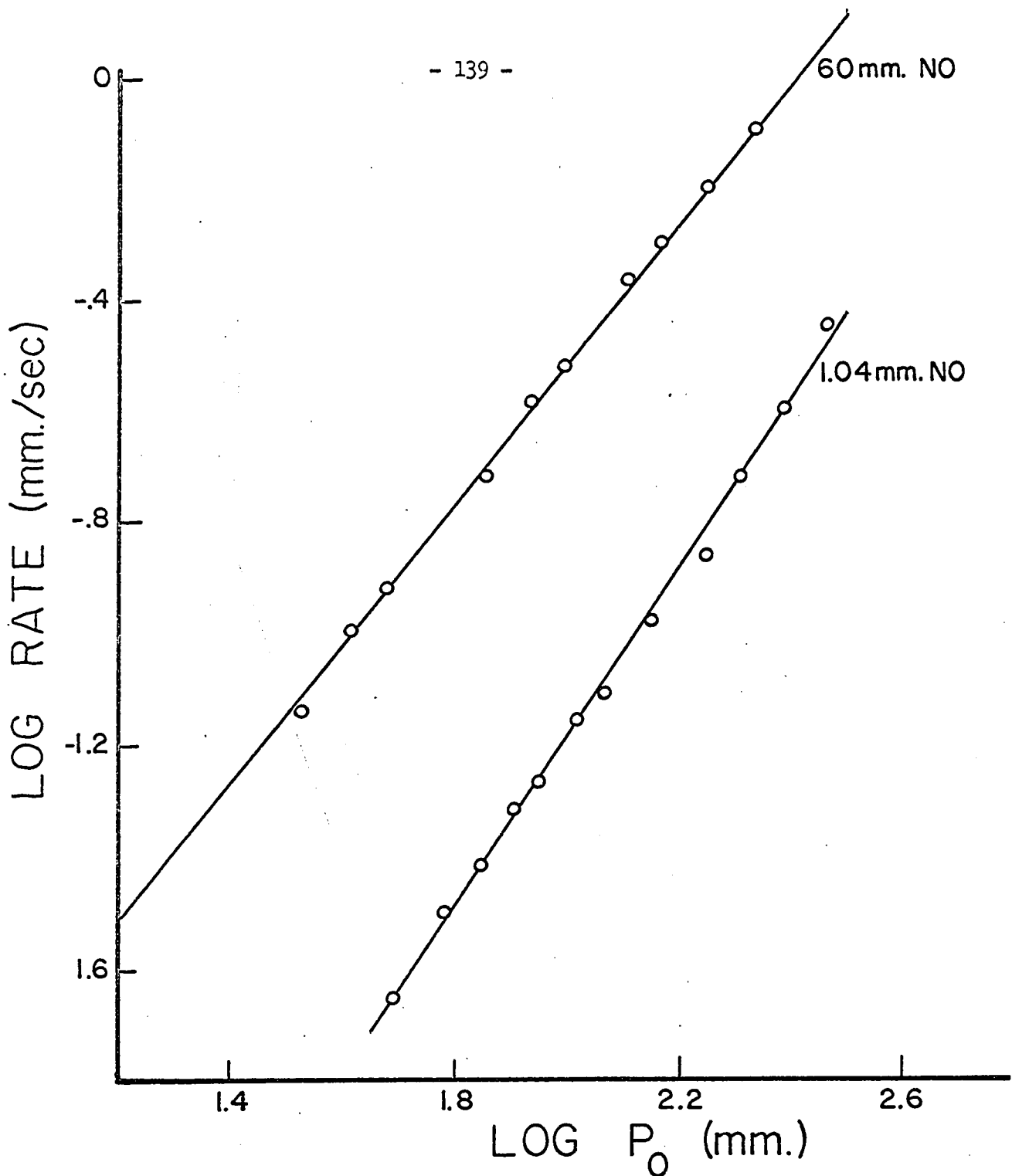


Figure 36. Plots of log rate against log pressure of propionaldehyde showing the effect of nitric oxide pressure on the order with respect to propionaldehyde.

Temperature = 540°C.

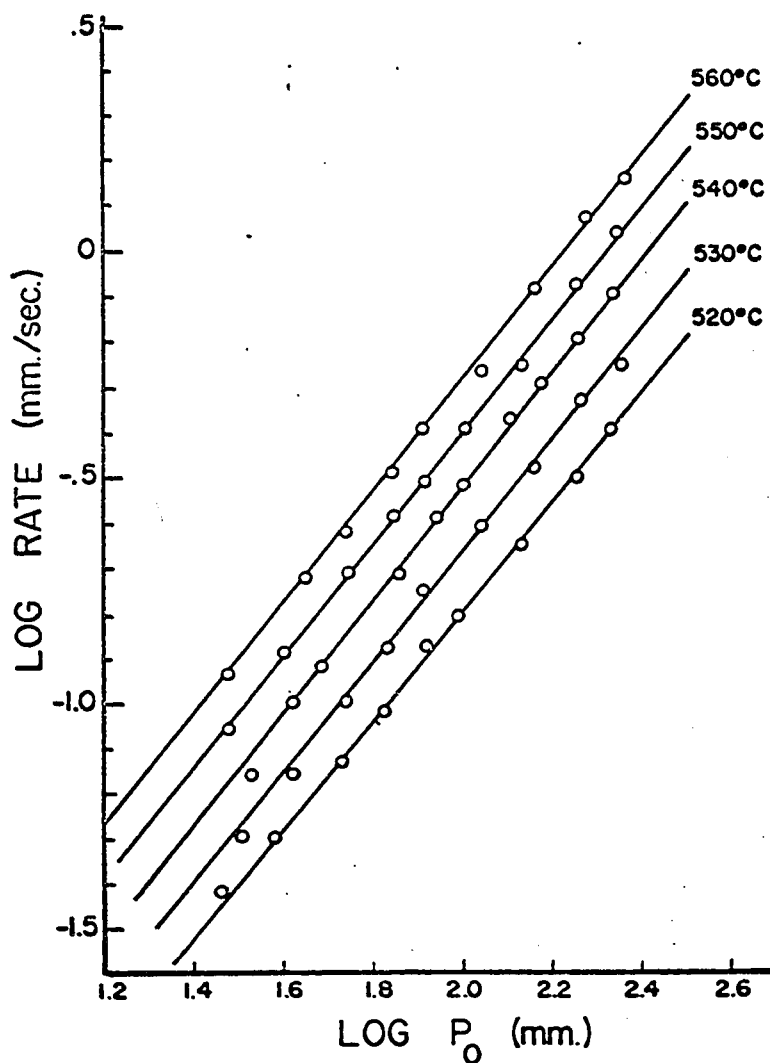


Figure 37. Plots of log rate against log pressure of propionaldehyde with 60 mm of nitric oxide at different temperatures.

propionaldehyde pressure (Figure 35), in contrast to the conclusion of Ho (125).

In Figure 38 is shown a plot of log relative rate against log pressure of nitric oxide at 50, 100 and 200 mm pressures of propionaldehyde. The order of the reaction is seen to be about 0.65 with respect to nitric oxide.

It will be shown in the discussion that the overall rate at high nitric oxide pressures can be divided into two parts and can be represented as

$$v = 2k_{24i} [C_2H_5CHO][NO] + k [C_2H_5CHO]^{3/2} [NO]^{1/2}$$

In Figure 39 is shown a plot of  $v_{NO/P_{C_2H_5CHO}}$  against  $P_{C_2H_5CHO}^{1/2}$  with 60 mm of nitric oxide at different temperatures,  $P_{C_2H_5CHO}$  being the initial pressure of propionaldehyde. The intercepts give  $2k_{24i}[NO]$  and the slopes  $k [NO]^{1/2}$ . The rate constants thus obtained are listed in Table 9.

Figure 40 shows an Arrhenius plot, the rate constants being obtained from Figure 39. The lower curve shows the plot  $k_{24i}$  and the upper curve that of  $k$ . The rate constants  $k_{24i}$  and  $k$  can be expressed as

$$k_{24i} = 4.19 \times 10^{12} e^{-\frac{36800}{RT}} \text{ cc mole}^{-1} \text{ sec}^{-1}$$

$$k = 2.35 \times 10^{14} e^{-\frac{42300}{RT}} \text{ cc mole}^{-1} \text{ sec}^{-1}$$

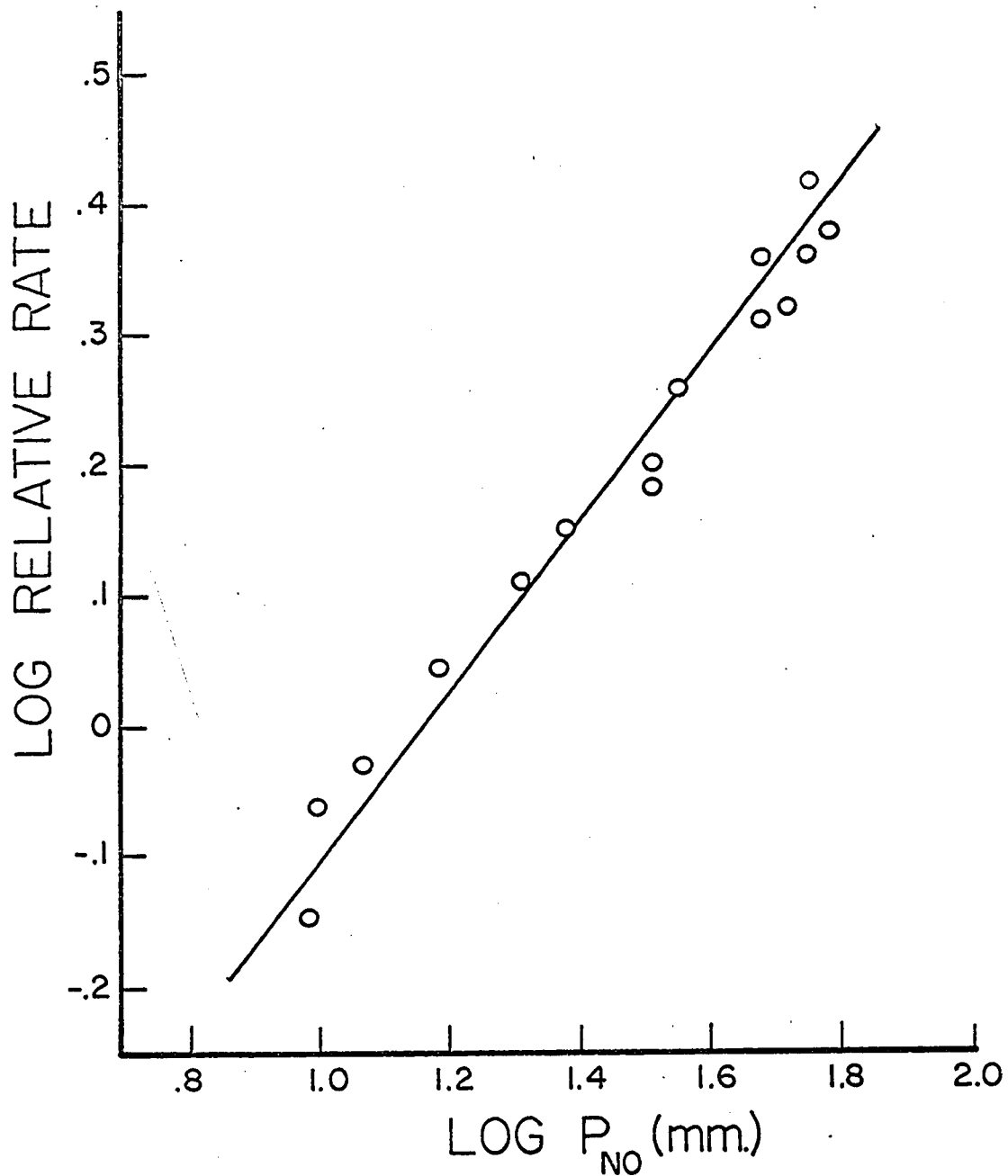


Figure 38. Plot of log relative rate against log pressure of nitric oxide in the region where relative rates are independent of propionaldehyde pressures (Figure 35)

Temperature = 540°C.

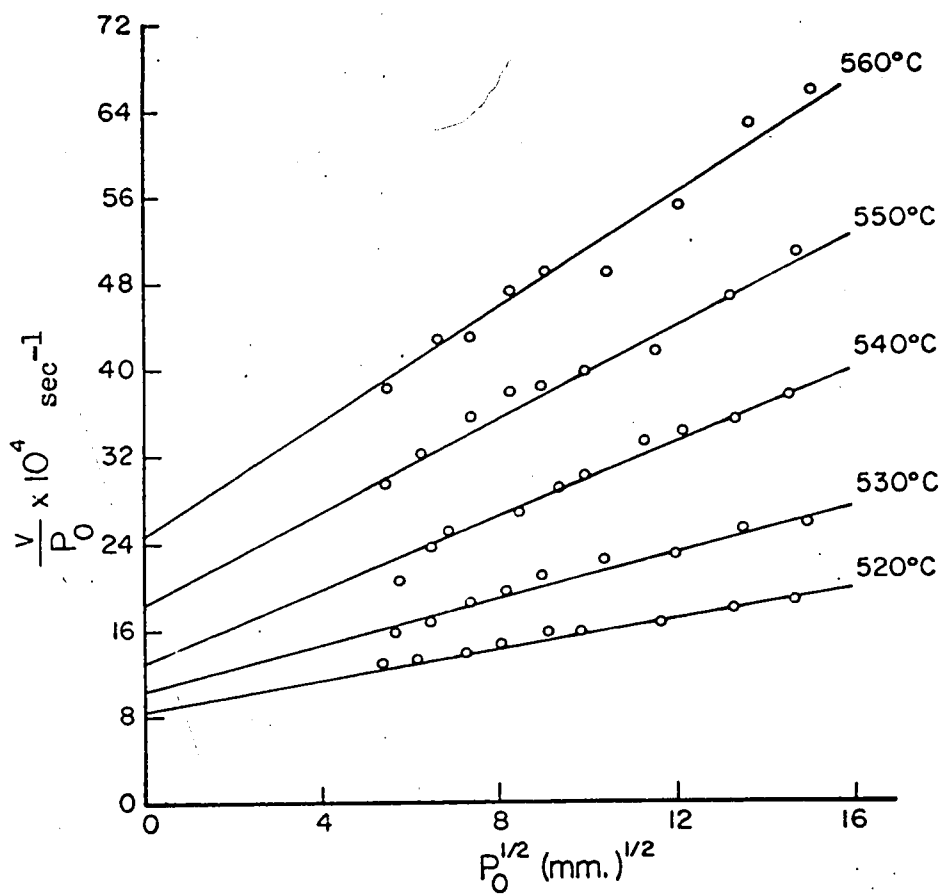


Figure 39. Plot of  $v/P_{\text{C}_2\text{H}_5\text{CHO}}^{1/2}$  against  $P_{\text{C}_2\text{H}_5\text{CHO}}^{1/2}$  with 60 mm of nitric oxide at different temperatures.

Table 9

RATE CONSTANTS CORRESPONDING TO THE

EQUATION  $v = 2k_{24i} [C_2H_5CHO][NO] + k [C_2H_5CHO]^{3/2}[NO]^{1/2}$

Initial Pressure of Nitric Oxide = 60 mm Hg.

Temperature (°C)	$k_{24i} \times 10^{-2}$ (cc mole <sup>-1</sup> sec <sup>-1</sup> )	$k \times 10^{-2}$ (cc mole <sup>-1</sup> sec <sup>-1</sup> )
520	3.46	4.59
530	4.34	6.72
540	5.57	10.99
550	7.87	14.30
560	10.73	18.23

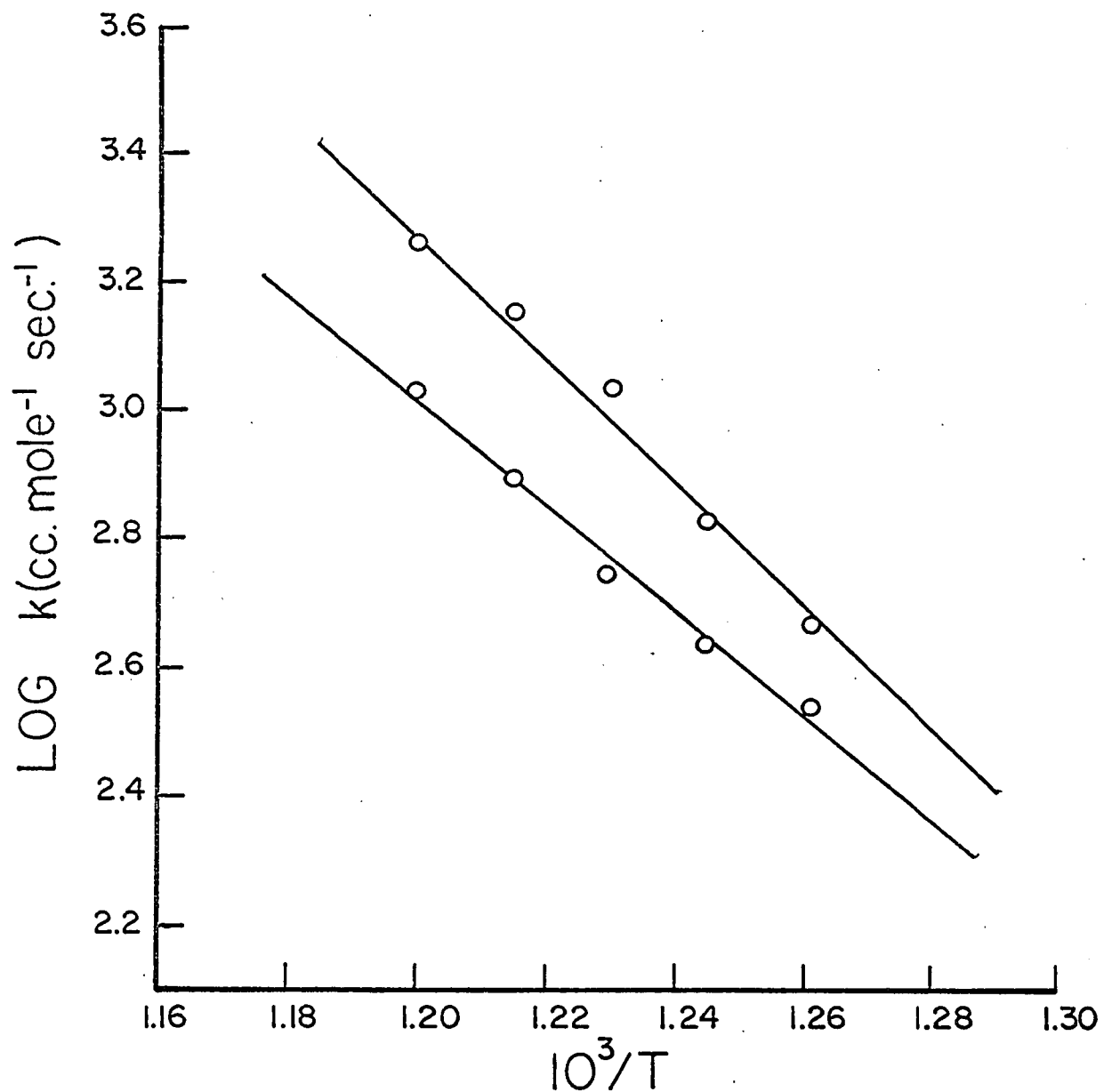


Figure 40. Arrhenius plots. The upper curve shows the plots of  $k_{25i} \left( \frac{k_{24i}}{k_{29i}} \right)^{1/2}$  and the lower one that of  $k_{24i}$  (Equation (68)), the rate constants being those obtained from Figure 39.

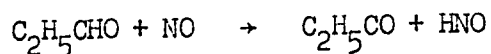
DISCUSSION

Overall Reaction Mechanism

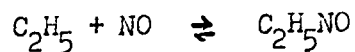
That the maximally uninhibited reaction is not a simple non-chain unimolecular process is shown by the following facts:

- (1) The maximally inhibited reaction has a non-integral order (1.5).
- (2) The degree of inhibition decreases with increase of propionaldehyde pressure.
- (3) In the catalytic region, the order of the reaction is non-integral with respect to both propionaldehyde and nitric oxide, indicating that the latter is involved in the chain reaction. The maximally inhibited reaction must, therefore, be the resultant of two opposing reactions - acceleration as well as inhibition by nitric oxide.
- (4) The increase of the ratio  $C_2H_4/H_2$  with nitric oxide pressure is consistent with a chain mechanism.
- (5) In the uninhibited reaction (Part 5) the contribution of a molecular process has been shown to be unimportant in comparison with that of a chain reaction.

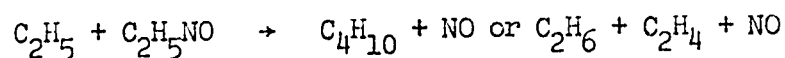
In line with previous work in these laboratories (101 - 107) it is suggested that nitric oxide initiates chains by the reaction



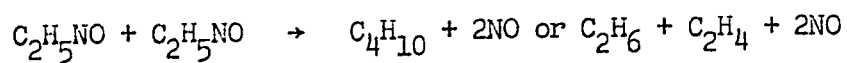
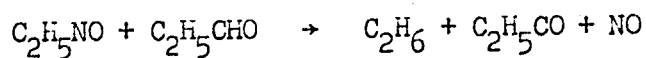
and that the most abundant radical  $C_2H_5$  is involved in the following equilibrium:



In order for the overall order of the maximally inhibited reaction to be three halves, the chain-ending step must be



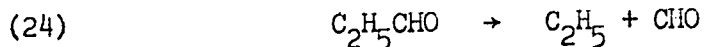
In the catalytic region, the order of the reaction with respect to propionaldehyde falls below three-halves and a plot of relative rate against nitric oxide concentration gives a negative curvature. In line with previous suggestions (Part 4) and the work of Szabó and Márta (111, 112) it is proposed that the reactions



become important at high nitric oxide pressures.

As in the case of acetaldehyde, in the present decomposition there is no flat region when rate is plotted against nitric oxide concentrations. One must, therefore, take into account all the processes in the uninhibited reaction in addition to those involving nitric oxide.

The complete scheme may be written as





$$[C_2H_5] = \frac{k_{24} + k_{24i} [NO]}{k_{29} + k_{29i} K_{31} [NO] + k_{29i}' K_{31}^2 [NO]^2}^{1/2} [C_2H_5CHO]^{1/2} \quad \dots (61)$$

$$[C_2H_5CO] = \frac{[C_2H_5CHO]}{k_{26}} (k_{24} + \frac{2k_{24i} [NO]}{24i} + k_{25} [C_2H_5] + k_{25i} [C_2H_5NO]) \quad \dots (62)$$

$$[C_2H_5NO] = k_{31} [C_2H_5] [NO] \quad K_{31} = \frac{k_{31}}{k_{-31}} \quad \dots (63)$$

$$v = 2k_{24} [C_2H_5CHO] + 2k_{24i} [C_2H_5CHO] [NO] + k_{25} [C_2H_5] [C_2H_5CHO] + k_{25i} [C_2H_5NO] [C_2H_5CHO] + k_{28} [C_2H_5] \quad \dots (64)$$

$$v = 2k_{24i} [C_2H_5CHO] [NO] + k_{25} \left(\frac{k_{24}}{k_{29}}\right)^{1/2} [C_2H_5CHO]^{3/2} \frac{\left(1 + \frac{k_{25i}}{k_{25}} K_{31} [NO]\right) \left(1 + \frac{k_{24i} [NO]}{k_{24}}\right)^{1/2}}{\left(1 + \frac{k_{29i} K_{31} [NO]}{k_{29}} + \frac{k_{29i}' K_{31}^2 [NO]^2}{k_{29}}\right)^{1/2}} + k_{28} \left(\frac{k_{24}}{k_{29}}\right)^{1/2} [C_2H_5CHO]^{1/2} \frac{\left(1 + \frac{k_{24i} [NO]}{k_{24}}\right)^{1/2}}{\left(1 + \frac{k_{29i}}{k_{29}} K_{31} [NO] + \frac{k_{29i}' K_{31}^2 [NO]^2}{k_{29}}\right)^{1/2}} \quad \dots (65)$$

Important special cases are as follows:

(1) If [NO] is zero, equation (65) reduces to

$$v = k_{25} \left( \frac{k_{24}}{k_{29}} \right)^{1/2} [C_2H_5CHO]^{3/2} + k_{28} \left( \frac{k_{24}}{k_{29}} \right)^{1/2} [C_2H_5CHO]^{1/2}$$

which is the rate expression for the uninhibited reaction.

(2) In the presence of nitric oxide ethylene production increases but not at the expense of ethane production (Figure 34); in the uninhibited reaction, on the other hand, the ethane and ethylene productions are in competition with each other. In the uninhibited reaction, the rates of formation of ethylene and hydrogen are approximately equal (Figure 34) but in the presence of nitric oxide the rate of formation of the latter is much less than that of the former (Figure 34). These facts suggest that the reaction



is unimportant in the presence of nitric oxide. This is understandable in view of the fact that using the kinetic parameters of Sagert and Laidler (105) the equilibrium constant  $K_{31}$  is calculated to be  $10^{12.66}$  at  $540^\circ C$ , and that the concentration of  $C_2H_5NO$  increases relative to that of  $C_2H_5$  with the increase of nitric oxide concentration. It is, therefore, suggested that most of the ethylene formed in the presence of nitric oxide comes from the chain-ending steps (29i) and (29'i). On the basis of the above considerations, equation (65) reduces to

$$v = 2k_{24i} [C_2H_5CHO][NO] + k_{25} \left(\frac{k_{24}}{k_{29}}\right)^{1/2} [C_2H_5CHO]^{3/2} \frac{\left(1 + \frac{k_{25i}}{k_{25}} K_{31} [NO]\right) \left(1 + \frac{k_{24i}}{k_{24}} [NO]\right)^{1/2}}{\left(1 + \frac{k_{29i}}{k_{29}} K_{31} [NO] + \frac{k'_{29i}}{k_{29}} K_{31}^2 [NO]^2\right)^{1/2}}$$

.... (66)

(3) At sufficiently low nitric oxide concentration

$$1 \gg \frac{k_{25i}}{k_{25}} K_{31} [NO] \text{ and } \left(1 + \frac{k_{29i}}{k_{29}} K_{31} [NO]\right) \gg \frac{k'_{29i}}{k_{29}} K_{31}^2 [NO]^2$$

Equation (66) then reduces to

$$v = 2k_{24i} [C_2H_5CHO][NO] + k_{25} \left(\frac{k_{24}}{k_{29}}\right)^{1/2} [C_2H_5CHO]^{3/2} \frac{\left(1 + \frac{k_{24i}}{k_{24}} [NO]\right)^{1/2}}{\left(1 + \frac{k_{29i}}{k_{29}} K_{31} [NO]\right)^{1/2}}$$

Approximately 1 mm pressure of nitric oxide gives maximum inhibition. The first term of the above equation can, therefore, be neglected. In the maximally inhibited region, the rates of the chain initiating steps (24) and (24i), and terminating steps (29) and (29i) may be compared in the following way:

$$\frac{v_{24i}}{v_{24}} = \frac{k_{24i} [C_2H_5CHO][NO]}{k_{24} [C_2H_5CHO]} = \frac{k_{24i}}{k_{24}} [NO] \approx 130 \text{ at } 540^\circ\text{C with 1 mm of}$$

nitric oxide.

$$\frac{v_{29i}}{v_{29}} = \frac{k_{29i} [\text{C}_2\text{H}_5][\text{C}_2\text{H}_5\text{NO}]}{k_{29} [\text{C}_2\text{H}_5][\text{C}_2\text{H}_5]} = \frac{k_{29i} K_{31} [\text{NO}]}{k_{29}} \approx 40 \text{ at } 540^\circ\text{C with 1 mm of}$$

nitric oxide. The values of the rate constants have been taken from Table 10. Application of the above considerations to equation (66) gives the following expression for the maximally inhibited rate.

$$v = k_{25} \left( \frac{k_{24i}}{k_{29i} K_{31}} \right)^{1/2} [\text{C}_2\text{H}_5\text{CHO}]^{3/2} \quad (67)$$

which is in complete agreement with experiment (Figure 36).

(4) At high nitric oxide pressures

$$\frac{k_{24i}}{k_{24}} [\text{NO}] \gg 1, \quad \frac{k'_{29i} K_{31}^2 [\text{NO}]^2}{k_{29}} \gg \left( 1 + \frac{k_{29i}}{k_{29}} K_{31} [\text{NO}] \right)$$

and  $\frac{k_{25i} K_{31} [\text{NO}]}{k_{25}} \gg 1$ . Equation (66) is, therefore, reduced to

$$v = 2k_{24i} [\text{C}_2\text{H}_5\text{CHO}][\text{NO}] + k_{25i} \left( \frac{k_{24i}}{k'_{29i}} \right)^{1/2} [\text{C}_2\text{H}_5\text{CHO}]^{3/2} [\text{NO}]^{1/2} \quad (68)$$

That at high nitric oxide pressures reaction (25) is unimportant in comparison with (25i) may be shown as follows:

Table 10

KINETIC PARAMETERS FOR ELEMENTARY REACTIONS

Reaction	Frequency factor*	Activation energy (kcal. mole <sup>-1</sup> )	Reference
(24)	1.7 x 10 <sup>15</sup>	82.8	Márta (124)
(24i)	4.19 x 10 <sup>12</sup>	36.8	See Text
(25)	2.36 x 10 <sup>11</sup>	7.6	Volman and Brinton (130)
(25i)	1 x 10 <sup>11</sup>	26.0	E calc. following Ree, Yang and Eyring (113) A est. from Volman and Brinton (130)
(31)	3.0 x 10 <sup>11</sup>	0	Sagert and Laidler (105)
(-31)	5.0 x 10 <sup>14</sup>	59	Sagert and Laidler (105)
(29)	1.6 x 10 <sup>13</sup>	0	Ivin and Steacie (133), and Shepp and Kutschke (134)
(29i)	7.0 x 10 <sup>9</sup>	0	Sagert and Laidler (105)

\* sec<sup>-1</sup> or cc mole<sup>-1</sup> sec.<sup>-1</sup>

$$\frac{v_{25i}}{v_{25}} = \frac{k_{25i} [C_2H_5NO][C_2H_5CHO]}{k_{25} [C_2H_5][C_2H_5CHO]} = \frac{k_{25i} K_{31} [NO]}{k_{25}}$$

Insertion of the values of the rate constants from Table 10 gives

$$\frac{v_{25i}}{v_{25}} \approx 26 \text{ at } 540^\circ\text{C with } 60 \text{ mm nitric oxide}$$

That equation (68) is the correct expression for the overall rate may be shown in the following way :

$$\frac{v}{[C_2H_5CHO]} = 2k_{24i} [NO] + k_{25i} \left( \frac{k_{24i}}{k_{29i}} \right)^{1/2} [C_2H_5CHO]^{1/2} [NO]^{1/2} \dots (69)$$

A plot of  $v/[C_2H_5CHO]$  against  $[C_2H_5CHO]^{1/2}$  at constant high nitric oxide pressure should give a straight line. Figure 39 shows such a plot with 60 mm nitric oxide at different temperatures. Good linearity within the experimental error at all temperatures lends strong support to the validity of equation (68) and hence to that of the suggested mechanism.

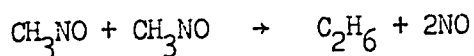
#### Activation Energies

Further support for equation (68) can be obtained from a comparison of the observed and predicted activation energies. Activation energies corresponding to the first and the second terms of equation (68) are 36.8 kcal. and 42.3 kcal per mole respectively (Figure 40). The observed

activation energy 36.8 kcal. for reaction (24i) compares well with its endothermicity 36.4 kcal. per mole (calculated on the basis of  $D(H - NO) = 48.6$  kcal (110) and  $D(C_2H_5CO - H) = 85$  kcal per mole; the latter value is assumed by comparison with  $D(CH_3CO - H) = 85$  kcal per mole (55)). The activation energy expression for the second term is

$$E_{25i} + \frac{1}{2} (E_{24i} - E'_{29i}) = 42.3 \text{ kcal per mole} \quad \dots (70)$$

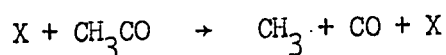
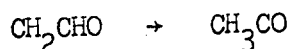
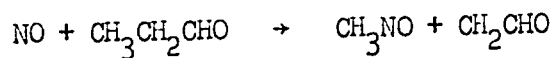
Insertion of the values of  $E_{25i}$  and  $E_{24i}$  from Table 10 leads to 4.2 kcal. per mole for reaction (29'i). This value may be compared with 3.9 kcal. per mole obtained for the similar reaction



in the pyrolysis of acetaldehyde (Part 4).

### The Production of Methane

In the uninhibited reaction only a trace amount of methane was detected and nitric oxide was found to increase the rate of production of methane. This fact may be explained through the occurrence of the following reactions :



Methane may also arise from the decomposition of  $C_4H_{10}$  formed in the chain-ending reactions.

### The Termination Steps

An important feature of the proposed mechanism is that chain termination in the presence of nitric oxide involves interaction between  $C_2H_5$  and  $C_2H_5NO$  (reaction 29i) and between two  $C_2H_5NO$  molecules (reaction 29'i). It has been shown by Pratt and Purnell (135) that in the decomposition of tetraethyl lead in the presence of nitric oxide at 252°C reaction (29i) is unimportant in comparison with reactions (32) and (33) and that reaction (33) is entirely heterogeneous. Szabó and Márta (111, 136) have found that nitric oxide is not consumed in the pyrolysis of propionaldehyde at 550°C. This fact suggests that under the conditions of propionaldehyde pyrolysis reactions (32) and (33) are unimportant, in contrast to the suggestion of Pratt and Purnell (135), and that nitric oxide is regenerated in some way. The occurrence of the surface reaction (33) to any significant extent in the pyrolysis of propionaldehyde is also excluded by the fact that the contribution of any heterogeneous reaction in this pyrolysis is negligible (125). Figure 34 shows that the ratio  $C_2H_4/C_2H_6$  is increased by the addition of nitric oxide. Since reaction (28) is, as shown above, unimportant in the presence of nitric oxide, the increase of  $C_2H_4/C_2H_6$  in the presence of nitric oxide and the regeneration of the latter are attributed to the occurrence of reactions (29i) and 29'i), i.e. the removal of ethyl radicals in the presence of

nitric oxide takes place by the radical-molecule complex mechanism which has recently been considered theoretically by Eusuf and Laidler (90).

CLAIMS TO ORIGINAL RESEARCH

1. Atom and free-radical combination reactions in the gas phase have been considered on the basis of the energy-transfer and radical-molecule complex mechanisms. Statistical-mechanical rate equations for the two types of mechanism are derived.
2. The resonance integral of the wave function of a charge-transfer complex has been estimated. This suggests numerous calculations of binding energies arising from charge transfer.
3. For the first time, the binding energies between iodine atoms and various chaperon molecules arising from charge transfer have been calculated.
4. The third-order rate constants for the combination of iodine atoms have been calculated on a purely theoretical basis. A conclusion has been drawn from a comparison of the experimental and calculated rate constants as to the type of mechanism applicable in the presence of a foreign molecule.
5. The dissociation of ethane and the combination of methyl radicals have been critically considered on the basis of the experimental results obtained in the photolysis and pyrolysis of various organic compounds.
6. It has been shown that all the known experimental facts can be explained only by putting the combination of methyl radicals in its third order region under the ordinary pyrolysis conditions.

7. The pyrolysis of acetaldehyde was studied and it was found that the overall order is three halves, in agreement with all the previous work.
8. The rate of ethane formation in the pyrolysis of acetaldehyde has been measured for the first time. It has been shown that the chain initiation in the pyrolysis of acetaldehyde is a second-order process.
9. It has been shown by calculation that the chain-initiation in the pyrolysis of acetaldehyde takes place by the transfer of a hydrogen atom from one acetaldehyde molecule to the other. This type of initiation has been shown to be consistent with all the known facts.
10. A new type of overall mechanism, which is consistent with all the available experimental results, has been proposed.
11. The pyrolysis of acetaldehyde in the presence of nitric oxide was studied over a wide range of acetaldehyde and nitric oxide pressures and for the first time a detailed investigation at low nitric oxide pressures was made. The overall order with respect to acetaldehyde first increases from three-halves with increase of nitric oxide pressures and then falls to three-halves again. The order with respect to nitric oxide at high nitric oxide pressures is one-half.
12. The occurrence of a reaction which is first-order in acetaldehyde and first-order in nitric oxide was shown for the first time. The activation energy of this reaction was found to agree with that of the hydrogen abstraction reaction suggested by Wojciechowski and Laidler (101).

13. A mechanism which is applicable over the whole range of nitric oxide pressures used has been proposed for the first time. This mechanism can explain satisfactorily all the experimental facts.
14. The pyrolysis of propionaldehyde was reinvestigated and it was found that the overall order is between 1.25 and 1.30. Inert gases were found to have no effect on the rates of formation of products.
15. It has been shown that the decomposition of the ethyl radical into ethylene and hydrogen is a pressure independent process under the ordinary pyrolysis conditions.
16. An overall mechanism consistent with the kinetic and analytical data has been proposed.
17. The unexpected fact that the rate of the uninhibited decomposition of acetaldehyde is higher than that of propionaldehyde has been explained.
18. The pyrolysis of propionaldehyde in the presence of nitric oxide was reinvestigated over a wide range of propionaldehyde and nitric oxide pressures. The overall order of the reaction first rises from 1.25 with the increase of nitric oxide pressures and then falls to 1.25 again. The order with respect to nitric oxide at high nitric oxide pressures is between one-half and one.

19. A detailed mechanism, for the propionaldehyde pyrolysis, applicable over the whole range of nitric oxide pressures used, has been proposed. The suggested mechanism is consistent with the kinetic and analytical results.

REFERENCES

1. G. Dixon-Lewis, M.M. Sutton, and A. Williams, Disc. Faraday Soc. 33, 205 (1962).
2. K. Hilferding and W. Steiner, Z. Physik. Chem. Ser. B, 30, 399 (1935).
3. K.E. Russell and J. Simons, Proc. Roy. Soc. (London) Ser. A, 217, 271 (1953).
4. M.I. Christie, R.G.W. Norrish, and G. Porter, Proc. Roy. Soc. (London) Ser. A, 216, 152 (1952).
5. M.I. Christie, A.J. Harrison, R.G. Norrish, and G. Porter, Proc. Roy. Soc. (London) Ser. A, 231, 446 (1955).
6. R.L. Strong, J.C.W. Chien, P.E. Graf, and F.E. Willard, J. Chem. Phys. 26, 1287 (1957).
7. D.L. Bunker and N. Davidson, J. Am. Chem. Soc. 80, 5085, 5090 (1958).
8. G. Porter and J.A. Smith, Proc. Roy. Soc. (London) Ser. A, 261, 28 (1961).
9. R. Engleman and N.R. Davidson, J. Am. Chem. Soc. 82, 4770 (1960).
10. R.E. Dodd and E.W.R. Steacie, Proc. Roy. Soc. (London) Ser. A, 223, 283 (1954).
11. A. Shepp, J. Chem. Phys. 24, 939 (1956).
12. J.C. Keck, J. Chem. Phys. 29, 410 (1958).
13. D. Husain and H.O. Prochard, J. Chem. Phys. 30, 1101 (1959).
14. D.W. Jepson and J.W. Hirschfelder, J. Chem. Phys. 30, 1032 (1959).
15. E.K. Gill and K.J. Laidler, Proc. Roy. Soc. (London) Ser. A, 250, 121 (1959).
16. J.C. Keck, J. Chem. Phys. 32, 1035 (1960).

17. G. Porter, Disc. Faraday Soc. 33, 198 (1962).
18. K.J. Laidler, Disc. Faraday Soc. 33, 294 (1962).
19. H.O. Pritchard, J. Phys. Chem. 65, 504 (1961).
20. H.O. Pritchard, J. Phys. Chem. 66, 2111 (1962).
21. D.L. Bunker, J. Chem. Phys. 32, 1001 (1960).
22. M.I. Christie, J. Am. Chem. Soc. 84, 4066 (1962).
23. J.C. Slater and J.G. Kirkwood, Phys. Rev. 37, 682 (1931).
24. K.S. Pitzer, J. Am. Chem. Soc. 78, 4565 (1956).
25. D.E. Peterson and K.S. Pitzer, J. Phys. Chem. 61, 1252 (1957).
26. J.A.A. Ketelaar, Chemical Constitution, Elsevier Publ. Co. Amsterdam, 1958 pp. 91, 201, 376.
27. J.O. Hirschfelder, C.F. Curtiss, and R.B. Bird, Molecular theory of gases and liquids. John Wiley and Sons, Inc., New York Chapman and Hall, Limited, London, 1954. pp. 1110 - 1112.
28. R.S. Mulliken, J. Am. Chem. Soc. 74, 811 (1952).
29. S.H. Hastings, J.L. Franklin, J.C. Schiller, and F.A. Matsen, J. Am. Chem. Soc. 75, 2900 (1953).
30. H. McConnel, J.S. Ham, and J.R. Platt, J. Chem. Phys. 21, 66 (1953).
31. M.C. Day Jr. and J. Selbin, Theoretical inorganic chemistry, Reinhold Publ. Corp., New York Chapman and Hall, Ltd. London, 1962. pp. 108, 110.
32. Handbook of Chemistry and Physics, 36th edition. Chemical Rubber Publ. Co. Ohio, 1954. p. 2341.
33. K. Watanabe, J. Chem. Phys. 26, 542 (1957).
34. P.G. Wilkinson, Can. J. Phys. 34, 596 (1956).

35. E. Rabinowitch, *Trans. Faraday Soc.* 33, 281 (1937).
36. A. Streitwieser Jr., *Molecular orbital theory for organic chemists.* John Wiley and Sons. New York, 1961. p. 191.
37. F.O. Rice and K.F. Herzfeld, *J. Am. Chem. Soc.* 56, 284 (1934).
38. L. Küchler and H. Theile, *Z. Physik. Chem. Ser. B*, 42, 359 (1939).
39. K.J. Laidler, N.H. Sagert, and B.W. Wojciechowski, *Proc. Roy. Soc. (London) Ser. A*, 270, 242 (1962).
40. K.J. Laidler and B.W. Wojciechowski, *Proc. Roy. Soc. (London) Ser. A*, 260, 91 (1961).
41. C.P. Quinn, *Proc. Roy. Soc. (London) Ser. A*, 275, 190 (1963).
42. C.P. Quinn, *Trans. Faraday. Soc.* 59, 2543 (1963).
43. K. Brill, P. Goldfinger, M. Letort, H. Mattys, and N. Niclause, *Bull. Soc. Chim. Belg.* 59, 263 (1950).
44. A.B. Trenwith, *J. Chem. Soc.* 4426 (1963).
45. A.F. Trotman-Dickenson and E.W.R. Steacie, *J. Chem. Phys.* 18, 1097, (1950).
46. R.K. Brinton, *J. Am. Chem. Soc.* 83, 1541 (1961).
47. C.J. Danby, A.S. Buchanan, and I.H.S. Henderson, *J. Chem. Soc.* 1426 (1951).
48. K.U. Ingold and F.P. Lossing, *J. Chem. Phys.* 21, 1135 (1953).
49. K.U. Ingold, I.H.S. Henderson and F.P. Lossing, *J. Chem. Phys.* 21, 2239 (1953).
50. G.B. Kistiakowski and E.K. Roberts, *J. Chem. Phys.* 21, 1637 (1953).
51. C.J. Danby, B.C. Spall, F.S. Stubbs and C.N. Hinshelwood, *Proc. Roy. Soc. (London) Ser. A*, 218, 450 (1953).

52. K.J. Laidler and B.W. Wojciechowski, Chem. Soc. Special Publication 16, 37 (1962).
53. L.A. Wall and W.J. Moore, J. Am. Chem. Soc. 73, 2840 (1951).
54. L.A. Wall and W.J. Moore, J. Phys. Coll. Chem. 55, 965 (1951).
55. E.W.R. Steacie, Atomic and free radical reactions, Reinhold Publ. Corp. New York, 1954.
56. C.J.M. Fletcher and C.N. Hinshelwood, Proc. Roy. Soc. (London) Ser. A, 141, 41 (1933).
57. C.N. Hinshelwood, C.J.M. Fletcher, F.H. Verhoek and C.A. Winkler Proc. Roy. Soc. (London), Ser. A, 146, 327 (1934).
58. C.A. Winkler and C.N. Hinshelwood, Proc. Roy. Soc. (London) Ser. A, 149, 355 (1935).
59. M. Letort, Thesis, University of Paris (1937).
60. M. Letort, J. Chim. Phys. 34, 206 (1937).
61. A. Boyer, M. Niclaude and M. Letort, J. Chim. Phys. 49, 337, 345 (1952).
62. G.R. Freeman, C.J. Danby, and C.N. Hinshelwood, Proc. Roy. Soc. (London) Ser. A. 245, 456 (1958).
63. N. Imai, Y. Yoshida, and O. Toyama, Bull. Chem. Soc. Japan, 35, 752 (1962).
64. F.O. Rice, W.R. Johnston, and B.L. Evering, J. Am. Chem. Soc. 54, 3529 (1932).
65. M. Burton, J.E. Ricci, and T.W. Davis, J. Am. Chem. Soc. 62, 265 (1940).
66. F. Patat, Z. Physik, Chem. Ser. B, 32, 294 (1936).
67. F. Patat and H. Sachsse, Naturwiss, 23, 247 (1935).

68. F. Patat and H. Sachsse, Z. Physik, Chem. Ser. B, 31, 105 (1935).
69. H. Sachsse and F. Patat, Z. Elektrochem. 41, 493 (1935).
70. J.C. Morris, J. Am. Chem. Soc. 63, 2535 (1941).
71. J.C. Morris, J. Am. Chem. Soc. 66, 584 (1944).
72. P.D. Zemaný and M. Burton, J. Am. Chem. Soc. 73, 499 (1951).
73. F.O. Rice and R.E. Varnerin, J. Am. Chem. Soc. 76, 2629 (1954).
74. A.O. Allen and D.V. Sickman, J. Am. Chem. Soc. 56, 2031 (1934).
75. D.V. Sickman and A.O. Allen, J. Am. Chem. Soc. 56, 1251 (1934).
76. F.E. Blacet and A. Taurog, J. Am. Chem. Soc. 61, 3024 (1939).
77. J.G. Calvert and J.T. Gruver, J. Am. Chem. Soc. 80, 1313 (1958).
78. F.P. Lossing, Can. J. Chem. 35, 305 (1957).
79. C.J.M. Fletcher, J. Am. Chem. Soc. 58, 534 (1936).
80. C.J.M. Fletcher and G.K. Rollefson, J. Am. Chem. Soc. 58, 2135 (1936).
81. F.O. Rice and W.D. Walters, J. Am. Chem. Soc. 63, 1701 (1941).
82. A. Boyer, M. Niclaude and M. Letort, J. Chim. Phys. 49, 345 (1952).
83. M. Niclaude and M. Letort, Compt. Rend., 226, 77 (1948).
84. K. Brill, P. Goldfinger, M. Letort, H. Mattys and M. Niclaude, Nature, 166, 405 (1950).
85. C.N. Hinshelwood and W.K. Hutchison, Proc. Roy. Soc. (London) Ser. A, 111, 380 (1926).
86. R.V. Seddon and M.W. Travers, Proc. Roy. Soc. (London) Ser. A, 156, 234 (1936).
87. E. Leifer and H.C. Urey, J. Am. Chem. Soc. 64, 994 (1942).
88. N. Imai and O. Toyama, Bull. Chem. Soc. Japan, 33, 1408 (1960).
89. M.H. Back, M. Eusuf and K.J. Laidler, To be published.
90. M. Eusuf and K.J. Laidler, Trans. Faraday Soc. 59, 2750 (1963).

91. S.W. Benson, The Foundation of Chemical Kinetics, McGraw-Hill Book Company Inc. 1960 pp. 383, 385.
92. D.J. McKenney and K.J. Laidler, Can. J. Chem. 41, 1984 (1963).
93. A.B. Trenwith, Private Communication.
94. F.E. Blacet and W.E. Bell, Disc. Faraday Soc. 14, 70 (1953).
95. J.N. Pitts, R.S. Tollberg, and T.W. Martin, J. Am. Chem. Soc. 70, 2843 (1954).
96. J.A. Kerr and A.K. Trotman-Dockenson, J. Chem. Soc. 3377 (1957).
97. F.H. Verhoek, Trans. Faraday Soc. 31, 1533 (1935).
98. L.A.K. Staveley and C.N. Hinshelwood, Nature 137, 29 (1936).
99. L.A.K. Staveley and C.N. Hinshelwood, J. Chem. Soc. 812 (1936).
100. J.R.E. Smith and C.N. Hinshelwood, Proc. Roy. Soc. (London) Ser. A, 180, 237 (1942).
101. B.W. Wojciechowski and K.J. Laidler, Can. J. Chem. 38, 1027 (1960).
102. B.W. Wojciechowski and K.J. Laidler, Trans. Faraday Soc. 59, 369 (1963).
103. K.J. Laidler and B.W. Wojciechowski, Proc. Roy. Soc. (London) Ser. A, 260, 103 (1961).
104. K.J. Laidler, N.H. Sagert and B.W. Wojciechowski, Proc. Roy. Soc. (London) Ser. A, 270, 254 (1962).
105. N.H. Sagert and K.J. Laidler, Can. J. Chem. 41, 848 (1963).
106. D.J. McKenney, B.W. Wojciechowski and K.J. Laidler, Can. J. Chem. 41, 1993 (1963).
107. K.J. Laidler and D.J. McKenney, to be published.
108. M. Eusuf and K.J. Laidler, Can. J. Chem. (1964).
109. E.E. Hughes, J. Chem. Phys. 35, 1531 (1961).

110. M.J.Y. Clement and D.A. Ramsay, *Can. J. Phys.* 39, 205 (1961).
111. Z.G. Szabó and F. Márta, *J. Am. Chem. Soc.* 83, 768 (1961).
112. Z.G. Szabó and F. Márta, *Acta Chim. Hung.* 32, 81 (1962).
113. T. Ree, H. Yang and H. Eyring, *Trans. Faraday Soc.* 58, 2375 (1962).
114. J.W. Mitchell and C.N. Hinshelwood, *Proc. Roy. Soc. (London) Ser. A*, 159, 32 (1937).
115. H.A. Taylor and H. Bender, *J. Chem. Phys.* 9, 761 (1941).
116. B.G. Gowenlock and J. Trotman, *J. Chem. Soc.* 4190 (1955).
117. W. Lüttke, *Z. Elektrochem.* 61, 302 (1957).
118. D.E. Hoare, *Can. J. Chem.* 40, 2012 (1962).
119. H.A. Taylor and V.v. Verselowsky, *J. Phys. Chem.* 39, 1095 (1935).
120. C.N. Hinshelwood and H.W. Thompson, *Proc. Roy. Soc. (London) Ser. A* 113, 221 (1936).
121. C.A. Winkler, C.J.M. Fletcher and C.N. Hinshelwood, *Proc. Roy. Soc. (London) Ser. A*, 146, 345 (1934).
122. J.J. Sworski and M.J. Burton, *J. Am. Chem. Soc.* 73, 3194 (1951).
123. A. Boyer and M. Niclause, *J. Chim. Phys.* 49, 354 (1952).
124. F. Márta, *Acta Chim. Hung.* 31, 415 (1962).
125. S.K. Ho, *Proc. Roy. Soc. (London) Ser. A*, 276, 278 (1963).
126. J.H. Purnell and C.P. Quinn, *Proc. Roy. Soc. (London) Ser. A*, 270, 267 (1962).
127. N.H. Sagert and K.J. Laidler, *Can. J. Chem.* 41, 838 (1963).
128. M. Swarc, *Chem. Rev.* 47, 75 (1950).
129. S.W. Benson, *The foundations of chemical kinetics*. McGraw-Hill Book Company Inc. 1960, pp. 662-671.

130. D.H. Volman and R.K. Brinton, *J. Chem. Phys.* 22, 929 (1954).
131. S. Bywater and E.W.R. Steacie, *J. Chem. Phys.* 19, 326 (1951).
132. A.F. Trotman-Dickenson, *J. Chem. Phys.* 21, 211 (1953).
133. K.J. Ivin and E.W.R. Steacie, *Proc. Roy. Soc. (London) Ser. A*, 208, 25 (1951).
134. A. Shepp and K.O. Kutschke, *J. Chem. Phys.* 26, 1020 (1957).
135. G.L. Pratt and J.H. Purnell, *Trans. Faraday Soc.* 60, 371 (1964).
136. Z.G. Szabó and F. Márta, *Acta Chim. Hung.* 32, 69 (1962).